

**SORTING OF INNER NUCLEAR MEMBRANE-DIRECTED
PROTEINS AT THE ENDOPLASMIC RETICULUM MEMBRANE**

A Dissertation

by

SURAJ SAKSENA

Submitted to the Office of Graduate Studies of
Texas A&M University
in partial fulfillment of the requirements for the degree of

DOCTOR OF PHILOSOPHY

December 2005

Major Subject: Biochemistry

**SORTING OF INNER NUCLEAR MEMBRANE-DIRECTED
PROTEINS AT THE ENDOPLASMIC RETICULUM MEMBRANE**

A Dissertation

by

SURAJ SAKSENA

Submitted to the Office of Graduate Studies of
Texas A&M University
in partial fulfillment of the requirements for the degree of

DOCTOR OF PHILOSOPHY

Approved by:

Chair of Committee, Max D. Summers

Committee members, Arthur E. Johnson

Ryland F. Young

James C. Hu

Sharon C. Braunagel

Head of Department, Gregory D. Reinhart

December 2005

Major Subject: Biochemistry

ABSTRACT

Sorting of Inner Nuclear Membrane- Directed Proteins at the Endoplasmic Reticulum
Membrane. (December 2005)

Suraj Saksena, B.S.; M.S. Biochemistry, University of Delhi

Chair of Advisory Committee: Dr. Max D. Summers

The current “diffusion-retention” model for protein trafficking to the inner nuclear membrane (INM) proposes that INM proteins diffuse laterally from the membrane of the endoplasmic reticulum into the INM and are then retained in the INM by binding to nuclear proteins or DNA. Because some data indicate that the sorting of baculovirus envelope proteins to the INM is protein-mediated, we have examined the early stages of INM protein integration and sorting using photocrosslinking. Both viral and host INM-directed proteins were integrated cotranslationally through the endoplasmic reticulum translocon, and their nonrandom photocrosslinking to two translocon proteins, Sec61 α and translocating chain-associated membrane protein (TRAM), revealed that the first transmembrane sequence (TMS) of each viral and host INM-directed protein occupied a very similar location within the translocon. Because few TMSs of non-INM-directed membrane proteins photocrosslink to TRAM, it seems that the INM-directed TMSs occupy different sites within the translocon than do non-INM-directed TMSs. The distinct proximities of translocon components to INM-directed TMSs strongly suggest that such TMSs are recognized and initially sorted within the translocon.

Previous work with the envelope protein ODV-E66 (E66) showed that E66 trafficking to the INM is mediated via an INM sorting signal (Sorting Motif or SM). In this study, using a site-specific crosslinking approach we demonstrate that following ER membrane integration, the SM is adjacent to two viral proteins: FP25K & BV/ODV-E26 (E26). Deletion of FP25K from the viral genome results in the accumulation of E66 at the ONM, suggesting that FP25K may facilitate protein movement at the nuclear pore. While the role of the E66-E26 interaction remains to be determined, these data suggest that E66 trafficking to the INM is a protein-facilitated process. Crosslinking experiments using E66 integration intermediates revealed that during co-translational integration at the ER, the SM is adjacent to two cellular proteins of ~10kDa and ~25kDa, referred to as SMAP 10 (SM associated protein of 10kDa) & SMAP25 respectively. Thus, contrary to the widely accepted “diffusion-retention” model for protein trafficking to the INM, our data indicate that protein sorting to the INM is a multistep process initiated upon membrane integration in which the INM sorting signal sequentially associates with various sorting factors.

DEDICATION

To my father, Late Ramesh Chandra Saksena, who didn't live to read this work, but
without whom this work would not have been possible

and

my mother, Chanda Saksena, who taught me my very first alphabets and whose courage,
strength, dedication, sacrifice and unmitigated endurance
are ideals I can only aspire to in my search for truth and meaning

ACKNOWLEDGEMENTS

I am indebted to my spiritual master, H.D. Swami Prakashanand Saraswati, for teaching me the true goal of my life. His endless love and compassion has had a calming influence during some of the most trying years of my life.

I am ever grateful to my mother, Chanda Saksena, for encouraging me to follow my dreams and exploring my full potential. No matter how bad, stressful or depressing things got in my professional or personal life, I always knew I could count on my mother for support and encouragement. I can't thank my mother enough for allowing me to come to the United States to attend graduate school. This is a true testament of her selfless love, as I know that in her heart she wants me to return home and be with her.

I thank my sister, Shalini Saksena, for being the best sister I could ask for. Throughout my stay in the U.S., she has willingly taken over all my responsibilities back home and I can't thank her enough for doing so. She has been a constant source of support and has always been the one to tell me that I need to settle for nothing but the best.

Good friends play a big role in lifting up one's spirits after a bad day at the office (or at the bench!). I surely have had my share of good friends who were there to support me when the going was tough, and to celebrate my moments of success. Specifically, I would like to thank Drs. Peter Cornish and Abbas Razvi for their friendship and support. I will always remember the fun times we spent together working on homework assignments or cramming for a test.

I am grateful to my true friend, Judit Wahlman, for coming into my life when I needed a supporting colleague and more importantly a friend. She has known me through anger, sadness and bitterness and has witnessed my moments of happiness and pride. I wish nothing but the best for the rest of her graduate work.

I would like to thank my fellow graduate student in the Summers lab, Jared Burks, who made a very significant contribution towards the completion of the last specific aim outlined in this study. His initial observation regarding the putative relation between E26 and SMAP-25, and the antibody generated by him against E26 proved to be key in the identification of SMAP-10. Over the years other members of the Summers lab have generated a number of tools that proved to be extremely critical for the execution of my experiments. I would like to thank Matthew Powers, Rebecca Parr, Hideo Beniya, Shawn Williamson, Tina Heyman, Robert Harrison for generating recombinant viruses, constructs, mutants, antibodies etc. that turned out to be useful for my experiments. I also want to thank Genevieve Ledwell and Virginia Cox for providing me with some of the microsomal membranes (vesicles) that were used in this study. I am thankful to Drs. Qi Ding, Zhenping Zhong, German Rosas-Acosta and Shawn Williamson for their support and friendship during my tenure in the lab.

I would also like to thank everyone in the Johnson lab (past and present) for being such excellent colleagues during my tenure. I would specially like to thank Drs. Ingmarie Nilsson, Andrey Karamyshev, Stephanie Etchells and Peter McCormick for their assistance during the initial stages of my project. I would like to thank Yiwei Miao and Yuanlong Shao who made sure that I had access to all the reagents needed for my

experiments year in and year out. I would also like to thank the student workers in the lab, Ashley Buhring, Lindsey Buhring, and Kristen Pfeiffer for their excellent technical assistance.

I am grateful to Drs. Ry Young, Jim Hu and Sharon Braunagel for serving on my advisory committee and making sure that my project was focused and that I was equal to the task. I am indebted to Dr. Art Johnson for being a good friend, a wonderful collaborator, and for allowing me to use the photocrosslinking technology established in his lab. I would also like to thank Sharon who worked very closely with me on the last part of my project. She not only designed the construct used for chemical crosslinking experiments but also taught me a number of techniques including primer extension, library screening, running 2D-gels and DNA sequencing gels that were instrumental in the identification of SMAP-10. In addition, her critical outlook towards experimental design and data was very helpful.

Finally, I thank my advisor Dr. Max Summers for giving me the freedom to explore many topics related to membrane proteins, protein trafficking and protein sorting. Over the years, he played a very important role in my maturation as a scientist, and in my ability to understand the difference between personal and scientific criticism (however difficult that may be!). He worked tirelessly on my presentation skills and was extremely supportive of my participation in scientific meetings at the departmental and national level. I also need to thank him for excusing my limited (yet growing) knowledge of Virology and for recognizing and understanding that I am a hardcore biochemist.

To conclude, Max and Art, it has been an honor to work with both of you.

TABLE OF CONTENTS

	Page
ABSTRACT.....	iii
DEDICATION.....	v
ACKNOWLEDGEMENTS.....	vi
TABLE OF CONTENTS.....	ix
LIST OF FIGURES.....	xii
CHAPTER	
I INTRODUCTION.....	1
Protein sorting at the ER membrane.....	1
The nuclear envelope and proteins of the	
INM: General features.....	16
Protein targeting to the INM.....	20
Diffusion-retention: Exceptions to the rule?.....	23
Protein transport to the INM: Lessons	
learned from Baculovirus.....	26
Identification of the viral INM sorting motif (SM).....	30
Sorting of E66 to the INM: Possible sites of regulation.....	34
Nucleocytoplasmic transport.....	40
Specific aims.....	51
II MATERIALS AND METHODS.....	54
Constructs used for photocrosslinking experiments.....	54
SM-C construct used for chemical crosslinking experiments.....	64
Primers used for generating different derivatives	
of clone 2.....	67
Preparation of Lys-tRNA ^{amb}	69
Chemical modification of Lys-tRNA ^{amb}	70
Characterization of modified Lys-tRNA ^{amb}	72
Preparation of wheat germ extract.....	73
Sf9 microsomes.....	74
Purification of signal recognition particle and	
canine pancreatic microsomes.....	76
PCR-generated translation intermediates.....	77

CHAPTER	Page
In vitro run-off transcription.....	77
In vitro translations using wheat germ extract.....	77
In vitro translations using rabbit reticulocyte lysate.....	78
Trichloroacetic acid precipitation.....	79
Generation of integration intermediates.....	80
Photoreactions.....	81
Chemical crosslinking.....	82
Purification of crosslinked products using TALON beads.....	82
Alkaline extraction.....	83
High-salt wash.....	83
Immunoprecipitations.....	84
SDS-PAGE electrophoresis.....	85
SDS-PAGE, western transfer and immunoblotting.....	87
cDNA expression library screen.....	87
DNA sequencing.....	89
Primer extension analysis.....	89
III COTRANSLATIONAL INTEGRATION AND INITIAL SORTING AT THE ER TRANSLOCON OF PROTEINS DESTINED FOR THE INM.....	91
Experimental design.....	91
Targeting of the SM to the ER membrane occurs cotranslationally and is SRP-dependent.....	94
Viral SM sequence proximity to translocon proteins.....	97
Mammalian INM TMS proximity to translocon proteins.....	100
Non-INM TMS proximity to translocon proteins.....	104
Nascent chain length-dependence of photocrosslinking.....	106
SM sequence crosslinking to non-translocon proteins.....	108
Membrane association of FP25K and E26.....	112
Not every substrate crosslinks to FP25K and E26.....	115
Discussion.....	117
IV IDENTIFICATION OF ACCESSORY PROTEINS INVOLVED IN THE SORTING OF E66 TO THE INM.....	123

CHAPTER	Page
Experimental design.....	123
The SM sequence is adjacent to two cellular proteins: SMAP-10 & SMAP-25.....	124
BV/ODV-E26 shares epitopes with SMAP-10.....	130
Antibody screening of an Sf9 cDNA expression library using E26 antibody identifies clone 2.....	134
Met ₃₁₀₋₄₅₄ is a translocon-associated protein.....	141
Met ₃₁₀₋₄₅₄ is derived via internal initiation of transcription.....	144
Met ₃₁₀₋₄₅₄ is an isoform of Sf9 importin α	147
Discussion.....	152
V SUMMARY.....	159
REFERENCES.....	168
VITA.....	198

LIST OF FIGURES

FIGURE	Page
1 Translocation across the ER membrane	4
2 Cotranslational translocation of a secretory protein.....	7
3 Posttranslational translocation in eukaryotes	9
4 SecA-mediated posttranslational translocation in eubacteria.....	10
5 X-ray structure of the <i>M. jannaschii</i> SecY complex	13
6 Cross-sectional view of the nuclear envelope showing its three main components.....	17
7 Trafficking of E66 to the INM, microvesicles and the ODV envelope	28
8 Sorting motif (SM) sequences.....	31
9 Comparison of the E66 SM sequence with cellular INM proteins	32
10 Localization of SM mutants	33
11 The specialized translocon model	36
12 The modular translocon model.....	37
13 Possible sites where the INM trafficking of E66 may be regulated.....	41
14 Overview of some major nuclear transport pathways in eukaryotic cells.....	45
15 The nucleoplasmic shuttling of importin α	46
16 Domain structure of importin α	48
17 Modeling of importin α	49
18 Constructs used for photocrosslinking	54
19 Schematic of clone 60	57

FIGURE	Page
20	Design of nurim construct 61
21	SM-C construct 65
22	Features of the SM-C construct..... 65
23	Translocation competence of Sf9 microsomes..... 75
24	Targeting of E66 to the ER membrane is cotranslational and SRP-dependent 96
25	Photocrosslinking of viral INM-directed TMSs to translocon proteins 98
26	Photocrosslinking of E25 TMS 99
27	Photocrosslinking of mammalian INM-directed TMSs to translocon proteins 102
28	Photocrosslinking of Nur1 TMS to translocon proteins..... 103
29	Photocrosslinking of Lep1 to translocon proteins 105
30	Nascent chain length-dependence of E66 photocrosslinking to translocon proteins 107
31	The E66SM crosslinks with FP25K and/or E26 110
32	Nascent chain length-dependence of SM chemical crosslinking to FP25K and E26 111
33	Membrane association of FP25K and E26 113
34	Membrane association of Sec61 α 114
35	FP25K and E26 are selective in their association 116
36	Chemical crosslinking of E66SM to SMAP-10 and SMAP-25 126
37	SMAP-10 crosslinking using different chemical crosslinkers and substrates 127

FIGURE	Page
38 SM sequence is in close proximity to SMAP-10 before and after leaving the translocon.....	129
39 E26 antiserum crossreacts with a ~25kDa cellular protein	130
40 E26 shares epitopes with cellular SMAP-10.....	132
41 Immunoprecipitations using E26 antiserum.....	133
42 Sf9 cDNA expression library screen.....	135
43 Clone 2 identified in the screen using E26 antiserum.....	137
44 Clone 2 derivatives and set up of chemical crosslinking reactions.....	138
45 Crosslinking of clone 2 derivatives.....	140
46 Membrane association of clone 2 derivatives	142
47 Met ₃₁₀₋₄₅₄ is a translocon-associated protein, which is selective in substrate selection	143
48 Primer extension analysis.....	146
49 SMAP-10 is an Sf9 importin α isoform.....	148
50 Immunoprecipitations using antibodies specific for Karyopherin alpha.....	149
51 Homology-based modeling	151
52 Cotranslational sorting of INM-directed TMSs at the ER translocon.....	161
53 Posttranslational sorting of INM-directed TMSs	162
54 SMAP-10 recruitment at the translocon.....	165
55 Translocon-bound SMAP-10 determines the binding site for INM-directed TMSs.....	166

CHAPTER I

INTRODUCTION

Protein sorting at the ER membrane

Nearly all proteins in eukaryotic cells are synthesized by cytosolic ribosomes, but many proteins ultimately perform their functions in other locations such as the various cellular organelles or, in the case of secreted proteins, outside the cell. Eukaryotic cells have developed elaborate mechanisms to ensure the efficient delivery of proteins to their final destinations (Barlowe et al., 2003). This process of delivering proteins to their final destinations is termed protein trafficking or protein sorting, and often involves the translocation of a protein substrate through a membrane bilayer.

A few fundamental principles control the sorting of soluble and membrane proteins in the cell. First, there must be a systematic method to identify the proteins that need to be sorted. This information is encoded in the primary structure of the protein and is referred to as the sorting signal, which contains the sequence and structural features necessary to determine the final intracellular localization of the protein. The sorting signal is often found near the amino-terminus of the protein allowing the sorting process to begin early in the biosynthetic pathway while the nascent protein is still bound to the ribosome (Johnson et al., 1999). Once the information within the sorting signal is decoded, a targeting mechanism is required to deliver each protein substrate to its

This dissertation follows the style and format of Cell.

final cellular destination or, in the case of membrane proteins, to the appropriate cellular membrane. The targeting process often involves specialized molecules in the cytoplasm, and unique receptors on the cytoplasmic side of the membrane to ensure accurate delivery of substrates.

The focus of this dissertation is the sorting of inner nuclear membrane (INM)-directed proteins at the endoplasmic reticulum (ER) membrane. Proteins destined to reside in the ER, Golgi, nuclear envelope (outer and inner nuclear membrane) and other organelles, as well as secretory proteins are directed first to the ER membrane. The first part of this chapter focuses on the fundamental principles of protein translocation across and protein integration into the membrane of the ER.

Targeting of proteins to the ER translocation site. In mammalian cells, ribosomes are found in the cytoplasm and at the membrane of the ER. These two classes of ribosomes differ in the nature of their translation products, with membrane-bound ribosomes engaged in the synthesis of secretory and membrane proteins. Membrane-bound ribosomes are identified by the presence of a nascent chain that contains a signal sequence at the N-terminus (Fig. 1). As the signal sequence emerges from the ribosome, it is recognized and bound by a ribonucleoprotein termed the signal recognition particle (SRP) (reviewed in Walter & Johnson, 1994). The binding of SRP induces a slowing or temporary halting of the protein-chain elongation process, and the “elongation-arrested complex” diffuses to the ER membrane. The ER targeting of the SRP-ribosome complex involves a specific interaction between SRP and SRP receptor (SR). The GTP-dependent interaction between SRP and its receptor initiates a series of events which includes the

binding of the ribosome-nascent chain complex to the translocation and integration machinery (translocon) at the ER membrane, release of the signal sequence from SRP, release of SRP and SRP receptor from the translocon, and resumption of peptide chain (translational) elongation by the ribosome, now engaged with the translocon (Fig. 1).

The Sec61/SecY complex. In every membrane, a complex of polypeptides associate together to form a protein-conducting channel (referred to as the 'translocon') that mediates protein translocation across the membrane. The proteins that form the translocation channel in the membrane of the ER were identified using an elegant approach that involved the cotranslational incorporation of photoreactive probes within the nascent chain (in the process of translocation or membrane integration). The photoreactive probes directly reported the proteinaceous environment of the substrate, and thus allowed the specific identification of ER membrane proteins that were adjacent to the nascent chain throughout its translocation or during its integration (Krieg et al., 1989; Wiedmann et al., 1989; High et al., 1991; Thrift et al., 1991). The information obtained from the photocrosslinking experiments was then used by several groups to purify the translocon proteins that crosslinked to the nascent chain, reconstitute them into proteoliposomes and demonstrate that they were successful in carrying out protein translocation and integration (Nicchitta & Blobel, 1990; Gorlich et al., 1992a,b; Gorlich & Rapoport, 1993). Using this approach, two protein components of the mammalian translocon were identified. The first component, the translocating chain-associated membrane protein (TRAM) (Gorlich et al., 1992a), was found to be essential for the translocation or integration of most, but not all, proteins (Gorlich & Rapoport, 1993;

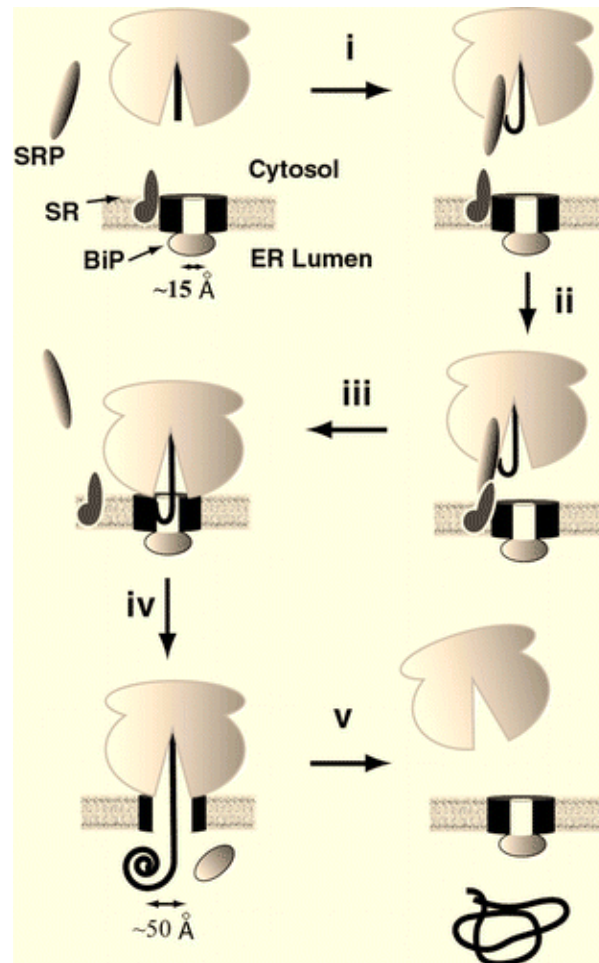


Figure 1. Translocation across the ER membrane. The ribosome-free translocon pore has an internal diameter of 9-15Å, and as shown in the figure is sealed at the luminal end directly or indirectly by the luminal chaperone BiP. Once the signal sequence emerges from the ribosome, it is bound by SRP resulting in the formation of an SRP-RNC (ribosome nascent chain) complex (i) that diffuses in the cytosol. The SRP-RNC complex is targeted to the membrane of the ER via an interaction between SRP and the SRP receptor (ii). The interaction results in ribosome binding to the translocon pore and the insertion of the nascent chain into the translocation channel. Fluorescence studies have revealed that following targeting to the ER membrane, the nascent chain initially remains in an aqueous environment inaccessible to either the cytoplasm or the ER lumen (iv). When the nascent chain reaches ~70 residues in length, BiP is released allowing translocation of the nascent chain into the ER lumen (iv). Following termination of translation, the secretory protein is released into the ER lumen, BiP seals the luminal end of the translocon pore and the ribosome is released into the cytosol (v). “Reprinted with permission from the *Annual Review of Cell and Developmental Biology*, Volume 15© 1999 by Annual Reviews www.annualreviews.org”

Oliver et al., 1995; Voigt et al., 1996). The second component identified using this approach was designated Sec61 α (Gorlich et al., 1992b) based on its homology with the yeast protein, Sec61p. Genetic screens for secretion mutants had previously identified and thus implicated Sec61p in the translocation process (Deshaies & Schekman, 1987; Stirling et al., 1992). Sec61 α was found to purify in a heterotrimeric complex with two other polypeptides termed, Sec61 β and Sec61 γ (Gorlich & Rapoport, 1993). Thus, the reconstitution experiments allowed the identification of the core components of the translocon, which include the heterotrimeric Sec61 complex and TRAM.

Identification of the core components of the mammalian translocon raised two important issues. First, which translocon component lines the protein-conducting channel? Second, what is the driving force for protein translocation at the ER membrane? Photocrosslinking experiments revealed that substrates with probes at different positions predicted to be within the membrane could be crosslinked to the α subunit of the Sec61 complex (High et al., 1993; Mothes et al., 1994), but not to other membrane proteins. Since, the α subunit was the primary crosslinking target within the pore, the photocrosslinking experiments suggested that the walls of the channel are formed by the α -helices of Sec61 α . This result was consistent with the observation that some of the Sec61 α transmembrane segments have limited hydrophobicity (Wilkinson et al., 1996).

Translocon-associated partners power the translocation process, and depending on the partner, the channel can function in three different translocation modes. During cotranslational translocation, the ribosome serves as the major channel partner.

Following SRP-mediated targeting to the ER membrane, the signal sequence is released from SRP and the ribosome-nascent chain complex binds to the protein-conducting channel formed by the heterotrimeric Sec61 complex (Fig. 2). Once docked at the translocon, the ribosome resumes protein synthesis, and the energy of translation (GTP hydrolysis) powers the movement of the nascent polypeptide chain into the translocation channel.

Both eukaryotes and yeast have a second mode of translocation at the ER membrane, in which substrate translocation is initiated following the termination of translation (posttranslational translocation). Proteins that use this mode generally have a signal sequence whose hydrophobicity is not sufficient to elicit an interaction with cytoplasmic SRP (Ng et al., 1996). Posttranslational translocation has been reconstituted in proteoliposomes containing Sec61p, Sbh1p and Sss1p (the yeast homologs of Sec61 α , Sec61 β , and Sec61 γ), in addition to the tetrameric Sec62/63 complex and the luminal chaperone BiP (Panzner et al., 1995; Rapoport et al., 1996). In yeast, the tetrameric Sec62/63 complex contains two essential proteins Sec62p and Sec63p, and two nonessential components Sec71p and Sec72p. Mammalian cells lack the proteins Sec71p and Sec72p but contain Sec62p and Sec63p (Meyer et al., 2000; Tyedmers et al., 2000).

Photocrosslinking experiments have revealed that the protein-conducting channel in the posttranslational translocon is formed, at least in part, by Sec61p (Musch et al., 1992; Sanders et al., 1992) and the other four membrane proteins have been suggested to be involved in other pathway-specific roles (Rapoport et al., 1996).

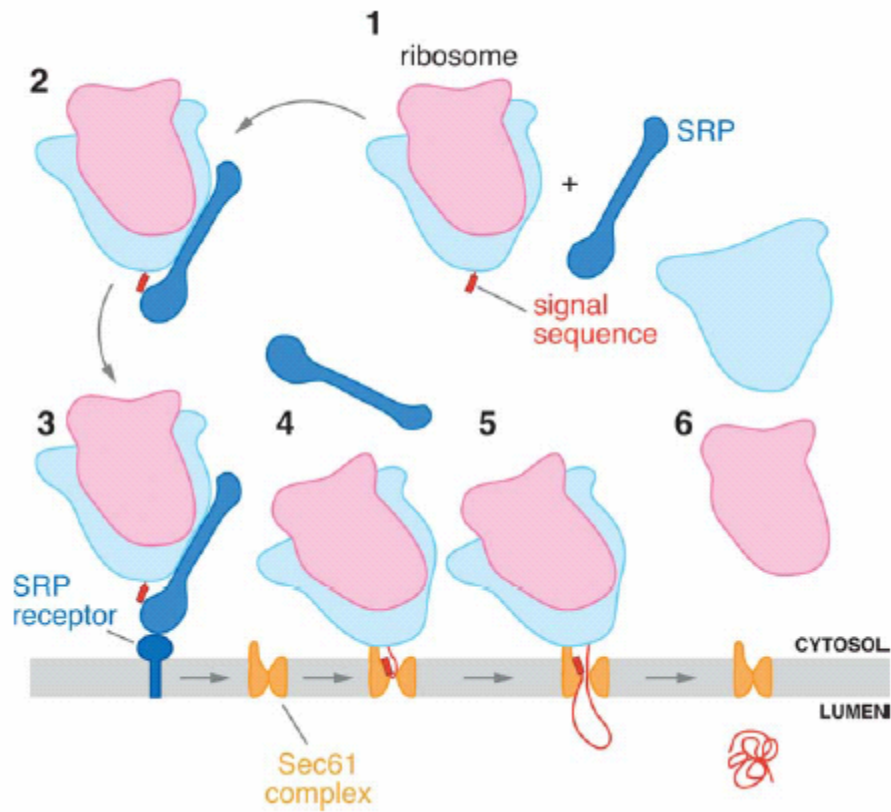


Figure 2. Cotranslational translocation of a secretory protein. (1-2) During the course of secretory protein synthesis, as the signal sequence emerges from the ribosome, it is bound by cytosolic SRP that also makes contacts with the ribosome (large subunit, *light blue*; small subunit, *pink*). The binding of SRP induces a temporary translational-elongation arrest and the SRP-RNC complex diffuses in the cytosol. The targeting of the SRP-RNC complex to the ER membrane is achieved via an interaction between SRP and SRP receptor (3). The interaction results in a series of events at the ER membrane, including release of SRP from the signal sequence, and the docking of the RNC complex at the translocon pore (4). The release of SRP relieves the elongation arrest, and the energy of translation drives the cotranslational translocation of the nascent chain into the lumen of the ER (5). Following termination of translation, the secretory protein is released into the ER lumen and the ribosome is released into the cytosol. “Reprinted with permission from the *Annual Review of Cell and Developmental Biology*, Volume 21© 2005 by Annual Reviews www.annualreviews.org”

Soluble Kar2p, the yeast homolog of mammalian BiP, is a member of the Hsp70 family that is localized at the posttranslational translocon via interactions with the J-domain of Sec63p (Brodsky & Schekman, 1993; Corsi & Schekman, 1997). A ratcheting mechanism is thought to provide the driving force for posttranslational translocation (Matlack et al., 1999). In this model, the interaction of ATP-bound BiP with the J-domain of Sec63p results in rapid ATP hydrolysis and the closure of the peptide binding cleft around the incoming polypeptide chain (Fig. 3), which prevents “back-sliding” and results in forward translocation. Once the polypeptide has moved a sufficient distance into the ER lumen, another BiP molecule binds to it, and this process is repeated until the polypeptide chain has completely traversed the channel. The exchange of ADP for ATP results in an opening of the peptide-binding pocket and the release of BiP from the polypeptide chain.

The third mode of translocation that is used by most secretory proteins in eubacteria occurs posttranslationally (reviewed in Mori & Ito, 2001), and is thought to involve the cytosolic ATPase, SecA. In this model, cytosolic SecA binds a polypeptide substrate with an N-terminal signal sequence, and the complex is targeted to the bacterial inner membrane via interactions between SecA and the translocon component, SecY (bacterial homolog of Sec61 α) Fig. 4). Following targeting, the polypeptide substrate inserts as a loop into the channel. The SecA polypeptide-binding groove opens, moves away from the channel, binds to the next section of the polypeptide chain and closes around it. The polypeptide-binding groove again moves towards the channel and pushes the polypeptide segment into the channel. These steps are repeated until the polypeptide

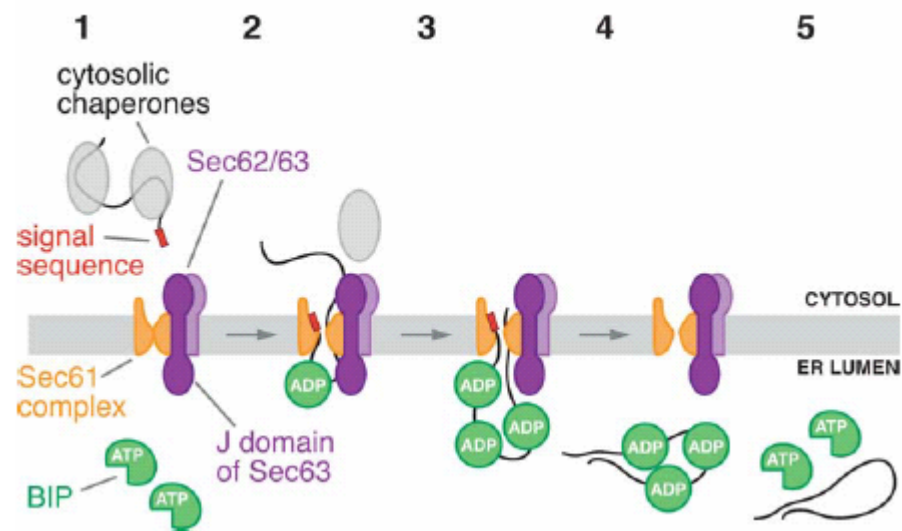


Figure 3. Posttranslational translocation in eukaryotes. (1) After synthesis in the cytosol, a posttranslational translocation substrate is kept in an unfolded, translocation-competent state by interactions with cytosolic chaperones. (2) The chaperone-bound substrate is targeted to the posttranslational translocon, comprised of the Sec61 complex, and the Sec62/63 complex via its signal sequence. The J-domain of Sec63 stimulates ATP hydrolysis by BiP, and the BiP-ADP complex binds to the polypeptide chain emerging into the ER lumen. (3) As the polypeptide enters the ER lumen, another BiP molecule can bind to it, resulting in forward translocation (pulling). (4) This process is repeated until the polypeptide chain has completely traversed the channel. (5) The exchange of ADP for ATP results in an opening of the peptide-binding pocket and the release of BiP from the polypeptide chain. “Reprinted with permission from the *Annual Review of Cell and Developmental Biology*, Volume 21© 2005 by Annual Reviews www.annualreviews.org”

chain is fully translocated across the membrane (Economou & Wickner, 1994).

Although the current data suggests that SecA-mediated translocation is processive (Joly & Wickner, 1993; Schiebel et al., 1991), a nonprocessive mechanism that involves the occasional disengagement of SecA cannot be ruled out.

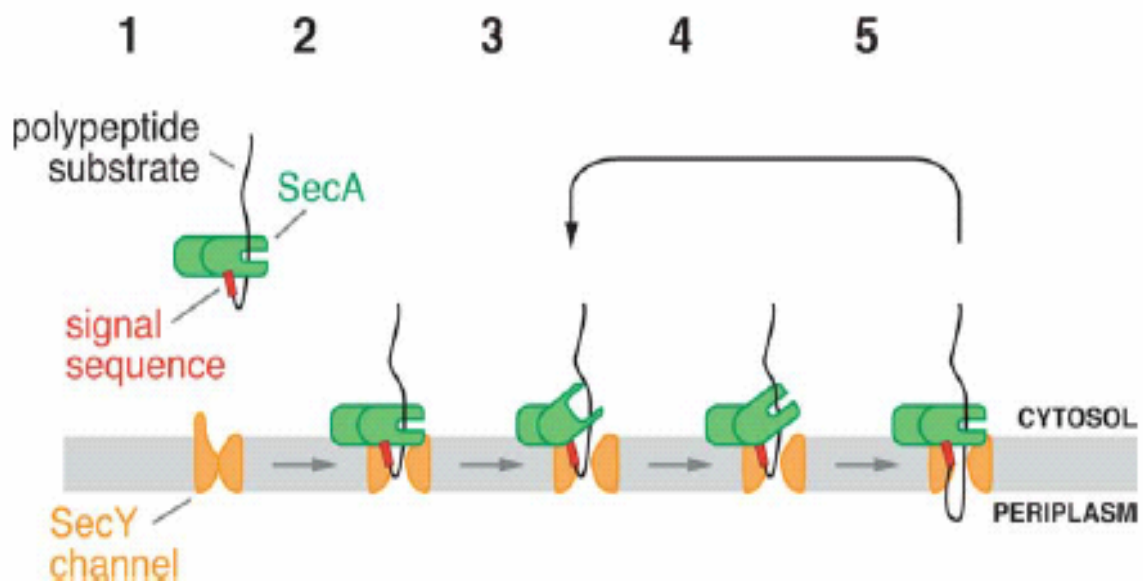


Figure 4. SecA-mediated posttranslational translocation in eubacteria. (1) Cytosolic SecA binds to a polypeptide substrate bearing an N-terminal signal sequence, and the complex is targeted to the SecY translocon (2). Following targeting to the translocon, the polypeptide-binding groove in SecA opens, moves away from the channel (3), and binds to the next section of the incoming polypeptide chain (4). The polypeptide-binding domains move towards the channel, pushing the polypeptide segment into the SecY channel (5). Steps (3)-(5) are repeated until the polypeptide chain is fully translocated across the membrane (not shown). “Reprinted with permission from the *Annual Review of Cell and Developmental Biology*, Volume 21© 2005 by Annual Reviews www.annualreviews.org”

Translocon composition and structure. The largest subunit of the heterotrimeric Sec61/SecY complex is the α -subunit, termed Sec61 α in mammals, Sec61p in *Saccharomyces cerevisiae*, and SecY in eubacteria and archaea (reviewed in Rapoport et al., 1996). The α -subunit has ten membrane-spanning domains and orients in the membrane with its N- and C-termini in the cytosol. The β -subunit is termed Sec61 β in mammals, Sbh1p in *S. cerevisiae*, SecG in eubacteria and Sec β in archaea. The γ -subunit is termed Sec61 γ in mammals, Sss1p in *S. cerevisiae*, and SecE in eubacteria and archaea.

Fluorescence lifetimes and collisional quenching studies have revealed that the protein-conducting channel has a hydrophilic interior (Crowley et al., 1994) that spans the entire membrane. The translocon pore is flexible, as indicated by its ability to translocate proteins containing bulky chemical moieties linked to amino acid side chains (Kurzchalia et al., 1988) or a disulfide-bonded peptide loop of 13 residues in a secretory protein (Tani et al., 1990). During the integration of membrane proteins, the channel allows lateral movement (partitioning) of the TMSs from the aqueous pore into the hydrophobic lipid bilayer. The ability of the protein-conducting channel to open in two directions, across the membrane (for forward translocation) and laterally within the membrane (for lateral exit of transmembrane segments) is not seen in other membrane channels.

The first image (view) of the channel came from freeze-fracture electron microscopy (EM) and subsequent cryo-EM studies of proteoliposomes reconstituted from purified and ribosome-associated Sec61 complexes. The translocon appeared to be an irregular

ovoid disc $\sim 100\text{\AA}$ wide and $50\text{-}60\text{\AA}$ high with an extensive luminal projection and a large central pore (Hanein et al., 1996; Menetret et al., 2000; Beckmann et al., 2001; Morgan et al., 2002). The size of the protein-conducting pore was consistent with the estimates derived from fluorescence-quenching studies (Hamman et al., 1997), and suggested that the translocon is formed from either three or four copies of the Sec61/SecY complex. Freeze fracture EM of the reconstituted proteoliposomes also revealed that the assembly of the Sec61- oligomeric structures is a regulated process. For instance, the number of oligomeric structures observed were higher when ribosomes were bound or when the Sec62/63 complex was co-reconstituted with Sec61 (Hanein et al., 1996), indicating that the binding of channel partners induces the formation of Sec61 oligomers.

A recent high-resolution (3.2\AA) structure of the SecY complex from the archaea, *Methanococcus jannaschii* revealed a $45\text{-}50\text{\AA}$ cuboidal structure with a central $5\text{-}8\text{\AA}$ pore (van den Berg et al., 2004). The α - subunit consists of two domains, TM1-5 (shaded blue in Fig. 5) and TM6-10 (shaded red in Fig. 5) that are clamped together by the essential γ -subunit which extends one TMS across the interface of the two domains and has an N-terminal amphipathic helix that lies flat on the surface of the cytoplasmic face of the membrane. The β -subunit contains a single TMS and makes limited contact with the α - subunit, which is consistent with its being non-essential.

The ten helices of the α - subunit surround a large water-filled cavity that has the shape of a funnel. The cavity is open on the cytoplasmic side and extends halfway across the plane of the membrane. The helices on the extracellular side of the membrane form a

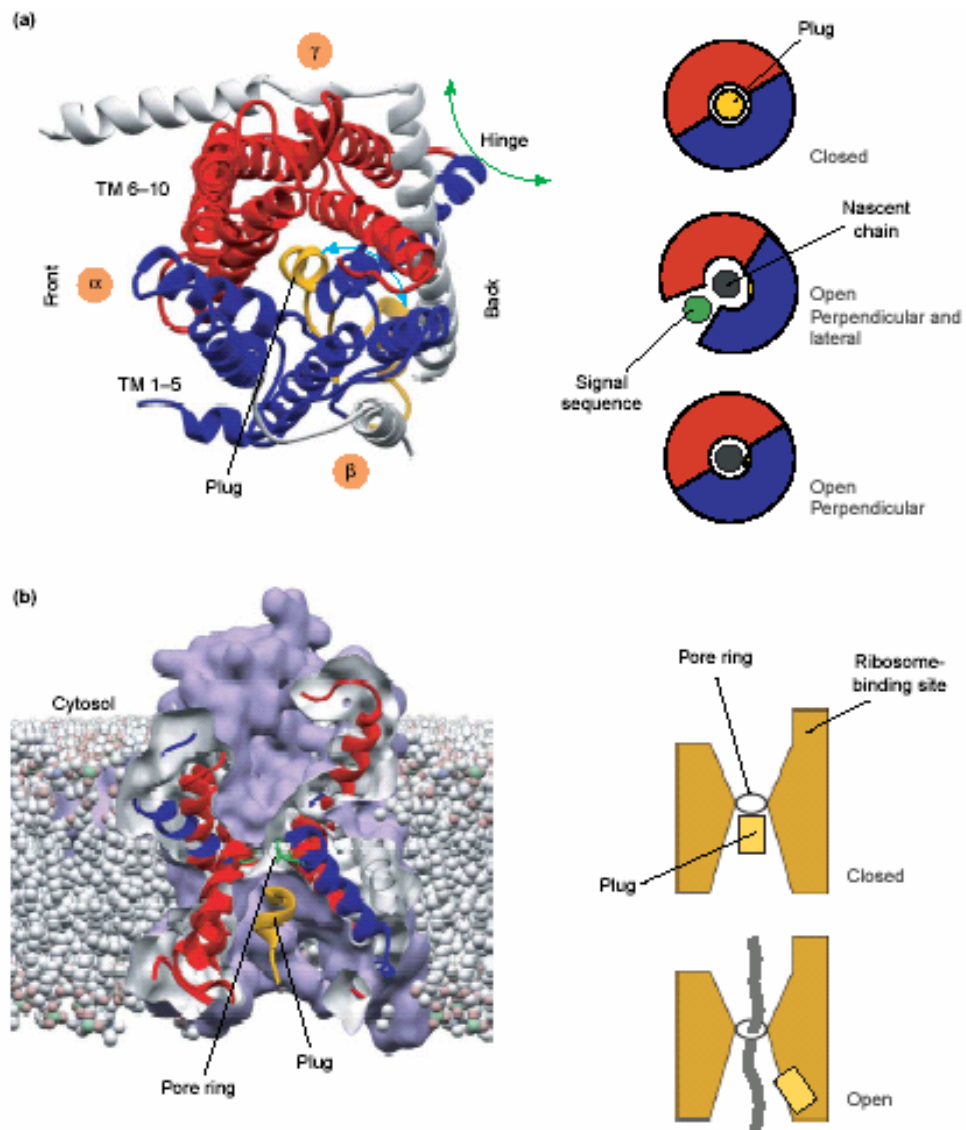


Figure 5. X-ray structure of the *M. jannaschii* SecY complex. (a) A view of the SecY complex from the cytoplasm. The two domains of the α subunit, the N-terminal domain (TM1-5) and the C-terminal domain (TM6-10) are depicted in blue and red respectively. The translocon pore is shown in its gated/closed state via the action of the 'plug' (TM2a), depicted in yellow. The β and γ subunits of the complex are depicted in white. (b) The interior of the translocon pore as revealed by slicing through the middle of the SecY complex. "Reprinted from Trends in Cell Biology, 14, Rapoport et al., Membrane protein integration and the role of the translocation channel, Page: 570, © 2005, with permission from Elsevier".

similar cavity, with the two cavities meeting in the center of the structure to form an “hourglass” structure (Fig. 5). A ring of six hydrophobic residues (mostly isoleucines) forms the constriction in the center of the membrane bilayer where the two aqueous (funnel-shaped) cavities meet. An additional short helix on the extracellular side that extends halfway through the membrane has been termed as the ‘plug’, which fills the center of the cavity. Upon engagement of the translocon by binding of both a ribosome and a signal sequence (or a TMS), the plug probably moves into a cavity on the extracellular side of the channel, resulting in pore opening (illustrated in Fig. 5B). This idea of pore opening as a result of plug movement is consistent with crosslinking experiments showing that residues in the plug helix can be crosslinked to the γ -subunit (Harris et al., 1999).

Based on the crystal structure of the substrate-free archeal SecYE β complex (Fig. 5), van den Berg et al. (2004) proposed that the translocon contains only a single heterotrimer. In addition, the authors also proposed that the pore residues could fit like a gasket around the translocating polypeptide and thus function in maintaining the membrane permeability barrier during cotranslational translocation. This model is different from the proposals derived from fluorescence studies in which the ribosome on the cytoplasmic side of the membrane, and BiP on the luminal side of the membrane maintain the permeability barrier during cotranslational translocation. (Crowley et al., 1994; Hamman et al., 1998).

One possible explanation of this discrepancy as outlined by Woolhead et al. (2004), is that in the absence of a preprotein substrate, the archeal SecYE β complex crystallizes

in a closed monomeric conformation. Also, since the crystal structure was resolved using detergent-purified SecYE β complex, it is possible that the purified complex lacks other translocon-associated proteins that are an integral part of the active translocon structure. Hence, the structure obtained by van den Berg et al. (2004) may reflect the conformation of an individual SecY (mammalian Sec61 α) complex prior to its association with other proteins, such as TRAM, TRAP, OST, Signal Peptidase (SP) etc. (discussed below) to form a translocation-competent, multimeric translocon.

Although the core translocation machinery consists of only Sec61 $\alpha\beta\gamma$, SRP and SR (Gorlich & Rapoport, 1993), fluorescence resonance energy transfer (FRET) studies aimed at probing the relative proximities of endogenously expressed translocon components in cells have shown that functional translocons contain multiple Sec61 heterotrimers and other translocon-associated proteins (Snapp et al., 2004). The translocon-associated proteins include the signal peptidase (SP), responsible for removing the signal sequence; the oligosaccharyl transferase (OST) complex, responsible for protein glycosylation; TRAM, involved in facilitating translocation (Gorlich et al., 1992; Gorlich & Rapoport, 1993; Hegde et al., 1998b), formation of the ribosome-translocon junction (Voigt et al., 1996; Hegde et al., 1998a,c) and membrane integration of TMSs (High et al., 1993; Martoglio et al., 1995; Do et al., 1996); and the translocon-associated protein (TRAP), which influences nascent chain orientation and facilitates initiation of post-targeting translocation (Fons et al., 2003).

The nuclear envelope and proteins of the INM: General features

In eukaryotic cells, the nucleus is separated from the cytoplasm by the nuclear envelope (NE). The NE is composed of three parts: the nuclear lamina, the nuclear pore complexes and the nuclear membranes (inner, outer and pore) (Fig. 6). The inner and outer membranes are separated by a narrow lumen (perinuclear space) and join periodically at the pore membrane where nuclear pore complexes (NPCs) are inserted. NPCs are large proteinaceous structures spanning the outer and inner nuclear membrane to form aqueous, gated channels that allow diffusion of small molecules and ions and the active transport of macromolecules.

The outer nuclear membrane (ONM) is directly continuous with and similar in composition to the endoplasmic reticulum (ER) membrane, whereas the nuclear lamina is linked to the inner nuclear membrane (INM) by integral proteins. The lamina is a fibrous meshwork of intermediate filament proteins called lamins (types A and B) that polymerize to form 10nm-diameter filaments (Aebi et al., 1986; Fisher et al., 1986; McKeon et al., 1986). Chromatin, the lamina, NPCs and proteins of the INM form a network of interactions responsible for nuclear and NE stability.

Although a recent proteomics analysis suggests that as many as eighty transmembrane proteins are localized to the INM (Schirmer et al., 2003), only a few have been characterized in detail. These proteins include the lamin B receptor (LBR), the lamina-associated polypeptide-1 (LAP1), the lamina-associated polypeptide-2 (LAP2), emerin, MAN1 (reviewed in Worman & Courvalin, 2000), Luma (Dreger et al., 2001),

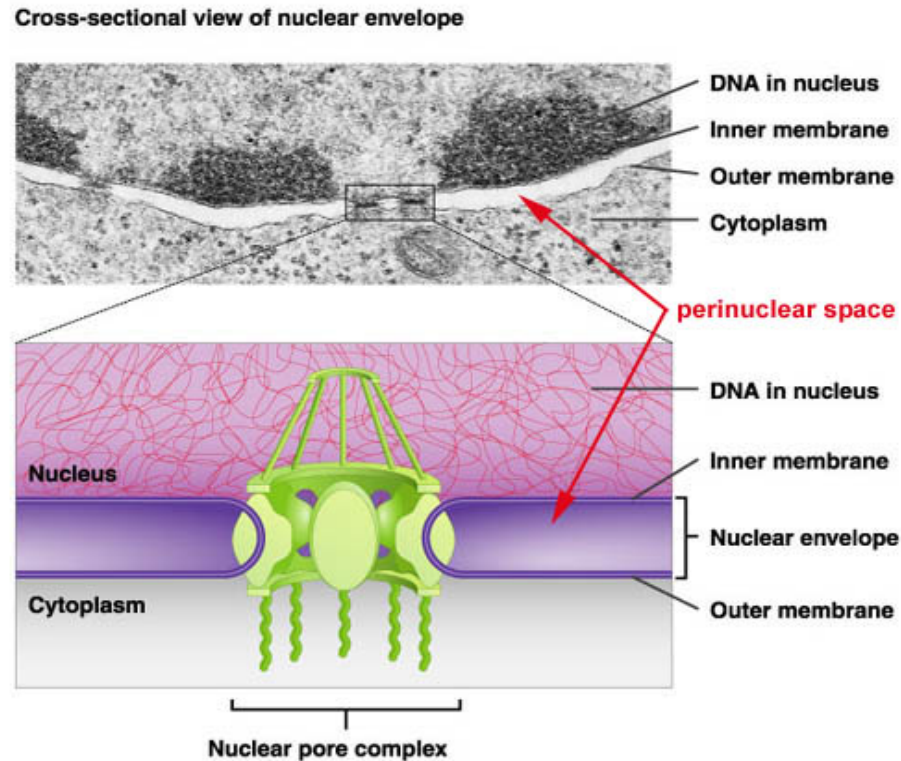


Figure 6. Cross-sectional view of the nuclear envelope showing its three main components. This figure was downloaded from the University of Miami website.

UNC-84 (Malone et al., 1999; Lee et al., 2002), and nesprins (Zhang, 2001). Other proteins including the IP_3/IP_4 receptors (reviewed in Rogue & Malviya, 1999), and the multifunctional protein Ire1 (Sidrauski & Walter, 1997) are also thought to localize in the INM, although definitive morphological evidence supporting an exclusively inner membrane localization of these proteins is lacking.

The common feature found in all these INM proteins is direct or indirect attachment to nuclear structures, such as the underlying nuclear lamina and/or chromatin, as

indicated by either resistance to detergent extraction or slow fluorescence recovery after photobleaching (FRAP) (Ellenberg et al., 1997; Rolls et al., 1999; Dreger et al., 2001).

The only sequence or structural features shared by the proteins of the INM is an N-terminal nucleoplasmic domain of >200 amino acids found in LBR, LAP1 and 2, MAN1 and emerin, and a short stretch of sequence similarity within this domain in LAP2, emerin and MAN1 {LEM domain} (Laguri et al., 2001). Finally, four INM proteins (LAP1, LAP2, MAN1 and emerin) possess coiled-coil motifs (Martin et al., 1995), which may be involved in formation of homo- or hetero- oligomeric structures in vivo.

A recent revolution occurred in the field of muscle pathophysiology when mutations in nuclear envelope proteins were shown to cause muscular dystrophy and cardiomyopathy (Worman & Courvalin, 2005; Gruenbaum et al., 2003; Bione et al., 1994; Bonne et al., 1999). Human LBR (615 residues) has an amino-terminal nucleoplasmic domain of ~210 amino acids and a hydrophobic domain consisting of eight membrane spanning segments. The hydrophobic domain of LBR exhibits high sequence similarity to sterol reductases in yeast, plants and mammals (Holmer et al., 1998; Schuler et al., 1994). Mutations in LBR cause Pelger-Huet anomaly, an autosomal dominantly inherited condition characterized by incomplete segmentation of granulocyte nuclei (Hoffmann et al., 2002). A homozygous LBR mutation was also found in a case of HEM/Greenberg skeletal dysplasia (Waterham et al., 2003). Patients suffering from this ailment exhibit skeletal dysplasia, short-limbed dwarfism, and notable bone calcification and cartilage disorganization. Cultured skin fibroblasts derived from these patients also exhibit elevated levels of cholesterol precursors, consistent with the

deficiency of the cholesterol biosynthetic enzyme 3- β -hydroxysterol delta (14)-reductase (Waterham et al, 2003). Thus most of the clinical manifestations of mutations in LBR are consistent with its known associations with nuclear structures such as lamins, chromatin, and its sequence similarity with sterol reductases.

Loss of function mutations in MAN1 have been implicated in a number of diseases including Osteopoikilosis (skeletal dysplasia), Buschke-Ollendorff syndrome, and Melorheostosis (muscle atrophy and skin lesions) (Hellemans et al., 2004). Similarly, mutations in the gene coding for emerin have been implicated in an X-linked form of muscular dystrophy characterized by a slow and progressive wasting of the muscles, and cardiomyopathy termed Emery-Dreifuss muscular dystrophy (Bione et al., 1994).

Although, the pathophysiological mechanisms of how mutations in proteins of the INM cause different diseases remains unknown, two hypotheses have been proposed (as reviewed in Muchir & Worman, 2004). According to the “mechanical stress” hypothesis, abnormalities in nuclear structure (either due to mutations in INM proteins or lamins) lead to increased susceptibility to cellular damage by physical strain. The “gene expression” hypothesis on the other hand is based on the interaction between the nuclear envelope and chromatin. Genetic and cell biological experiments have suggested that the coupling of chromatin domains to the nuclear envelope results in their transcriptional inactivation (Andrulis et al., 1998), implying that the INM serves to concentrate transcriptional silencers or chromatin-remodelling factors. Thus, the “gene expression” model proposes that mutations in lamins and associated proteins alter the interaction

between chromatin and the nuclear envelope, which regulates tissue-specific gene expression.

Protein targeting to the INM

The use of highly sensitive protein-imaging and detection methods has greatly enhanced our understanding of nuclear envelope dynamics (envelope disassembly and assembly) during the cell cycle (Ellenberg et al., 1997; Lee et al., 2000; Lenart & Ellenberg, 2003). However, interphase protein sorting to the INM poses a unique challenge since proteins of the INM are immobilized at their final destination, making intermediates in the trafficking pathway difficult to discern or visualize. Despite these challenges, a number of groups have used a range of innovative approaches to define the important features of the pathway (discussed below).

Although the physio-chemical properties of the nuclear membranes have not been directly determined, studies using intact nuclei and nuclei lacking large pieces of the ONM have suggested that the inner and outer membranes have essentially the same lipid mobility and lipid composition (Schindler et al., 1985). In addition, a structural relatedness between the NE and the ER membrane has been suggested by observations that NE assembly in *Xenopus* extracts involves ‘rough’ vesicles and tubular intermediates, which bear morphological resemblance to the ER cisternae (Wiese et al., 1997; Dreier & Rapoport, 2000). These observations suggest that the NE can be thought of as a specialized domain of the ER.

Integral membrane proteins of the INM can diffuse freely between the ER and the interconnected inner, pore and outer nuclear membranes (Ellenberg et al., 1997; Ostlund

et al., 1999). Although, the ER and the NE represent a continuum, the proteins of the INM and the pore membrane do not 'leak' to the ONM or the peripheral ER and remain stably localized in the corresponding territories (reviewed in Gant & Wilson, 1997). This is believed to be a result of the difference in mobility of the INM proteins localized in the ER versus the INM. FRAP studies on the well-characterized INM proteins such as LBR, emerin and MAN1 have shown that these proteins freely diffuse laterally in the ER membrane, where they are synthesized (Ellenberg et al., 1997; Ostlund et al., 1999; Wu et al., 2002). However, their diffusional mobilities are significantly reduced in the INM. Protein retention at the INM is believed to be the result of protein-protein interactions either between the nucleoplasmic domains of these proteins and other nuclear structures (chromatin, lamins etc.) or between transmembrane segments in the plane of the membrane. Consistent with this notion, the major nuclear envelope targeting domain of most INM proteins has been found to contain lamin- and/or chromatin- binding determinants. For example, the nucleoplasmic domain of the well-characterized INM protein, lamin B receptor (LBR), which confers INM retention (Soullam & Worman, 1993, 1995; Ellenberg et al., 1997), binds to B-type lamins (Worman et al., 1988; Ye & Worman, 1994), DNA (Ye & Worman, 1994), chromatin (Pyrpasopoulou et al., 1996) and HP-1, a chromatin-binding protein (Ye and Worman, 1996). The transmembrane domain of LBR (Smith & Blobel, 1993) and nurim (Rolls et al., 1999) are also involved in INM retention possibly via interactions with transmembrane segments of other resident proteins. As seen with LBR, the major nuclear envelope targeting domain of LAP2 contains a lamin-binding site (Furukawa et al., 1998).

The results of a number of studies are consistent with a “diffusion-retention” model for the targeting of integral membrane proteins to the INM (Worman & Courvalin, 2000). The model proposes that proteins synthesized on the rough ER with cytoplasmic domains less than ~60kDa appear to travel through the continuous outer nuclear membrane and enter into the INM by diffusion through the pore membrane. It is believed that once the proteins arrive at the INM, they are retained there by binding to nuclear ligands or via interactions with the transmembrane segments of other resident proteins. Integral membrane proteins with cytoplasmic domains in excess of 60kDa are excluded from the INM because of steric constraints imposed by the lateral channels of the nuclear pore complexes. On the other hand, integral proteins with nucleocytoplasmic domains less than 60kDa that do not bind to nuclear ligands (lamins, chromatin), cytoplasmic structures or endoplasmic reticulum proteins such as the KDEL receptor (involved in protein retention at the ER) ultimately enter the secretory pathway.

In support of this model, most integral membrane proteins of the INM have nucleoplasmic domains less than 60kDa, consistent with the size constraints imposed by the 10nm lateral channels of the nuclear pore complex (Hinshaw et al., 1992) and FRAP analysis shows that INM proteins are freely mobile in the ER membrane and immobilized at the INM (Ellenberg et al., 1997; Ostlund et al., 1999; Wu et al., 2002). An alternate mechanism to explain the transit of integral proteins to the INM involves periodic fusion of the INM and ONM to provide transient connections to allow diffusional exchange of protein between the two membranes. However, a recent study demonstrated that protein accumulation at the INM is inhibited by antibodies specific for

the nuclear pore protein, gp210, and to a significant, albeit lesser, degree by the lectin WGA that is known to block the central channel of the nuclear pore complex (Ohba et al., 2004). The results of Ohba et al. (2004) indicate that the antibodies and lectin act by sterically occluding protein movement to the INM. Although the authors note the possibility that the antibodies and the lectin could induce conformational changes in the NPC, which indirectly affect protein channels that allow integral proteins to pass around the pore membrane, these data provide strong evidence that as proposed by the “diffusion-retention” model, the nuclear pore membrane is the conduit for movement of integral membrane proteins from the ONM to the INM. In the same report the authors also reported that the movement of a reporter protein to the INM was completely inhibited by ATP depletion, and also by cooling cells to 20°C. Although these results suggested that membrane-fusion may be involved in the movement of integral membrane proteins to the INM, pretreatment of cells with inhibitors of vesicular trafficking that block fusion between cytosolic membrane surfaces was found to have no significant effect on reporter movement to the INM. These data argue against the membrane fusion model and strongly suggest that the nuclear pore membrane is involved in protein transport to the INM.

Diffusion-retention: Exceptions to the rule?

Although the results of many studies are consistent with the “diffusion-retention” model (described above), a number of observations suggest that protein transport to the INM may be regulated by something more complex than passive diffusion and retention.

The model predicts that specific interactions with other proteins or chromatin result in protein immobilization at the NPC or the INM, respectively. Consequently, one would expect pore membrane proteins lacking their protein-interaction domain to diffuse in the ER and ultimately enter the secretory pathway. However, POM121 [1-129]-GFP which lacks signal(s) for targeting to the NPC, was found to distribute exclusively in the ER-nuclear membrane system and was absent from the Golgi, annulate lamellae (AL) or plasma membrane (Imreh et al., 2003). Using experiments blocking retrograde vesicular transport from the Golgi to the ER as well as fluorescence loss in photobleaching (FLIP) experiments, the authors also demonstrated that POM121 [1-129]-GFP was strictly restricted to the ER.

Studies on proteins of the INM and pore membrane, which were unable to target to their proper location either due to excessive overexpression or deletion of their targeting/retention domain(s), have shown that the majority of proteins including LBR (Smith & Blobel, 1993; Soullam & Worman, 1993; Soullam & Worman, 1995; Ellenberg et al., 1997), LAP2 (Furukawa et al., 1995), MAN1 (Lin et al., 2000), and nurim (Rolls et al., 1999) distributed in the ER. The only exception was emerin, which, when overexpressed, distributed in the INM, ER and the plasma membrane (Ostlund et al., 1999). These results suggest the existence of a regulatory mechanism that prevents even excess INM proteins from entering the secretory pathway.

If protein movement from the ER to the interconnected nuclear membranes was governed by simple diffusion alone as proposed by the “diffusion-retention” model, one would predict INM localization of a substrate (of interest) to be independent of any other

protein(s) or putative interacting partner(s). However, a recent report by Murthi et al (2005) shows that YIL090W/Ice2p, an integral membrane protein located in the ER, is necessary for efficient tethering of Trm1p-II-GFP (tRNA specific m²G methyltransferase) to the INM. *YIL090W*Δ was identified in a genome-wide deletion study as being synthetically lethal with *kar3*Δ (Tong et al., 2004), and Kar3p is known to be required for nuclear fusion during mating (Rose et al., 1996). However, YIL090W was recently identified as Ice2p, an integral membrane protein with eight transmembrane domains. GFP-tagged versions of YIL090W reside in the ER rather than the INM, and play an important role in the structure of the cortical ER (Martin et al., 2005). Murthi et al (2005) eliminated the possibility that *YIL090W*Δ*ice2*Δ disrupts the structure of the nuclear membranes by showing that the deletion has no effect on nuclear pore structure. Instead they favor the explanation that Ice2p is an ER component that indirectly affects the INM tethering of Trm1p-II-GFP perhaps by directing authentic tether(s) to the INM. While it remains to be seen whether Ice2p is involved in the tethering of other INM proteins, the requirement of Ice2p in the INM-tethering/localization of Trm1p-II-GFP indicates the participation of other proteins in this pathway.

Clearly, there is growing evidence that protein transport to the INM is not completely a function of or is not simply defined by simple diffusion in the interconnected ER and nuclear membranes. Instead, the INM transport process instead appears to be mediated by other proteins that are involved in the active restructuring of the NPC to facilitate protein movement across the lateral channels (discussed above). Also, the INM transport process exhibits remarkable specificity, contrary to the

randomness predicted by simple diffusion in the interconnected membranes. This specificity reflects the existence of sorting events mediated by putative INM-sorting factors, which confer directionality to protein transport towards the INM and prevent random protein distribution.

Protein transport to the INM: Lessons learned from Baculovirus

The baculovirus *Autographa californica* nucleopolyhedrovirus (AcMNPV) is an enveloped, double-stranded DNA virus (132kbp), which is distinguished by a unique biphasic life cycle in its Lepidopteran host. Infection results in two forms of progeny virus, budded virus (BV) and occlusion-derived virus (ODV), which mature at different cellular membranes. The proteins of the BV envelope are transported to the cell surface where they are incorporated into the viral envelope as the nucleocapsids bud through the plasma membrane (Kawamoto et al., 1977; Volkman & Goldsmith, 1985; Fraser et al., 1986; Adams & McClintock, 1991). In contrast, the strategy employed by the ODV to obtain its envelope is unique. The maturation and envelopment of the ODV occurs within the nucleoplasm of infected cells. *AcMNPV* infection is also characterized by the appearance of foci of unit membrane structures within the nucleus, which are referred to as “microvesicles” based on their small size and vesicle-like appearance (Fraser et al., 1986). Although there was a suggestion that the intranuclear microvesicles were formed as a result of *de novo* membrane morphogenesis (Stoltz et al., 1973), ultrastructural studies revealed that viral infection results in extensive proliferation and invagination (into the nucleoplasm) of the INM, raising the possibility that the INM serves as the source of the intranuclear microvesicles (Summers et al., 1969; Fraser et al., 1986; Hong

et al., 1994). When the ODV-envelope proteins, ODV-E66 (Hong et al., 1994) and ODV-E56 (Braunagel et al., 1996), were overexpressed, the protein was detected in the intranuclear microvesicles, the viral envelope, the outer and inner nuclear membranes and the ER membrane, suggesting that the INM indeed serves as the source of the intranuclear microvesicles and the viral envelope. Hence, the envelope proteins of the ODV must be transported into the INM prior to incorporation into the viral envelope. These proteins therefore constitute excellent substrates for examining the molecular mechanisms that mediate protein movement into the INM.

There are significant similarities between the trafficking of viral ODV-envelope proteins and resident proteins of the INM (Fig. 7). Both viral and cellular proteins utilize the continuous membranes of the ER and the nuclear envelope (ONM & INM) to traffic to the INM, and the budding of the INM to form the intranuclear microvesicles removes proteins from the diffusible pool as effectively as retention. However, experimental data obtained with the viral envelope protein ODV-E66 (E66) suggests that transport to the INM may be regulated by something more complex than passive diffusion and retention. As observed with cellular proteins of the INM (LBR, LAP2, MAN1 and nurim), when E66 was overexpressed, the protein was found in the ER membrane, ONM and the INM, but was not found in the plasma membrane or non-ER cytoplasmic membranes (Hong et al., 1997). This result suggests the existence of a sorting event which prevents INM-directed proteins (viral & cellular) from entering the secretory pathway.

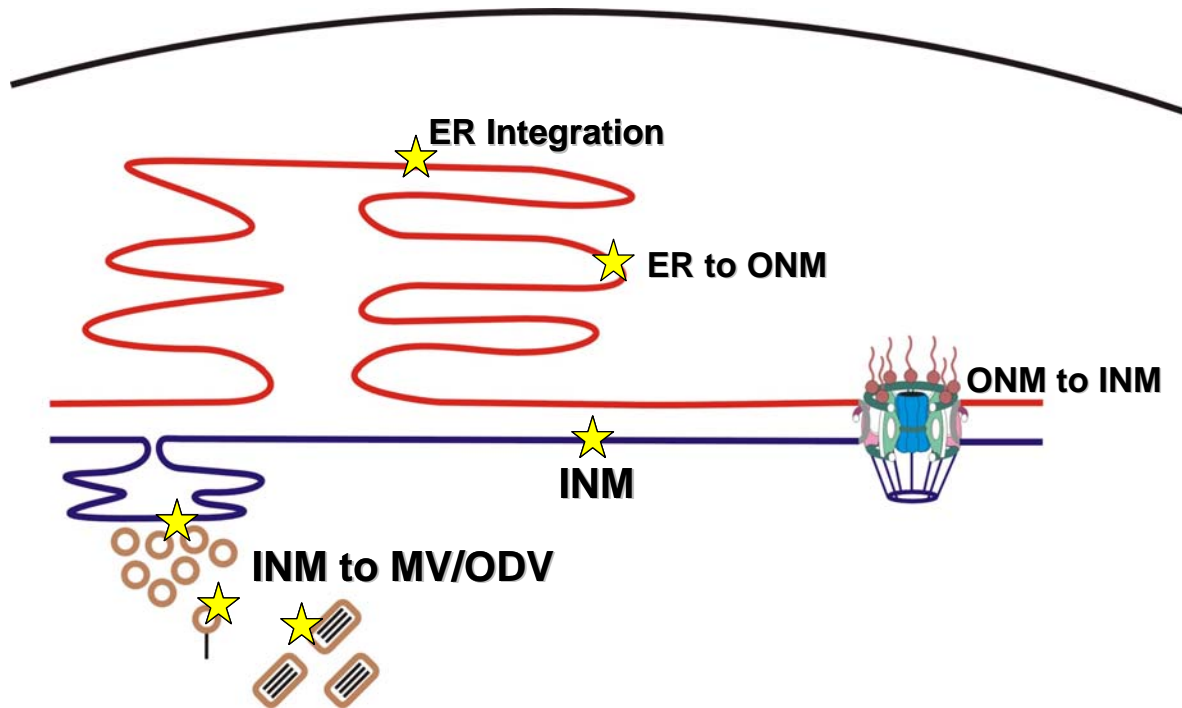


Figure 7. Trafficking of E66 to the INM, microvesicles and the ODV envelope. The trafficking of E66 to the microvesicles, which are the source of the viral envelope, is similar to the INM trafficking of resident INM proteins. The first step involves the cotranslational integration of the protein into the membrane of the ER via the translocon. Once integrated into the membrane of the ER, the protein diffuses in the continuous membranes of the ER and the ONM. Since the ONM and the INM join periodically at the nuclear pore complexes, the protein (E66) uses the lateral channels of the nuclear pore complex (pore membrane) to move from the ONM to the INM. Resident proteins of the INM are immobilized there by binding to nuclear proteins or DNA, but E66 accumulates in regions of the INM that undergo extensive proliferation and invagination (into the nucleoplasm) as a result of viral infection. The invaginations of the INM bud/pinch off into the nucleoplasm to produce unit membrane structures (vesicle-like in appearance) referred to as microvesicles (MV). The microvesicles fuse together to form the envelope of the maturing virus particle within the nucleoplasm of the infected cell.

Simple diffusion from the ER to the INM would predict that the INM-trafficking of E66 should be independent of the involvement of any other gene products. However, when the gene coding for FP25K was deleted from the viral genome, the trafficking of E66 during infection appeared to be blocked at the nuclear envelope. E66 was found to accumulate in punctate regions associated with the ONM, but was clearly not detected in the INM or the intranuclear microvesicles (Rosas-Acosta et al., 2001). The effect of the FP25K deletion was E66-specific, since the trafficking of another ODV envelope protein, ODV-E25 to the INM and microvesicles was unaffected (Rosas-Acosta et al., 2001).

Protein sorting to the ER and post-ER compartments occurs at several levels, requires multiple sorting signals and sorting events, and is regulated by protein-protein and protein-lipid interactions (Rothman & Wieland, 1996; Gomord et al., 1999; Mellman & Warren, 2000). Although it is possible that the continuous membranes of the ER, ONM, pore membrane and INM require a less elaborate mechanism of trafficking, it is also possible that more than one mechanism exists for protein trafficking from the ER to the INM. The diffusion-retention model (Worman & Courvalin, 2000) may describe the essential features for some resident INM proteins; however, proteins with large cytoplasmic/nucleoplasmic domains may require other factors for movement across the 10nm lateral channels of the nuclear pore complexes. The viral protein E66 may be an example of such a protein since its cytoplasmic domain is at the upper limit (~76kDa) of free passage across the lateral channels of the nuclear pore complexes. Taken together, these observations suggest that diffusion-retention does not fully describe the trafficking

of E66 from the ER to the INM (en route to the microvesicles/ODV envelope). Instead, the sorting of E66 to the INM appears to be a regulated process involving the active participation of other proteins (sorting factors).

Identification of the viral INM sorting motif (SM)

A deletion analysis of E66 revealed that the N-terminal 33 amino acids of E66 are sufficient to traffic fusion proteins to the microvesicles and ODV envelope with efficiency similar to wild type E66 (Fig. 8, #1 and 2) (Hong et al., 1997). Because of the functional ability to direct proteins fused to it to the INM, this sequence has been termed an INM- sorting motif (SM). The SM consists of a stretch of 16-18 nonpolar residues that form a transmembrane sequence (TMS) and positively charged amino acids that are located 5-8 residues from the TMS on the nucleoplasmic or cytoplasmic face of the membrane. If the charged amino acids flanking the TMSs are maintained, this INM-sorting motif sequence can be shortened to 23 amino acids (Fig. 8, # 3). As observed with E66, when the SM-fusions are overexpressed, the protein can be detected in the ER membrane, and the nuclear membranes (ONM & INM) (Braunagel et al., 2004).

Since, E66 and SM fusion proteins traffic to the INM, identification of the INM-sorting signal within E66 raises the issue whether resident proteins of the INM have an SM or SM-like sequence. Sequence comparison revealed that known resident proteins of the INM also have an SM-like sequence (Fig. 9) (Braunagel et al., 2004), even though many are oriented in the opposite direction in the bilayer and are inserted into the bilayer by different mechanisms (either via a translocon-mediated process or as C-tail anchored proteins {Wattenberg et al., 2001}). Since, some INM proteins are multispinning

1. ODV-E66: MSIVLIIVIVVIFLICFLYL SNSNNKNDANKNNAFIDLNP-----
2. 33-GFP: MSIVLIIVIVVIFLICFLYL SNSNNKNDANKNAGAMVSK-----
3. 23-GFP: MSIVLIIVIVVIFLICFLYL SNSKDPVPELM-----

Figure 8. Sorting motif (SM) sequences. (1) The N-terminal sequences of wild type E66; and the sorting motif fusions (2) and (3) are shown. The TMS is highlighted in yellow; the charged amino acids are highlighted in red (basic) and blue (acidic); and the GFP sequence is highlighted in green.

membrane proteins (nurim, LBR etc.), the comparison was made with the TMS that is critical for protein accumulation at the INM (TMS 1 of nurim and LBR).

The features conserved among the viral (E66) SM sequence and the resident INM proteins include the lack of any charged amino acid within the TMS and the presence of positively charged amino acids on the cytoplasmic/nucleoplasmic face of the membrane within 3 to 8 residues from the TMS. Studies on the viral SM fusion (23 GFP; Fig. 8, # 3) have shown that the spacing between the charged residues and the end of the TMS seems to be critical for protein accumulation at the INM (Braunagel et al., 2004). When the spacing was increased to 11 residues, a less intense nuclear rim (indicative of protein accumulation at the INM) was observed and more protein was detected in the peripheral ER (Fig. 10; Group 2) (for reference the localization of 23 GFP is shown in Fig. 10; Group 1). Deletion of the lysine residues and increase in the length of the TMS resulted in protein accumulation at the cell surface (Fig. 10; Group 3), and a decrease in the

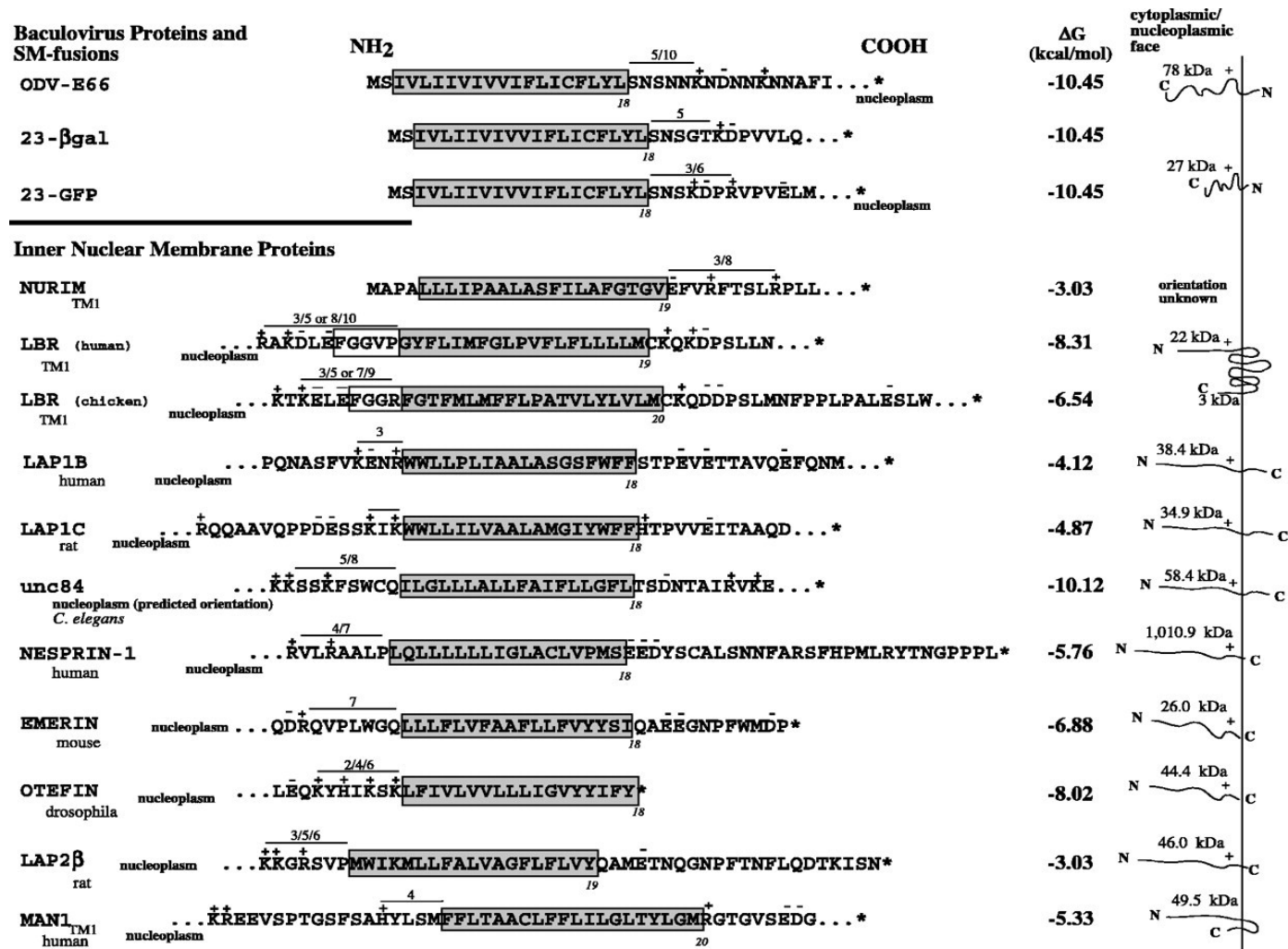


Figure 9. Comparison of the E66 SM sequence with cellular INM proteins. The TMS and flanking sequences most likely to influence INM localization are shown.

Reprinted in accordance with Copyright ©1993-2004 by The National Academy of Sciences of the United States of America, all rights reserved (Braunagel et al., 2004).

spacing between the charged residues and the end of the TMS resulted in protein distribution throughout the peripheral ER in a manner indistinguishable from the ER-marker protein, calreticulin (Fig. 10; Group 4). These data indicate that the lysine residues within the SM are at or near a functionally important site that influences the INM trafficking of the SM fusion. Since, the essential features of the viral (E66) SM are conserved within resident INM proteins of mammalian cells, E66 seems to be a relevant substrate to examine the sorting of mammalian INM proteins.

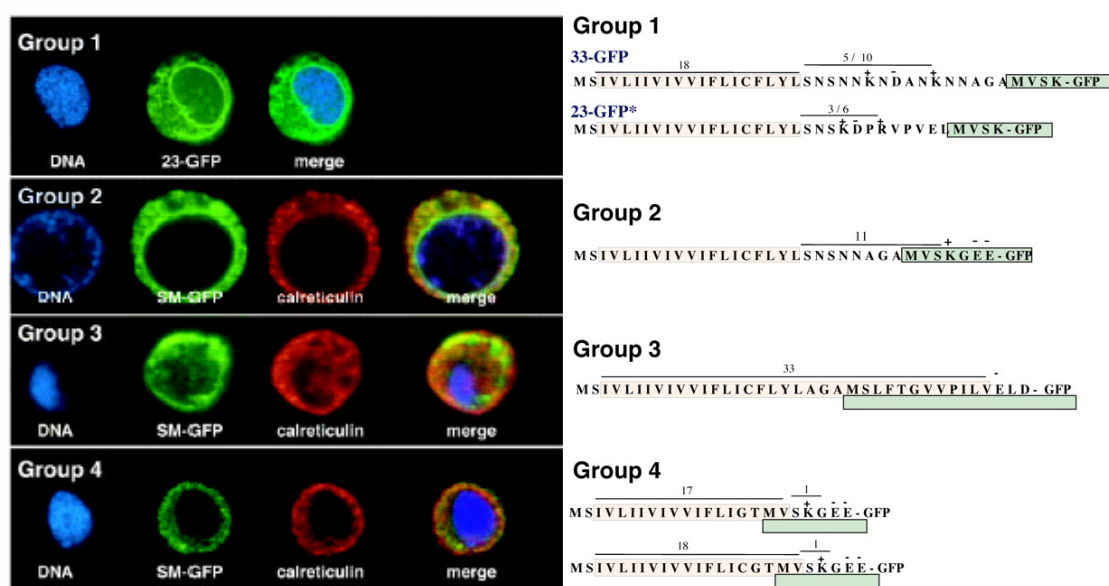


Figure 10. Localization of SM mutants. Clones from each group were transiently expressed in Sf9 cells, and a representative Z section is shown. ER was identified using antibodies specific for calreticulin and DNA was labeled with the dye DAPI, while the SM-fusion was detected by GFP autofluorescence. If two clones are represented within the same group, the results were visually indistinguishable. Reprinted with permission from Proc. Natl. Acad. Sci. (Braunagel et al., 2004).

Sorting of E66 to the INM: Possible sites of regulation

Since the SM of E66 is sufficient to direct non-nuclear proteins into the INM when only 13 and 2 residues are exposed on the cytoplasmic and luminal sides, respectively, of the INM or ER INM or ER bilayer (Braunagel et al., 2004), SM sorting must be mediated by the TMS and/or sequences close to the membrane surface. Now that the TMS of E66 has been identified to be critical for sorting to the INM, the stage has been set to ask a different type of question: is the key cellular event of TMS integration into the ER membrane (the first step in the trafficking of proteins to the INM) subject to regulation? In other words: is the ER translocon involved in protein sorting? This is a provocative question to ask, considering the multitude of integral membrane proteins handled by the translocon. The ER membrane serves as the site of integration not just for resident ER membrane proteins, but also for proteins of the nuclear envelope (outer and inner nuclear membranes) and the secretory pathway. Following membrane integration, these proteins destined for different intracellular locations need to be sorted and exported, which involves multiple sorting signals and sorting events. Although, the sorting signals and factors involved in the transport of proteins to post-ER compartments such as the Golgi, plasma membrane are well characterized (Barlowe et al., 2003), most of these sorting events have been found to function at the post-translational level or after the full-length protein has been synthesized, released from the ribosome and integrated into the membrane bilayer. It is unclear how early in the biosynthesis of the protein (substrate) can the sorting process initiate. Can sorting factors associate with the substrate cotranslationally while the nascent protein is in the process of membrane

integration? Does the translocon 'know' or 'sense' whether a TMS in the process of integration represents a resident ER substrate versus a protein of the INM?

If sorting indeed could initiate cotranslationally or early in the biosynthesis of the substrate, one can envision two scenarios: first, all disengaged (empty) translocons are associated with a different set of (relevant) sorting factors (Fig. 11) that makes them specialized/dedicated to handle (exclusively) a particular class of substrates (resident ER/INM/plasma membrane substrates). This implies that all disengaged (empty) translocons are not equal (same in overall protein composition) but instead there are different subpopulations of translocon specialized to handle proteins destined for the INM, the resident ER membrane proteins, and proteins destined for the cell surface. This idea of translocons associated with different interacting protein (partners) was recently reported in yeast (Yan & Lennarz, 2005). The second possibility is that all disengaged (empty) translocons are equal (same in overall protein composition) but modular in nature, implying that the core translocation/integration machinery is the same but is subject to the action of regulatory factors (sorting factors) recruited by the core machinery in a substrate-dependent manner (Fig. 12). This model predicts a more dynamic and active role for the translocon in protein sorting, whereby once engaged, it not only 'senses' the substrate (resident ER versus INM versus plasma membrane protein) in the translocation channel, but also responds via recruiting the appropriate sorting factor(s). In short, the difference between the two models is that while the first model predicts the pre-existence of specialized translocons, the second model predicts

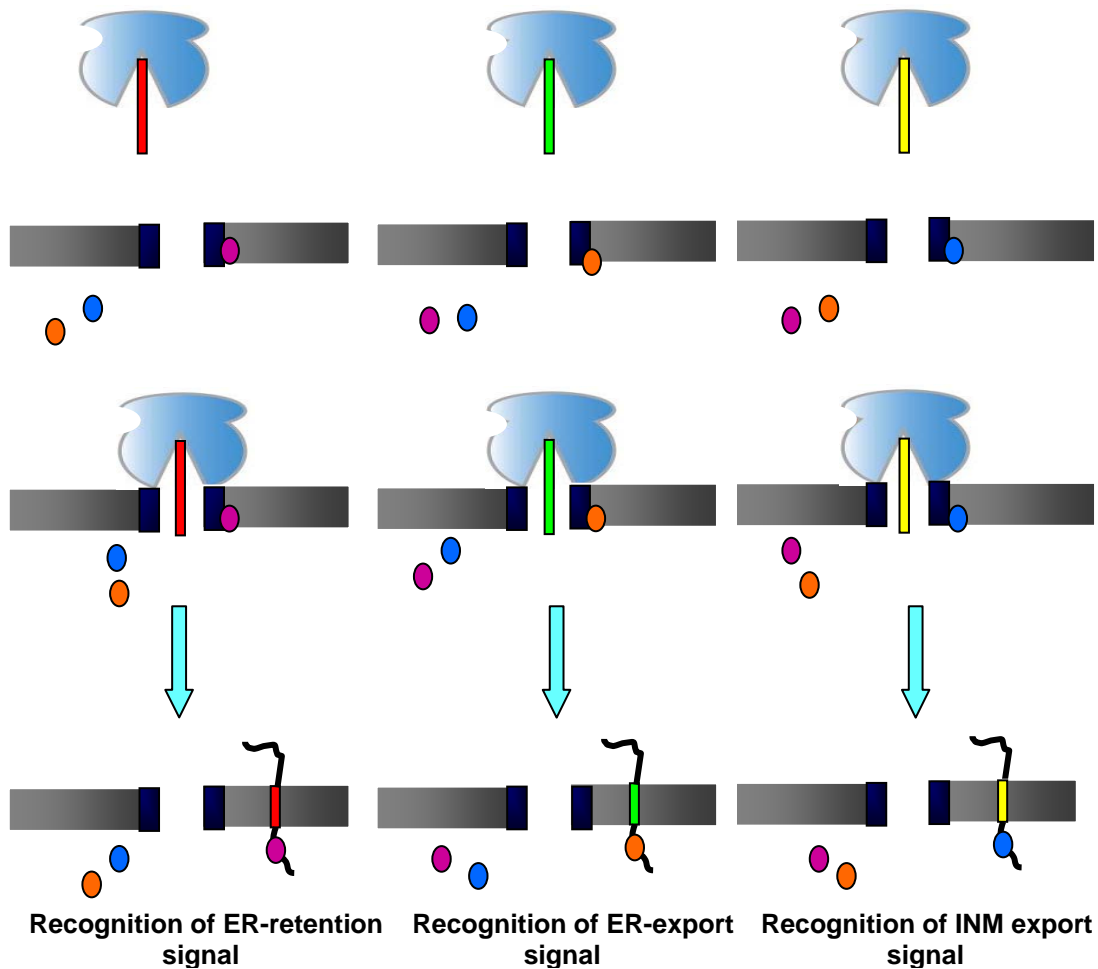


Figure 11. The specialized translocon model. For simplicity, three (among numerous) empty translocons are depicted in the first row of events. A translocon specialized for handling resident ER membrane proteins is associated with a sorting factor (depicted in purple), which is able to recognize the ER-retention signal on resident ER membrane proteins. Thus, a cytosolic ribosome in the process of translating a resident ER membrane protein (depicted in red) is targeted to the translocon associated with the ER-specific sorting factor (depicted in purple). Following, termination of translation the sorting factor may either continue to be proximal to the resident ER membrane protein (as depicted in this figure) or it may hand off the substrate to the next sorting factor (not shown) in the pathway. In the same way, the ER membrane has translocons specialized for handling proteins of the INM (depicted in yellow) via the association of INM-specific sorting factor(s) (depicted in blue), and translocons specialized for handling proteins destined for the plasma membrane (depicted in green) via the association of sorting factor(s) (depicted in orange) capable of recognizing the ER-export signal.

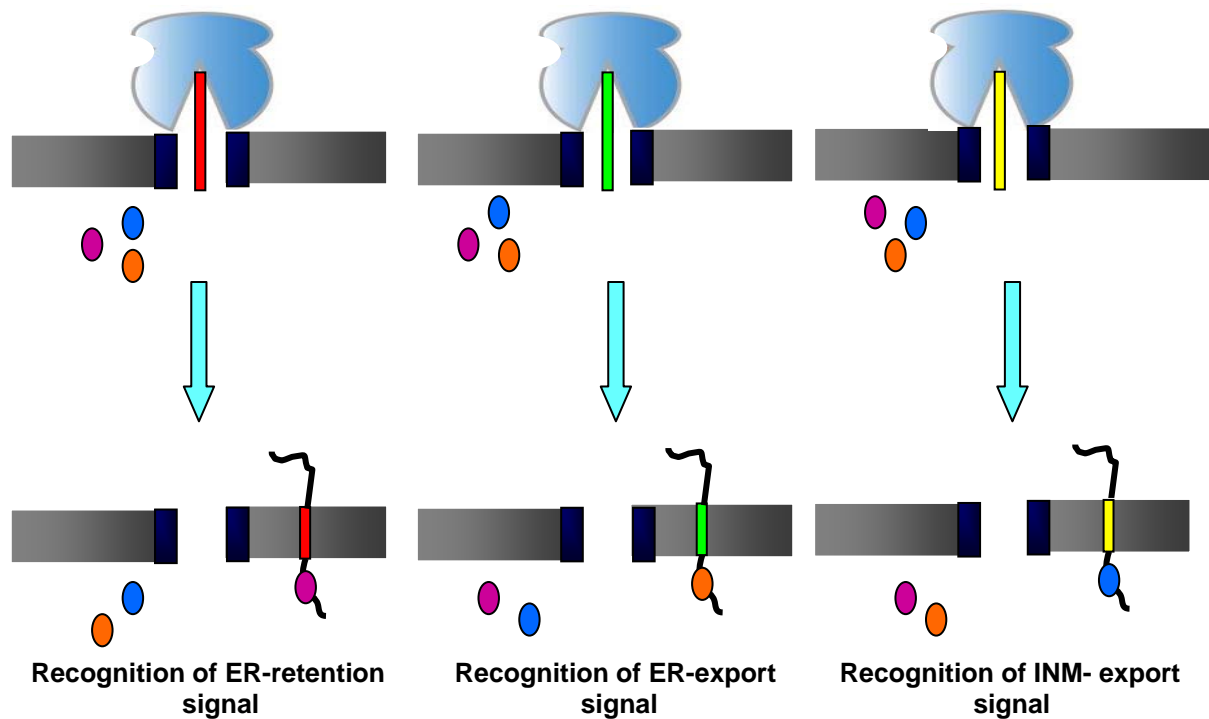


Figure 12. The modular translocon model. For simplicity, three (among numerous) engaged translocons are depicted in the first row of events. When engaged with a ribosome translating a resident ER membrane protein (depicted in red), the translocon is able to recruit an ER-specific sorting factor (depicted in purple) from a pool of luminal sorting factors. Note that although the figure shows the different sorting factors to be luminal, they may be present in the cytosol or both in the lumen and cytosol. Following termination of translation, the ER-specific sorting factor may either continue to stay associated with the substrate (as shown in the figure) or it may dissociate and hand off the substrate to the next sorting factor in the pathway (not shown). Similarly, a translocon engaged with a ribosome translating a plasma membrane protein (depicted in green) is able to recruit the ER-export specific sorting factor (depicted in orange), while a translocon engaged with an INM protein (depicted in yellow) recruits an INM-specific sorting factor (depicted in blue).

that translocons become specialized only when engaged with substrate. While it is experimentally difficult to test which between the two models is correct, the second model (modular translocon) is more likely to represent the physiological operational state of the translocon.

There are a number of parallels to support the modular translocon model. Key cellular events such as transcription, splicing, translation and protein degradation are all carried out by core machinery subject to the action of regulatory factors. There is growing evidence that the stability of the ribosome-translocon junction may be physiologically regulated, depending on specific properties of the signal sequence and its dependence on translocation-associated factors (TrAFs) such as TRAM, or TRAP (Hegde & Lingappa, 1997,1999; Hegde et al., 1998). There is also a body of evidence to suggest that the translocon is not merely a passive pore during protein translocation or membrane protein integration. Protein-protein interactions have been shown to exist between the nascent chain and the translocon during cotranslational membrane protein integration (McCormick et al., 2003). However, as proposed by the modular translocon model, once engaged by a particular substrate, the translocon needs to recruit the appropriate sorting factor(s). How might such events be regulated? It is possible that topogenic sequences within the nascent chain are 'recognized' /'sensed' by the translocation machinery to initiate dynamic changes in the translocon. Several experimental results support the existence of such long-range signal transduction pathways, where topogenic sequences within the ribosomal tunnel are able to initiate

changes in the translocon structure and dynamics (Liao et al., 1997; Hamman et al., 1998; Woolhead et al., 2004).

If the modular translocon model, in which the translocon is able to ‘sense’ the substrate in the translocation channel to initiate sorting, is accurate, how might such substrate ‘sensing’ occur? Although, it is known that there are protein-protein interactions between the nascent chain and the translocon during cotranslational membrane protein integration (McCormick et al., 2003), a number of interesting issues remain unanswered. Does every TMS interact with the same site in the translocon (e.g. a particular translocon α helix)? Is it possible that nascent chains move to different sites within the translocon depending on their TM sequences? One possible mechanism by which the translocon may initiate cotranslational membrane protein sorting is if TMSs of INM-directed proteins occupied a (binding) site within the translocon that is different from the site occupied by the TMS of a resident ER protein. And further, if this binding site (exclusive for TMSs of INM-directed proteins) is proximal to the site for association of INM-specific sorting factors that function downstream (post-integration) in the sorting of proteins to the INM.

Although, the role of the translocon in the sorting of proteins during cotranslational membrane integration remains to be examined, the arguments discussed above certainly present a compelling case to test the possibility that protein sorting may begin during cotranslational integration into the ER membrane. In other words, is it possible that the first step in the trafficking of proteins (E66) to the INM (Fig. 13) may be regulated? Also, since preliminary data indicates that the sorting of E66 to the INM is a regulated

process involving the active participation of other accessory proteins (sorting factors), what is the identity of these accessory proteins? Are there viral proteins that (during infection) facilitate the trafficking of E66 from the ER to the ONM and the INM (Fig. 13)? And more interestingly and importantly, are there any cellular proteins that facilitate the trafficking of E66 to the INM? Are these accessory proteins translocon-associated and what stage of biosynthesis (cotranslational or post-translational) do they associate with the substrate? These are some of the issues that will be addressed in this study. It is possible that once at the INM, the accumulation of E66 into regions (microdomains) of the INM that undergo extensive invagination and proliferation is also regulated either by protein-protein or protein-lipid interactions. Also, the budding of the INM into microvesicles within the nucleoplasm and protein incorporation into the viral envelope may be tightly regulated events as well. However, studies examining these steps of the pathway are beyond the scope of this study.

Nucleocytoplasmic transport

In contrast, to the trafficking of integral membrane proteins to the nuclear membranes (ONM & INM), the movement of soluble cargo between the nucleus and the cytoplasm has been characterized in extensive detail. The signals mediating nuclear import and export are well characterized, and the proteins involved in the nucleocytoplasmic shuttling process have not only been identified but also characterized at the structural level.

Cargoes and signals. In eukaryotic cells, the separation of the nucleus and cytoplasm by the nuclear envelope implies that there is rapid and vectorial exchange of

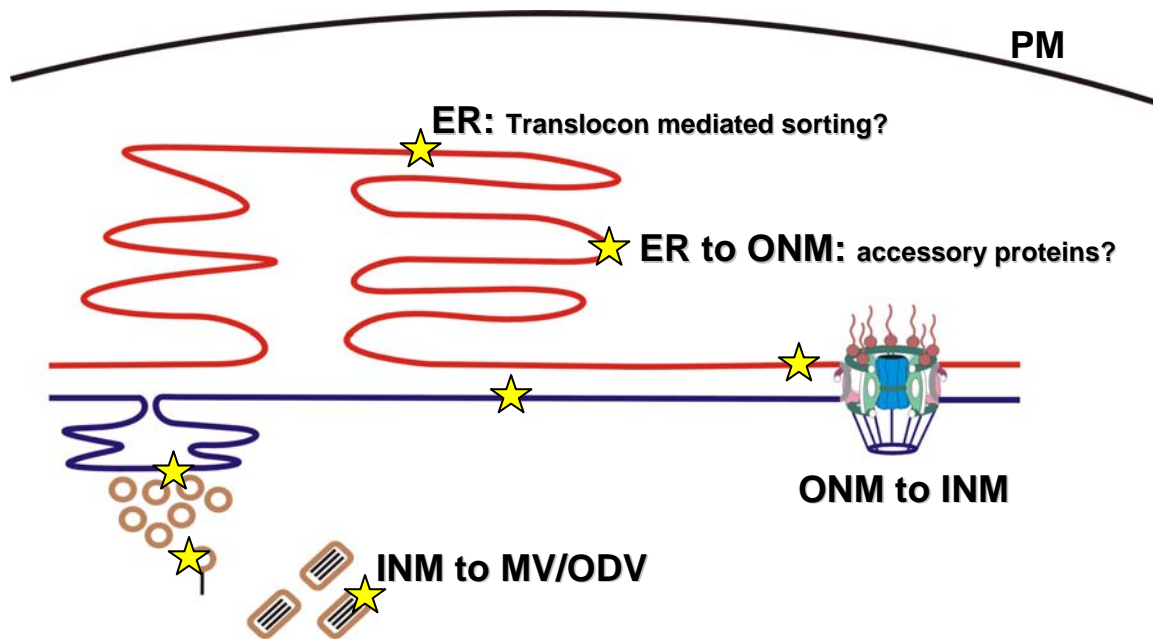


Figure 13. Possible sites where the INM trafficking of E66 may be regulated. Step 1: Integration into the membrane of the ER via the translocon. Step 2: Protein movement from the ER to the ONM may be facilitated by other accessory proteins (viral and/or cellular). Step 3: Protein movement across the lateral channels of the NPC may be protein-mediated. Step 4: Accumulation of protein in regions of the INM that undergo invagination into the nucleoplasm. Step 5: Budding of the INM to produce microvesicles. Step 6: Protein incorporation into the envelope of the virus particle.

macromolecules such as proteins and RNAs between the two aqueous compartments. Most of these transport processes (pathways) are facilitated by soluble transport factors, which are members of the karyopherin β family. Based on the importance of their cellular function, human cells contain at least twenty members of this family, while yeast contains fourteen members (Mosammaparast et al., 2004).

The large and diverse repertoire of substrates (cargoes) that need to be moved between the nucleus and the cytoplasm raises questions regarding the mechanism of karyopherin: cargo recognition. Studies have shown that karyopherins directly bind to their cargoes via recognition of a nuclear localization sequence (NLS) for nuclear import or a nuclear export sequence (NES) for export (Fried et al., 2003; Weis et al., 2003). However, the nuclear transport process does not always involve require direct cargo binding by the karyopherins. For some cargoes, karyopherin binding is mediated by adaptor proteins, most commonly via the related protein karyopherin α .

Careful analysis of the well-characterized NLSs from SV40 Large-T antigen and nucleoplasmin revealed the essential features of a classical NLS, which consists of one or two clusters of basic amino acids separated by a linker (Gorlich et al., 1999). NLSs, such as the one found in SV40 Large T-antigen (PKKKRKV), which contains a single cluster of basic amino acids, are referred to as monopartite NLSs. In contrast, bipartite NLSs such as the NLS of nucleoplasmin (KRPAATKKAGQAKKKK) that contain two clusters of basic amino acids are referred to as bipartite NLSs. However, recent studies have shown that nuclear import is not regulated by import signals (NLSs) alone. NLS activity can be regulated by a number of mechanisms including signal modification or

signal masking (Kaffman et al., 1999). In addition, modification of residues proximal to the NLS has also been shown to result in altered binding to the adaptor protein, karyopherin α (Harreman et al., 2004).

The karyopherin-mediated nuclear transport process is regulated by the interaction between karyopherins and Ran (Fig. 14). Ran cycles between its GDP- and GTP- bound states. Cytoplasmic Ran is in the GDP-bound state that is promoted by the cytoplasmic Ran GTPase activating protein (RanGAP). In contrast, nuclear Ran is in the GTP-bound state that is maintained by the Ran guanine-nucleotide-exchange factor (RanGEF), whose nuclear localization is mediated via interactions with chromatin. The resulting Ran gradient provides directionality to the nuclear transport process (Weis et al., 2003).

Karyopherins that mediate import bind to their cargoes in the cytoplasm via recognition of the nuclear localization signal (NLS) (Fig. 14). The nuclear translocation of the import complex is mediated via interactions with NPC proteins (nucleoporins). Once in the nucleus, the karyopherin: RanGTP complex results in cargo dissociation and recycling of karyopherin to the cytoplasm. Conversely, karyopherins that mediate export bind cargo in the nucleus via recognition of a nuclear export signal (NES). Karyopherin binding to export cargoes occurs co-operatively with RanGTP, which results in formation of a karyopherin: cargo: RanGTP ternary complex (Fig. 14) that is translocated to the cytoplasm. Thus, Ran regulates both the assembly and the disassembly of karyopherin: cargo complexes.

Karyopherin- α and the basic NLS. Importin α functions as an adaptor that links cNLS-containing cargo molecules with the nuclear transporter, importin β . The ternary

complex formed in the cytoplasm diffuses to reach the nuclear pore complex, where protein-protein interactions between importin β and the nucleoporins facilitate the translocation of the ternary complex through the central channel of the NPC (Fig. 15). In the nucleus, the binding of the small nuclear GTPase Ran-GTP to importin β triggers the dissociation of the ternary complex, resulting in the recycling of importin α to the cytoplasm bound to the exportin CAS-Ran-GTP. The export complex is disassembled in the cytoplasm by Ran-GAP (GTPase activating protein)-induced hydrolysis of GTP by Ran that releases free importin α in the cytoplasm. Ran-GDP and CAS are recycled back to the nucleus for further rounds of transport, where Ran-GDP is converted to Ran-GTP by the guanine nucleotide exchange factor RCC1.

Membrane association of importin α . A recent study demonstrated that a significant proportion (~50%) of importin α fractionates with *Xenopus* egg membranes (Hachet et al., 2004). The association of importin α with membranes in interphase was shown to be independent of any of the previously characterized binding partners of importin α , including importin β , CAS and Ran. Interestingly, an importin α mutant that does not bind NLS proteins, the ED mutant (Gruss et al., 2001), also associates with membranes and apparently functions in NE assembly, indicating that membrane association of importin α is independent of substrate-binding as well.

The localization of importin α to either the membrane or cytosolic fractions correlates with post-translational modification of the protein. The soluble form of

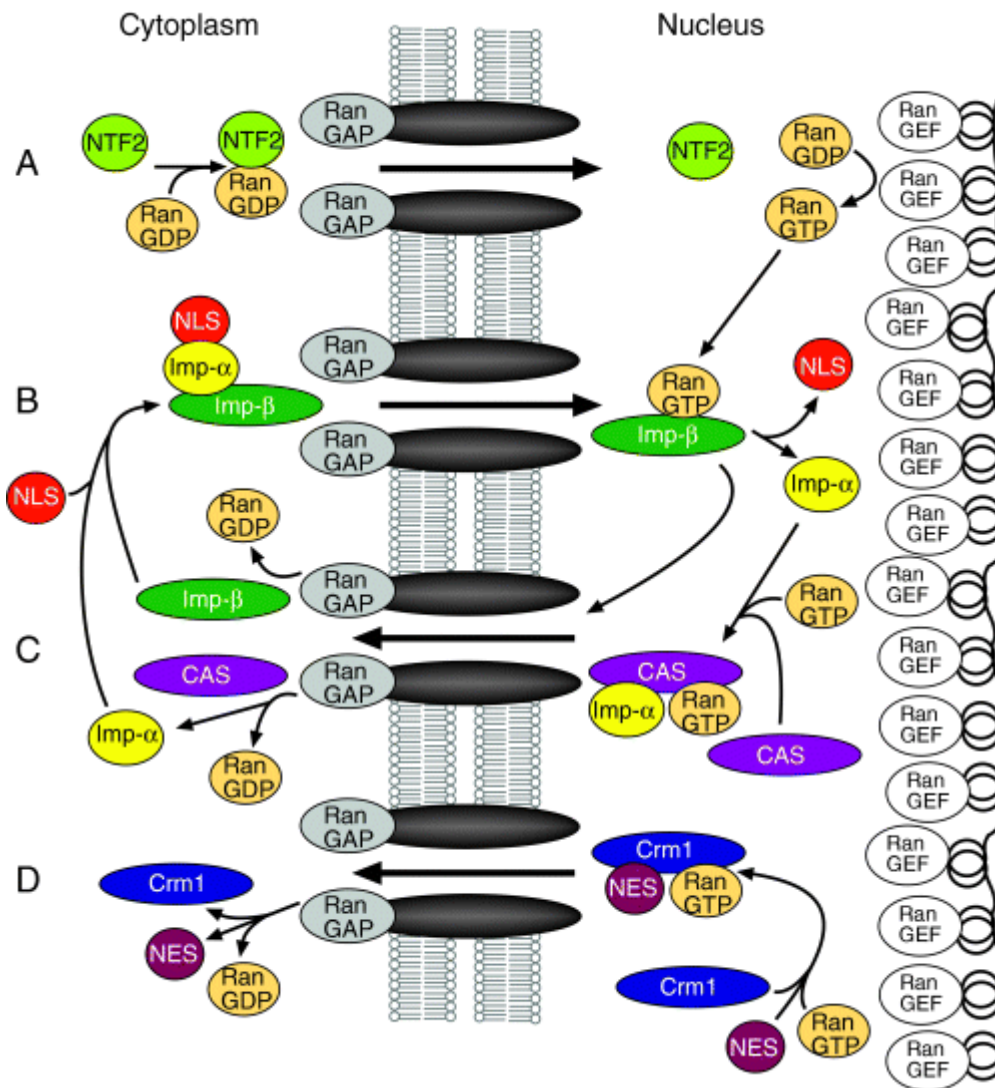


Figure 14. Overview of some major nuclear transport pathways in eukaryotic cells.

A) Nuclear import of RanGDP mediated by NTF2. B) Nuclear import of nuclear localization sequence (NLS) cargo mediated by the karyopherin- α : importin- β 1 heterodimer (abbreviated as Imp- α and Imp- β). C) Nuclear export pathways that mediate recycling of importin- β 1 and karyopherin- α ; the latter requires CAS as an export receptor. D) Nuclear export of nuclear export sequence (NES) cargo mediated by Crm1. RanGAP is anchored to the cytoplasmic side of the NPC and RanGEF is shown bound to chromatin. For simplicity, the model depicts only the minimal components necessary to form the pretranslocation transport complexes, and post-translocation intermediates and accessory factors are not shown. Reprinted with permission from Traffic (Pemberton & Paschal, 2005).

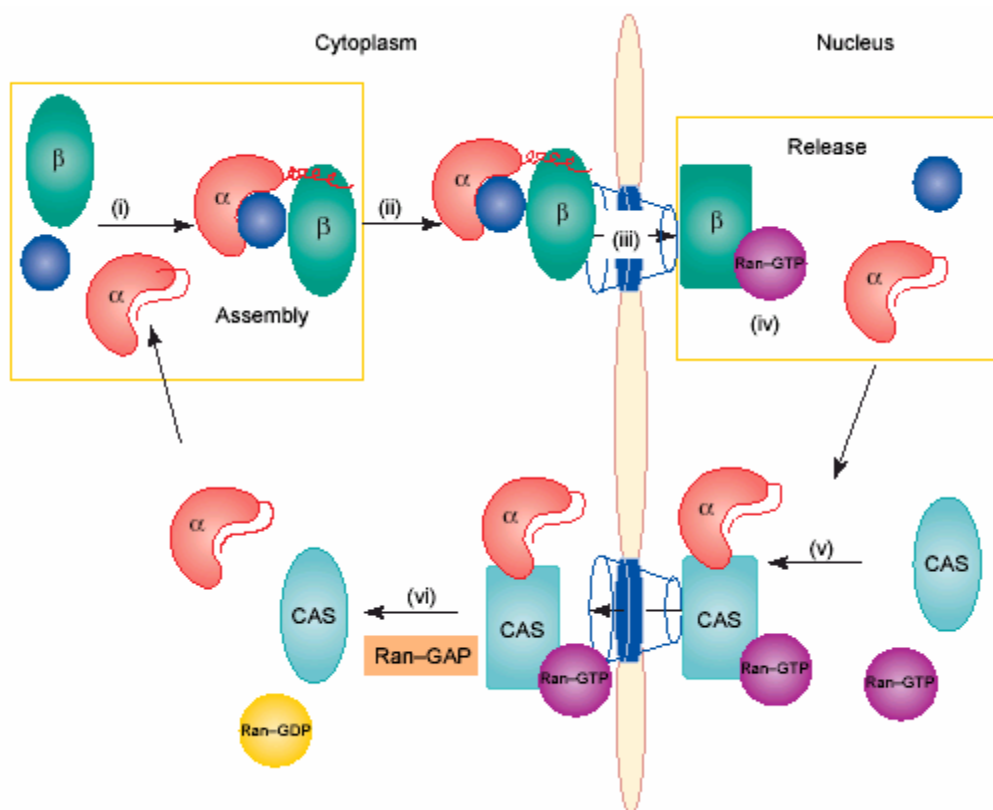


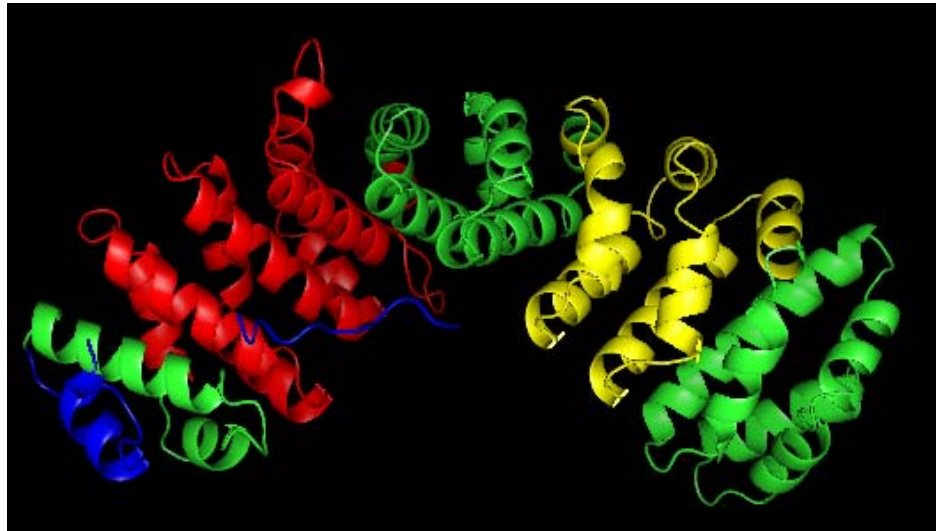
Figure 15. The nucleocytoplasmic shuttling of importin α . (i) Importin α (α) forms a ternary complex with importin β (β) and cargo (blue circles). (ii) The ternary complex docks at the nuclear pore complex (NPC) and (iii) translocates into the nucleus. (iv) Binding of Ran-GTP triggers the dissociation of the ternary complex. (v) Importin α binds to the exportin CAS-Ran-GTP complex and is exported to the cytoplasm. (vi) Ran-GAP-stimulated hydrolysis of GTP by Ran triggers the dissociation of the exportin complex and releases free importin α into the cytoplasm for another transport cycle.

“Reprinted from Trends in Cell Biology, 14, Goldfarb et al., Importin alpha: a multipurpose nuclear-transport receptor, Page: 508, © 2005, with permission from Elsevier”.

importin α present in the cytosolic fraction was found to be more highly phosphorylated than the membrane-bound form, as determined both by mobility change on SDS-PAGE and by phosphopeptide mapping (Hachet et al., 2004). The authors proposed that the modification-dependent membrane association of importin α in principle allows regulation via the action of phosphatases and kinases. Although the membrane-bound form of importin α has been suggested to be involved in formation of a closed nuclear envelope, it is clear that this form functions in quite a different way than the better understood soluble form.

Structural basis of importin α function. Data from structural analyses and *in vitro* binding studies have provided insights into how importin α binds to and regulates interactions with NLS-containing cargoes (Herold et al., 1998; Conti et al., 1998; Fontes et al., 2000). These studies have revealed that the NLS-binding pocket on importin α is composed of a series of series of armadillo (ARM) repeats, which are related to HEAT repeats, the structural building block for the importin β karyopherins (Figs. 16 and 17).

A.



B.

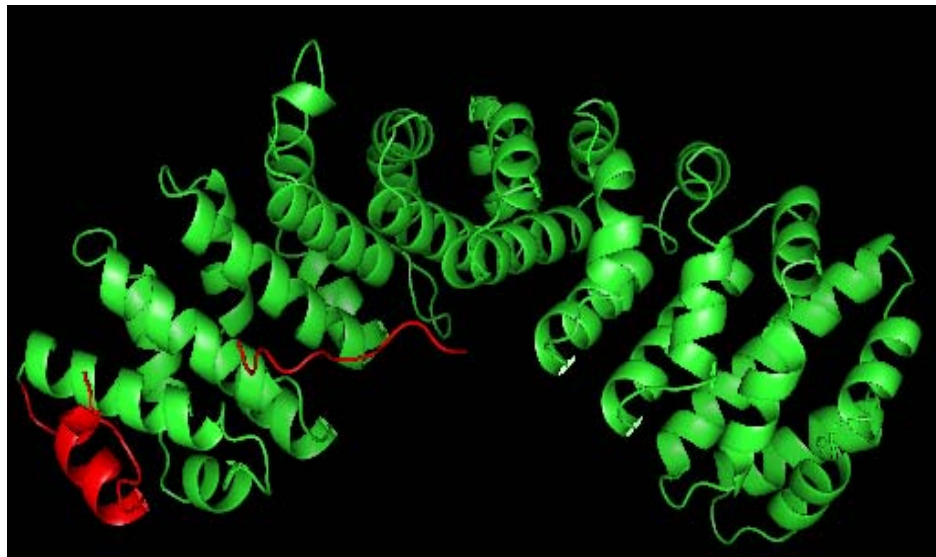
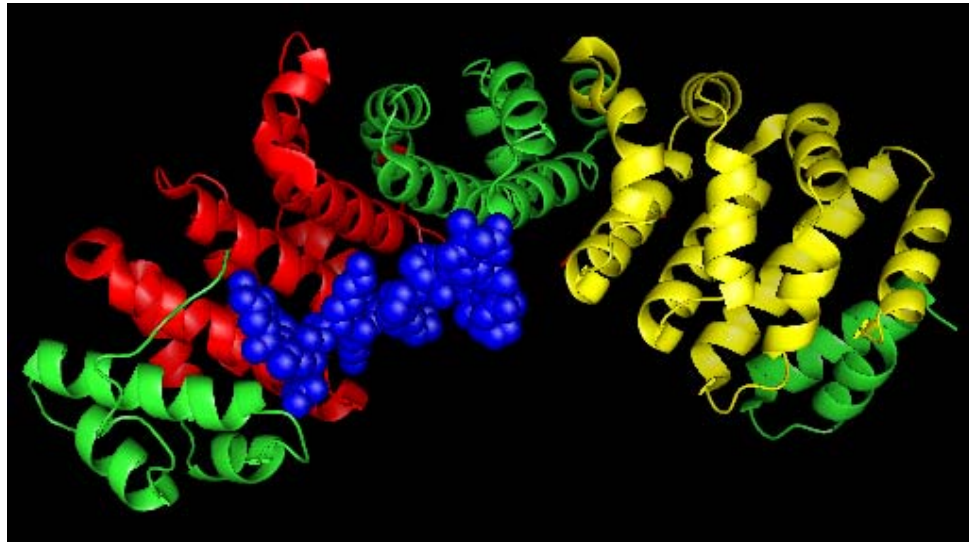


Figure 16. Domain structure of importin α . (A). Mouse importin alpha (PDB: 1IQ1) (monomer) with the IBB highlighted in blue; major NLS-binding site (ARMs 2-4) highlighted in red; minor NLS-binding site (ARMs 7-9) highlighted in yellow. (B). IBB (highlighted in red) masking the major-NLS binding site of mouse importin alpha in the absence of cargo. The shading of the different functional parts of the mouse importin alpha structure was done using PyMol (DeLano, 2002).

A.



B.



Figure 17. Modeling of importin α . (A) Mouse importin alpha (PDB: 1EJL) with the SV40 antigen (shown in blue) bound to the major NLS-binding site (ARMs 2-4) (and highlighted in red). The minor NLS-binding site (ARMs 7-9) is highlighted in yellow and the rest of the ARM repeats are indicated in green. (B). Binding of a cargo molecule containing a bipartite NLS is depicted using PyMol (DeLano, 2002). Yeast importin alpha (PDB: 1EE4) is shown with the c-myc peptide (blue) bound to both the major NLS-binding site (highlighted in cyan), and the minor NLS-binding sites (highlighted in orange).

Importin α has an N-terminal domain that binds to importin β (the IBB) (shaded blue in Fig. 16), the central ARM domain that constitutes the cNLS-binding pocket and a C-terminal region, including the tenth ARM repeat that seems to be important for binding to the export receptor CAS/Cse1 (Fig. 16).

The structure of truncated *Saccharomyces cerevisiae* importin α (amino acid residues 89-530) complexed with a cNLS peptide, provided a detailed picture of how the central ARM domain of importin α creates specific binding pockets for cNLS cargo (Conti et al., 1998) (Fig. 17). These structural studies revealed the presence of two cNLS-binding sites on importin α (ARM repeats 2-4 and 7-9). Structure of the full-length mouse importin α solved in the absence of cargo, showed that the N-terminal IBB forms an intramolecular interaction with the cNLS-binding pocket, resulting in masking of the cNLS-binding pocket in the absence of cargo (Kobe et al., 1999). These structural studies have provided molecular snapshots of the architecture of importin α and its interaction with cargo molecules that have greatly advanced our understanding of the importin α transport cycle.

Specific aims

Previous studies on ODV envelope proteins suggest that the movement of these proteins could be mediated via cytoplasmic membranes and the nuclear envelope (Hong, 1997). Although this model predicts that ODV envelope proteins are incorporated into the ER and transported to the outer and inner nuclear membranes, there have been no studies that directly address the first step in the INM-trafficking process of ODV envelope proteins i.e. targeting to and integration at the ER membrane. Specifically, do viral envelope proteins such as E66 integrate into the ER membrane and diffuse through the continuous membranes of the ER and the nuclear envelope in a manner analogous to INM proteins? If so, is the putative ER-integration process mediated by interactions of the viral envelope protein with components of the Sec61 translocon? Following ER-integration, what is the mechanism by which these INM-directed proteins are sorted away from resident ER proteins or proteins of the secretory pathway? Is the sorting process protein-mediated, and if so are these sorting factors translocon associated? The research outlined in this proposal will use the viral envelope protein E66 to address these questions regarding the sorting of INM-directed proteins at the ER membrane. The experimental approach will entail a combination of crosslinking techniques: chemical crosslinking as well as site-specific incorporation of photoreactive probes using aminoacyl tRNA analogs.

- 1) Is the membrane targeting of E66 cotranslational and SRP-dependent or posttranslational and SRP-independent?** Full-length E66 has been observed to insert into membranes post-translationally, albeit at low efficiency (Hong et al.,

1997). Hence, it is necessary to ascertain whether E66 is normally targeted to the ER membrane in an SRP-dependent manner and integrated cotranslationally.

- 2) **To examine the role of the ER translocon in sorting of proteins destined for the INM.** Since the SM of E66 is sufficient to direct non-nuclear proteins into the INM when only 13 and 2 residues are exposed on the cytoplasmic and luminal sides, respectively, of the INM or ER bilayer (Hong et al., 1997), SM sorting must be mediated by the TMS and/or sequences close to the membrane surface. In this study viral and cellular SM-like sequences will be used to address three issues that are critical to our understanding of protein sorting to the INM. First, photochemical and chemical crosslinking will be used to detect and identify proteins that are located adjacent to, and presumably interact with, nascent INM proteins at different stages of integration. Second, to determine whether viral and host INM proteins use the same sorting machinery and are sorted in the same way, the photoadducts obtained with two host and two viral INM proteins will be compared. Third, to ascertain at what point, if any, during integration the SM sequence directs INM membrane proteins into a different pathway than that taken by proteins destined for other cellular membranes, the photocrosslinking of nascent chains directed to either the INM or another membrane will be compared.
- 3) **Identification of accessory proteins involved in the sorting of E66 to the INM.** Previous work has shown that the lysine residues within the E66SM are at or near a functionally important site that influences the trafficking of the SM fusion (Braunagel, 2004). Hence, the proteinaceous environment of the lysine residue(s)

within the E66SM will be analyzed using lysine specific chemical crosslinkers to identify any accessory proteins (sorting factors) that are able to recognize and associate with the E66 SM. Chemical crosslinking experiments will be performed using both (insect) Sf9 microsomes as well as virus-infected Sf9 microsomes to identify any cellular or viral proteins that are involved in the trafficking/sorting of E66 to the INM.

CHAPTER II

MATERIALS AND METHODS

Constructs used for photocrosslinking experiments

Cotranslational membrane integration of five different TMSs was analyzed in this study using photocrosslinking. To analyze the proteinaceous environment of the TMSs from four different sides of the TMS α -helix surface, a single amber codon per mRNA was substituted in place of each of four sequential in-frame codons in each mRNA examined (Fig. 18). Photoreactive probes were incorporated cotranslationally using the modified amber-suppressor tRNA (ϵ ANB-Lys-tRNA^{amb}) (Flanagan et al., 2003).

		10	11	12	13																			
E66:	M	<u>S</u>	<u>I</u>	<u>V</u>	<u>L</u>	<u>I</u>	<u>I</u>	<u>V</u>	<u>I</u>	V	V	I	F	L	I	C	F	L	Y	L	S	N	-	-
E25:	M	<u>W</u>	<u>G</u>	<u>I</u>	<u>V</u>	<u>L</u>	<u>L</u>	<u>I</u>	<u>V</u>	L	L	I	L	F	Y	L	Y	W	T	N	A	L	-	-
LBR1:	M	<u>F</u>	<u>G</u>	<u>G</u>	<u>V</u>	<u>P</u>	<u>G</u>	<u>V</u>	<u>F</u>	L	I	M	G	G	L	P	V	F	L	F	L	L	L	-
Nur1:	M	<u>A</u>	<u>P</u>	<u>A</u>	<u>L</u>	<u>L</u>	<u>L</u>	<u>I</u>	<u>P</u>	A	A	L	A	S	F	I	M	A	F	G	T	G	V	-
Lep1:	M	A	N	<u>M</u>	<u>F</u>	<u>A</u>	<u>L</u>	<u>I</u>	<u>L</u>	V	I	A	T	L	V	T	G	I	L	W	C	V	D	-

Figure 18. Constructs used for photocrosslinking. The N-terminal sequences of E66 and E25 are shown with the TMS underlined, as are the N-terminal sequences of the constructs containing the first TMS of LBR (LBR1), nurim (Nur1), and Lep (Lep1). In each case, an amber codon was substituted for the codon shown at position 10, 11, 12, or 13 (boxed in figure) to position the photoreactive probe at a single nascent chain location in each sample.

ODV-E66. Two constructs, clone 91 and 92 (pGEM 4z based vector), were available in the lab (generated by Matthew Powers; MDS) that contained an amber codon at positions 10 and 12, respectively, within the coding region of E66 (sequence confirmed).

Clone 91: ATG TCT ATC GTA TTG ATT ATT GTC ATA TAG GTA ATA TTT -----
 M S I V L I I V I * V I F -----

Clone 92: ATG TCT ATC GTA TTG ATT ATT GTC ATA GTT GTA TAG TTT -----
 M S I V L I I V I V V * F -----

To generate integration intermediates of E66 that were 70 residues long and contained an amber codon at position 10, PCR was performed using clone 91 as the template and following set of primers:

Forward primer: pGMFW: 5' CGATTAAGTTGGGTAACGCC 3'

Reverse primer: E66 70mer: 5' TTGCCGAAAGGCCACTATGC 3'

To generate integration intermediates of E66 that were 70 residues long and contained an amber codon at position 12, PCR was performed using clone 92 as the template and following set of primers:

Forward primer: pGMFW: 5' CGATTAAGTTGGGTAACGCC 3'

Reverse primer: E66 70mer: 5' TTGCCGAAAGGCCACTATGC 3'

Following the PCR reaction, the PCR product was purified using the PCR purification kit (Qiagen Catalog # 28106), analyzed by agarose-gel electrophoresis, and used as template in an *in vitro* transcription reaction to generate mRNA encoding E66 70mer with an amber codon at position 10 or 12.

An amber codon was introduced at positions 11 and 13 in E66 using a two-step PCR-based mutagenesis approach. In the first step, the amber codon was introduced at position 11 or 13 using clone 60 (generated by Shawn Williamson; MDS) as the template (Fig. 19). The PCR reaction involved the following primers:

Forward primers: TAG11-E66 and TAG13-E66

TAG11-E66: 5' ATGTCTATCGTATTGATTATTGTCATAGTTTAGATATTTTT
AATATGTTTTTTGTACC 3'

TAG13-E66: 5' ATGTCTATCGTATTGATTATTGTCATAGTTGTAATATAGTT
AATATGTTTTTTGTACCTATC 3'

Reverse primer: E66 70mer: 5' TTGCCGAAAGGCCACTATGC 3'

Following the PCR reaction, the PCR product was purified using the QIAquick PCR purification kit (Qiagen, Catalog # 28106). The purified PCR product was analyzed by agarose-gel electrophoresis, and was then used as a template for the second PCR reaction. The second PCR reaction involved the following primers:

Forward primer: SP6 Kozak E66: 5' GATTTAGGTGACACTATAGAGGAAACAG
CCACCATGTCTATCGTATTGATTATTG 3'

Reverse primer: E66 70mer: 5' TTGCCGAAAGGCCACTATGC 3'

Following the second PCR reaction, the PCR product was purified using the PCR purification kit (described above), analyzed by agarose-gel electrophoresis, and used as a template in the transcription reaction(s) to generate mRNAs encoding E66 70mer with an amber codon at position 11 or 13.

Cloning information. Clone 48 containing the E66 gene was digested using Bam HI, and the ~2.0 kb fragment of E66 was gel purified. The vector pGEM4z was also digested

using Bam HI and gel purified. The E66 fragment was then ligated into the cut pGEM4z and to generate clone 60.

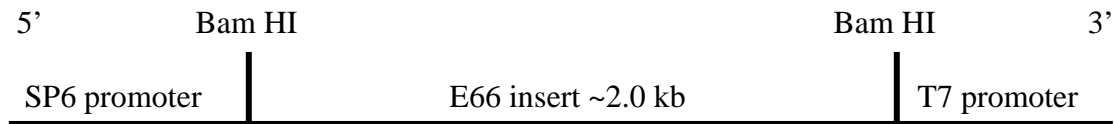


Figure 19. Schematic of clone 60. Clone 60 was generated by ligating the Bam HI digested products of clone 48 (containing the E66 gene) and pGEM4z.

ODV-E25. The viral envelope protein gene ODV-E25 (E25) was PCR-amplified from the *Autographa californica* nucleopolyhedrovirus (strain E2) HindIII C fragment and cloned into pBluescript II KS (generated by Rebecca Parr; MDS). The E25 gene was then subcloned into the in vitro translation competent vector pGEM4z to generate the pGEM4z-E25 clone.

To generate integration intermediates of E25 that were 70 residues long and contained an amber codon at position 10, 11, 12, and 13 a two-step PCR based mutagenesis approach (as described above for E66) was employed using the pGEM4z-E25 vector as the template. The first PCR reaction involved the following set of primers:

a) to generate E25 with an amber codon at position 10:

Forward primer: ODV-E25TAG10: 5' ATGTGGGGAATCGTGTTACTTATCGTTTAGCT
CATACTGTTTTATCTTTATTGG 3'

Reverse primer: ODV-E25 70mer: 5' CAATTTATTATCGCCGTGTGC 3'

b) to generate E25 with an amber codon at position 11:

Forward primer: ODV-E25TAG11: 5' ATGTGGGGAATCGTGTTACTTATCGTTTTGTAG

ATACTGTTTTATCTTTATTGGACG 3'

Reverse primer: ODV-E25 70mer: 5' CAATTTATTATCGCCGTGTGC 3'

c) to generate E25 with an amber codon at position 12:

Forward primer: ODV-E25TAG12: 5' ATGTGGGGAATCGTGTTACTTATCGTTTTGCTC

TAGCTGTTTTATCTTTATTGGACG 3'

Reverse primer: ODV-E25 70mer TAG12: 5' CAATTTATTATCGCCGTGTG 3'

d) to generate E25 with an amber codon at position 13:

Forward primer: ODV-E25TAG13: 5' ATGTGGGGAATCGTGTTACTTATCGTTTTGCTC

ATATAGTTTTATCTTTATTGGACGAATGC 3'

Reverse primer: ODV-E25 70mer: 5' CAATTTATTATCGCCGTGTGC 3'

Following the PCR reaction, the PCR product was purified using the QIAquick PCR purification kit (Qiagen, Catalog # 28106). The purified PCR product was analyzed by agarose-gel electrophoresis, and was then used as a template for the second PCR reaction. The second PCR reaction involved the following primers:

Forward primer: SP6/Kozak ODVE25: 5'GATTTAGGTGACACTATAGAGGAAACAGCC

ACCATGTGGGGAATCGTGTTACTTATC 3'

Reverse primer: ODV-E25 70mer: 5' CAATTTATTATCGCCGTGTGC 3'

Following the second PCR reaction, the PCR product was purified using the PCR purification kit (described above), analyzed by agarose-gel electrophoresis, and used as a template in the transcription reaction(s) to generate mRNAs encoding E25 70mer with an amber codon at position 10, 11, 12 or 13.

Lamin B Receptor (LBR). The lamin B receptor-green fluorescent protein fusion clone (LBR-GFP) was kindly provided by J. Ellenberg, and this was used as a template to PCR a truncated version of LBR. The LBR1 sequence (generated by Tina Heyman; MDS) is: MFGGVPGVFLIMFGLPVFLFLLLMCKQKDPPVATM.....GFP, where the second residue (F) corresponds to residue 208 in native LBR, the amino acids added in cloning are underlined, and “M.....GFP” at the C-terminus represents the GFP sequence.

To generate integration intermediates of LBR that were 72 residues long and contained an amber codon at position 10, 11, 12, and 13 a two-step PCR based mutagenesis approach (as described above for E66 & E25) was employed using the LBR-GFP clone as the template. The first PCR reaction involved the following set of primers:

a) to generate LBR with an amber codon at position 10:

Forward primer: LBR TAG10: 5' ATGTTTGGAGGAGTACCTGGTGTGTTTTAGATCATG
TTTGGCCTGCCTGTG 3'

Reverse primer: LBR 72mer: 5' GTAGGTGGCATCGCCCTCG 3'

b) to generate LBR with an amber codon at position 11:

Forward primer: LBR TAG11: 5' ATGTTTGGAGGAGTACCTGGTGTGTTTCTCTAGAT
GTTTGGCCTGCCTGTGTTC 3'

Reverse primer: LBR 72mer: 5' GTAGGTGGCATCGCCCTCG 3'

c) to generate LBR with an amber codon at position 12:

Forward primer: LBR TAG12: 5' ATGTTTGGAGGAGTACCTGGTGTGTTTCTCATCTAG
TTTGGCCTGCCTGTGTTCCTC 3'

Reverse primer: LBR 72mer: 5' GTAGGTGGCATCGCCCTCG 3'

d) to generate LBR with an amber codon at position 13:

Forward primer: LBR TAG13: 5' ATGTTTGGAGGAGTACCTGGTGTGTTTCTCATCATG

TAGGGCCTGCCTGTGTTTCCTC 3'

Reverse primer: LBR 72mer: 5' GTAGGTGGCATCGCCCTCG 3'

Following the PCR reaction, the PCR product was purified using the QIAquick PCR purification kit (Qiagen, Catalog # 28106). The purified PCR product was analyzed by agarose-gel electrophoresis, and was then used as a template for the second PCR reaction. The second PCR reaction involved the following primers:

Forward primer: SP6/Kozak LBR: 5' GATTTAGGTGACACTATAGAGCTTACAGCC

AGCATGTTCCGGAGGAGTACCTGGTGTG 3'

Reverse Primer: LBR 72mer: 5' GTAGGTGGCATCGCCCTCG 3'

Following the second PCR reaction, the PCR product was purified using the PCR purification kit (described above), analyzed by agarose-gel electrophoresis, and used as a template in the transcription reaction(s) to generate mRNAs encoding LBR 72mer with an amber codon at position 10, 11, 12 or 13.

Nurim. The nurim construct used for photocrosslinking studies was generated by Matthew Powers (MDS) using the following approach: two complementary sets of oligonucleotides were synthesized. Oligonucleotides 1 and 2 contained a 5' XbaI site followed by the nurim sequence. The second set of oligonucleotides contained overlapping regions with the first, the sequence of Nurim through amino acid #55 and a 3' PstI site. Each set was annealed in equimolar ratios, then the two sets allowed to anneal to each other and cloned into pGEM 4Z (Fig. 20).

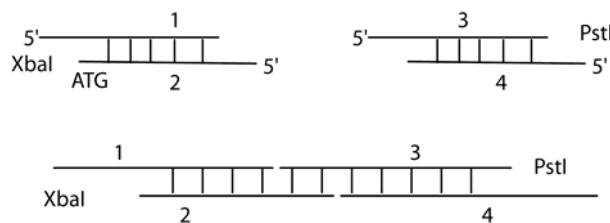


Figure 20. Design of nurim construct. The oligos used for generating the nurim construct are shown along with the restriction sites used for cloning into pGEM4Z.

The same technique was used to add amino acids 55 through 92. The final Nurim clone contains a conservative amino acid change at position 17 (L→M). The nurim sequence was obtained from Genbank #AF143676 (Rolls et al., 1999).

To generate integration intermediates of Nurim that were 72 residues long and contained an amber codon at position 10, 11, 12, and 13 a two-step PCR based mutagenesis approach (as described above for E66 & E25) was employed using the pGEM4z-Nurim clone as the template. The first PCR reaction involved the following set of primers:

a) to generate Nurim with an amber codon at position 10:

Forward primer: Nurim TAG 10: 5' ATGGCCCCTGCACTGCTCCTGATCCCTTAGGTCC
TCGCCTCTTTCATCATG 3'

Reverse primer: Nurim 72mer: 5' GTGATGGTGATGGTGATGGTGATGGTGATGTAGGG
AGACAAGCTTGCATG 3'

b) to generate Nurim with an amber codon at position 11:

Forward primer: Nurim TAG 11: 5' ATGGCCCCTGCACTGCTCCTGATCCCTGCTTAGC
TCGCCTCTTTCATCATGG 3'

Reverse primer: Nurim 72mer: 5' GTGATGGTGATGGTGATGGTGATGGTGATGTAGGG
AGACAAGCTTGCATG 3'

c) to generate Nurim with an amber codon at position 12:

Forward primer: Nurim TAG 12: 5' ATGGCCCCTGCACTGCTCCTGATCCCTGCTGCCT
AGGTCTCTTTCATCATGGCCTTTG 3'

Reverse primer: Nurim 72mer: 5' GTGATGGTGATGGTGATGGTGATGGTGATGTAGGG
AGACAAGCTTGCATG 3'

d) to generate Nurim with an amber codon at position 13:

Forward primer: Nurim TAG 13: 5' ATGGCCCCTGCACTGCTCCTGATCCCTGCTGCCC
TCTAGTCTTTCATCATGGCCTTTGGC 3'

Reverse primer: Nurim 72mer: 5' GTGATGGTGATGGTGATGGTGATGGTGATGTAGGG
AGACAAGCTTGCATG 3'

Following the PCR reaction, the PCR product was purified using the QIAquick PCR purification kit (Qiagen, Catalog # 28106). The purified PCR product was analyzed by agarose-gel electrophoresis, and was then used as a template for the second PCR reaction. The second PCR reaction involved the following primers:

Forward primer: SP6/Kozak Nurim: 5' GATTTAGGTGACACTATAGAGGAAACACCC
ACCATGGCCCCTGCACTGCTC 3'

Reverse primer: Nurim 72mer: 5' GTGATGGTGATGGTGATGGTGATGGTGATGTAGGG
AGACAAGCTTGCATG 3'

Following the second PCR reaction, the PCR product was purified using the PCR purification kit (described above), analyzed by agarose-gel electrophoresis, and used as a

template in the transcription reaction(s) to generate mRNAs encoding nurim 72mer with an amber codon at position 10, 11, 12 or 13.

Leader peptidase 1 (Lep1). A plasmid containing *E. coli* leader peptidase (signal peptidase I) gene (*lepB*) in vector pGEM 1 was a generous gift of Ingmarie Nilsson (Stockholm University, Sweden).

To generate integration intermediates of Lep1 that were 70 residues long and contained an amber codon at position 10, 11, 12, and 13 a two-step PCR based mutagenesis approach was employed using the Lep1 clone as the template. The first PCR reaction involved the following set of primers:

a) to generate Lep1 with an amber codon at position 10:

Forward primer: LepB TAG 10: 5' ATGGCGAATATGTTTGCCCTGATTCTGTAGATTGC
CACACTGGTGACGG 3'

Reverse primer: LepB 70mer: 5' TACCGGAAAAACAGAAGCACC 3'

b) to generate Lep1 with an amber codon at position 11:

Forward primer: LepB TAG 11: 5' ATGGCGAATATGTTTGCCCTGATTCTGGTGTAGGC
CACACTGGTGACGGGC 3'

Reverse primer: LepB 70mer: 5' TACCGGAAAAACAGAAGCACC 3'

c) to generate Lep1 with an amber codon at position 12:

Forward primer: LepB TAG 12: 5' ATGGCGAATATGTTTGCCCTGATTCTGGTGATTTA
GACACTGGTGACGGGCATTTT 3'

Reverse primer: LepB 70mer: 5' TACCGGAAAAACAGAAGCACC 3'

d) to generate Lep1 with an amber codon at position 13:

Forward primer: LepB TAG 13: 5' ATGGCGAATATGTTTGCCCTGATTCTGGTATTGC

CTAGCTGGTGACGGGCATTTTATG 3'

Reverse primer: LepB 70mer: 5' TACCGGAAAAACAGAAGCACC 3'

Following the PCR reaction, the PCR product was purified using the QIAquick PCR purification kit (Qiagen, Catalog # 28106). The purified PCR product was analyzed by agarose-gel electrophoresis, and was then used as a template for the second PCR reaction. The second PCR reaction involved the following primers:

Forward primer: SP6/Kozak LepB H1: 5' GATTTAGGTGACACTATAGAGGAAACAGC
CACCATGGAGTTTGCCCTGATTCTGG 3'

Reverse primer: LepB 70mer: 5' TACCGGAAAAACAGAAGCACC 3'

Following the second PCR reaction, the PCR product was purified using the PCR purification kit (described above), analyzed by agarose-gel electrophoresis, and used as a template in the transcription reaction(s) to generate mRNAs encoding Lep1 72mer with an amber codon at position 10, 11, 12 or 13.

SM-C construct used for chemical crosslinking experiments

The SM-C construct was designed by Dr. Sharon C. Braunagel and was constructed by Matthew Powers (MDS). Features of the SM-C construct (Figs. 21 & 22) that was used for chemical crosslinking experiments are the following: (i) The E66-SM sequence (N-terminal 33 amino acids of E66) is fused to a lysine/cysteine free domain of Bcl-2. (ii) The encoded protein contains an in frame T7 epitope (MASMTGGQMG) and the histidine tag (at the C-terminus). The two affinity tags can be used either singly or in tandem for the detection or purification of any crosslinked complex(es). (iii) Protein expression is driven by the SP6 promoter, and the vector backbone is the in vitro transcription/translation competent: pGEM4Z.

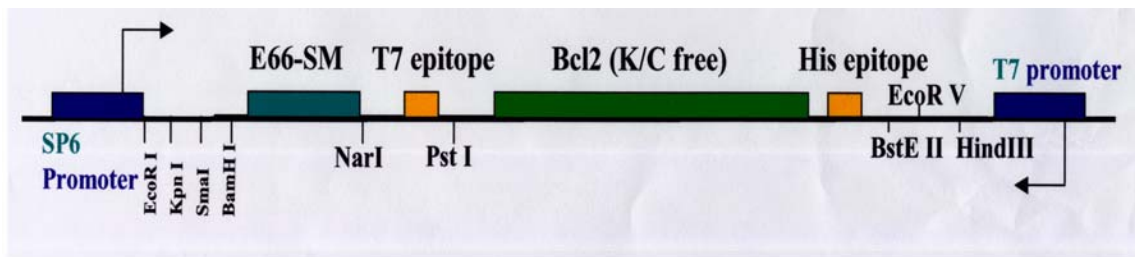


Figure 21. SM-C construct. The basic components of the SM-C construct such as the E66SM, T7 epitope, Bcl-2 domain and the His epitope are depicted. The different restriction sites available for further manipulation of the construct are also indicated.

MSIVLIIVIVVIFLICFLYLSNSNNKNDANKNNAFIGANAMASMTGGQQMGMLQ
MVAISR VVHLTLRQAGDDFSRRYRRDFAEMSSLHLPFTARGRFATVVEELFR
DGVNWGRIVAFFEFGGVIAAAAHHHHHHH

Figure 22. Features of the SM-C construct. Translation of the SM-C construct (driven by the SP6 promoter) yields a 136 residue-polypeptide whose sequence is shown. The E66SM sequence, the T7 epitope, the lysine/cysteine free domain of Bcl-2, and the histidine epitope have been highlighted in blue, yellow, green and red respectively.

The integration intermediates used in the crosslinking experiments contained nascent chains of the following lengths: 60mer, 74mer, 105mer, 120mer, 130mer and the full-length (normally terminated) 136mer. These different nascent chain lengths were generated in vitro using a PCR-based approach. Using the SM-C construct as the template, PCR reactions were conducted using different reverse primers (described below) (and the same forward primer) to generate DNA products of varying lengths. The corresponding PCR products were used in transcription reactions to generate mRNAs encoding the different nascent chain lengths.

(i) E66SM 60mer

Forward primer: pGMFW: 5' CGATTAAGTTGGGTAACGCC 3'

Reverse primer: E66SM 60mer: 5'GTGATGGTGATGGTGATGCTAGAAATCGCAAC
CATCTG 3'

(ii) E66SM 74mer

Forward primer: pGMFW: 5' CGATTAAGTTGGGTAACGCC 3'

Reverse primer: E66SM 74mer: 5'GTGATGGTGATGGTGATGGGAGAAGTCG
TCGCCGGG 3'

(iii) E66SM 105mer

Forward primer: pGMFW: 5' CGATTAAGTTGGGTAACGCC 3'

Reverse primer: E66SM 105mer: 5' GTGATGATGATGATGATGCTCCTCCACCA
CCGTG 3'

(iv) E66SM 120mer

Forward primer: pGMFW: 5' CGATTAAGTTGGGTAACGCC 3'

Reverse primer: E66SM 120mer: 5' GTGATGGTGATGGTGATGAAAGAAGGCCA
CAATCCTC 3'

(v) E66SM 130mer

Forward primer: pGMFW: 5' CGATTAAGTTGGGTAACGCC 3'

Reverse primer: E66SM 130mer: 5' GTGATGGTGATGGTGATGAGCTGCAGCTA
TGACCCC 3'

(vi) E66SM 136mer (136-R)

Forward primer: pGMFW: 5' CGATTAAGTTGGGTAACGCC 3'

Reverse primer: Summers reverse: 5' GTATGTTGTGTGGAATTGTGAGC 3'

Primers used for generating different derivatives of clone 2

1) To generate the full-length clone 2 initiating at the first methionine residue (Met₁) and T7-tagged at the C-terminus, the following primers were used:

Forward primer: SP6/Kozak initial 2-2 start (MSG--): 5' GATTTAGGTGACACTATAGAG
GAAACACCCACCATGTCCGAGGAGGGCGAG 3'

Reverse primer: T7/ STOP 2-2: 5' CTAGAATGATATTGCGACCATTTCAGCATTGATG
AAGACTCCCTCTGTG 3'

2) To generate the internal derivative of clone 2 (Met₁₃₀₋₄₅₄) that is T7-tagged at the C-terminus, the following primers were used:

Forward primer: SP6/Kozak internal 2-2 start (MLEAL...): 5'GATTTAGGTGACACTATA
GAGGAAACACCCACCATGCTGGAGGCGCTGCCC 3'

Reverse primer: T7/ STOP 2-2: 5' CTAGAATGATATTGCGACCATTTCAGCATTGATG
AAGACTCCCTCTGTG 3'

3) To generate the Met₃₁₀₋₄₅₄ derivative of clone 2 that is T7-tagged at the C-terminus, the following primers were used:

Forward primer: SP6/Kozak 2-2: 5' GATTTAGGTGACACTATAGAGGAAACACCCACC
ATGTGCGCCGCTGTCC 3'

Reverse primer: T7/ STOP 2-2: 5' CTAGAATGATATTGCGACCATTTCAGCATTGATG
AAGACTCCCTCTGTG 3'

4) To generate the Met₃₅₆₋₄₅₄ derivative of clone 2 that is T7-tagged at the C-terminus, the following primers were used:

Forward primer: 2-2 Start: 5' GATTTAGGTGACACTATAGAGGAAACACCCACC
ATGCCGCGCCTGCCCAC 3'

Reverse primer: T7/ STOP 2-2: 5' CTAGAATGATATTGCGACCATTTCAGCATTGATG
AAGACTCCCTCTGTG 3'

5) To generate the Met₁₋₃₀₉ derivative of clone 2 that is T7-tagged at the C-terminus, the following primers were used:

Forward primer: SP6/Kozak initial 2-2 start (MSG.....): 5' GATTTAGGTGACACTATAGA
GGAAACACCCACCATGTCCGAGGAGGGCGAG 3'

Reverse primer: T7 Internal stop/2-2: 5' CTAGAATGATATTGCGACCATTTCAGCATG
ACCCACAGCAGCCGCAG3'

6) To generate the Met₁₃₀₋₃₀₉ derivative of clone 2 that is T7-tagged at the C-terminus, the following primers were used:

Forward primer: SP6/Kozak internal 2-2 start (MLEAL...): 5' GATTTAGGTGACACTATA
GAGGAAACACCCACCATGCTGGAGGCGCTGCCC 3'

Reverse primer: T7 Internal stop/2-2: 5' CTAGAATGATATTGCGACCATTTGCAGCATG
ACCCACAGCAGCCGCAG3'

Preparation of Lys-tRNA^{amb}

Lys-tRNA^{amb} was prepared by Yiwei Miao and Yuanlong Shao using the protocol described below. Using a plasmid encoding the wild-type *Escherichia coli* (*E.coli*) lysine tRNA gene, site-directed mutagenesis was performed to change the anticodon loop to CUA and thus create an amber suppressor tRNA (hereafter termed tRNA^{amb}) that was a generous gift from Dr. Greg Beckler (Promega, Madison, WI). PCR was performed to amplify the region of the plasmid that contained the T7 promoter sequence and the amber-suppressor tRNA gene. A typical PCR reaction contained in 100 μ l: 1X Ex TaqTM polymerase buffer (supplied with Ex TaqTM polymerase from Panvera, Madison, WI), 1.5mM MgCl₂, 200 μ M dNTPs, 100pmol upstream primer (1035-YM), 100pmol of downstream primer (1043-YM), and 2.5 units of Ex TaqTM polymerase. The reaction was started with 2 min at 94°C, followed by 30 cycles of denaturation (94°C for 15 s), annealing (60°C for 15 s) elongation (72°C for 15 s), followed by a final extension step of 10 min at 72°C. Next a 10 μ l aliquot of the PCR reaction was run on a 1.6% agarose/TBE [90mM Tris-borate, 2mM EDTA pH 8.0] gel to confirm the size of the desired product. Following purification of the PCR product using the Qiagen PCR purification product, the purified product was then *in vitro* transcribed in a standard 100 μ l reaction that contained 80mM HEPES (pH 7.5), 16mM Mg Cl₂, 2mM spermidine, 10mM DTT, 4mM ATP, 4mM CTP, 0.4mM GTP, 4mM UTP, 12 μ l of the purified PCR product, 0.1 units of pyrophosphatase, 2 units of RNasinTM (Promega, Madison, WI) and

2.5 μ l of T7 RNA polymerase (1.35-1.45 A₂₈₀ units/ml). The reaction was incubated at 37°C for at least 4 hours.

An aliquot of the transcription reaction was analyzed on a 1.6% agarose /TBE gel and following confirmation of the expected product, the remainder of the sample underwent purification by anion exchange chromatography using a Mono Q HR 10/10 column on an FPLC (Pharmacia). The tRNA was eluted in 10mM NaOAc (pH 4.5), 5mM MgCl₂ using a 115ml linear gradient of NaCl from 480mM to 1M.

Aminoacylation was performed to determine which fractions were enriched in tRNA^{amb} as described previously (Crowley et al., 1983; Johnson et al., 1982; Krieg et al., 1989) with the modification that 6mM MgCl₂ and no KCl was used. The majority of the tRNA eluted near 550mM NaCl and the fractions with the highest functional tRNA^{amb} content were aminoacylated with [¹⁴C]-Lysine and stored at -80°C until needed (Flanagan et al., 2003).

Chemical modification of Lys-tRNA^{amb}

Aminoacylation and purification of *E.coli* tRNA^{amb} was performed by Yuanlong Shao and Yiwei Miao as outlined above and described previously (Flanagan et al., 2003). The specific activity of an aminoacylated tRNA sample is expressed in pmoles Lys/A₂₆₀ units of tRNA, with pure Lys-tRNA^{amb} having a specific activity near 1600 pmol Lys/A₂₆₀ unit tRNA. Chromatographically purified Lys-tRNA^{amb}, usually at a specific activity in excess of 1000 pmol Lys/A₂₆₀ unit was used for the chemical modification process along with the N-5-azido-2-nitrobenzoic acid (ANB-NOS; Pierce Chemicals). In a typical reaction, ANB-NOS reagent (stored at -20°C) was allowed to

come to room temperature in the dark, and 7.5 g of ANB-NOS was added to 1.75 ml of dimethylsulfoxide (DMSO; Gold Label, Aldrich Chemicals) for each reaction. Fresh solutions of 4M KOH, 4M HOAc, 2M KOAc (pH 5.0), and 500mM potassium phosphate (pH 7.0) were also prepared. A 3 dram vial and a 2mm x 7mm stir bar were washed with ddH₂O and acetone to ensure that they were clean and nuclease-free. The 3 dram vial was then set in an ice water bath and held in place using a retort stand and clamp. The ice water bath was set on top of a stir plate to ensure constant stirring during the course of the entire labeling reaction. All of the following steps were performed in the dark room illuminated only with red safety lights, the kind used in photographic dark rooms. [¹⁴C]Lys-tRNA^{amb} (5000pmoles) was added to the vial along with ddH₂O and 0.5M potassium phosphate (pH 7.0) to yield a final concentration of 50mM of the latter in a total volume of 750μl. Then 1.75 ml of the ANB-NOS/DMSO solution was added and the stirring speed was quickly reset due to the increased volume of the solution. Next 15μl of 4M KOH was added, and the reaction was allowed to proceed for only 14 sec (absolutely no longer than 14 sec) at which point 15μl of 4M HOAc was added along with 2.5 ml of 2M KOAc (pH 5.0). The KOH was added to deprotonate the ε-amine group of the lysine residue and initiate the nucleophilic attack of the ANB-NOS reagent. The HOAc was added to stop the reaction by lowering the pH back to neutral. The contents of the 3 dram vial were then transferred to an SW-28 polyallomer centrifuge tube and 26 ml of cold 100% EtOH was added to precipitate the tRNA. After a second reaction volume was added to the same SW-28 polyallomer centrifuge tube (Beckman

Instruments), the tubes were wrapped in aluminum foil to prevent exposure to light and placed at -20°C overnight.

The next day the samples were loaded in the dark in an SW-28 rotor (Beckman Instruments) and centrifuged at 28,000 rpm for 2.5 hrs at 4°C . The supernatant, which contains free ANB, was discarded, and the pellet was dried under a stream of nitrogen gas. The dried pellet was resuspended in 300 μl of tRNA buffer [1mM KOAc (pH 5.0), 2mM MgCl_2]. The modified Lys-tRNA^{amb}, N^ε-(ANB)-[^{14}C]Lys-tRNA^{amb} (termed $\epsilon\text{ANB-Lys-tRNA}^{\text{amb}}$ from here on), was then dialyzed against 3 volumes of tRNA buffer for 2 hrs at 4°C in the dark by wrapping everything in aluminum foil. The tRNA solutions were then split into 25 μl aliquots in microfuge tubes, wrapped in aluminum foil, frozen in liquid N_2 , and stored at -80°C . An aliquot of the sample was then used in the characterization of the $\epsilon\text{ANB-Lys-tRNA}^{\text{amb}}$.

Characterization of modified Lys-tRNA^{amb}

$\epsilon\text{ANB-Lys-tRNA}^{\text{amb}}$ was normally characterized by Yiwei Miao and Yuanlong Shao prior to its use in photocrosslinking experiments. Typically 2 μl of the dialyzed $\epsilon\text{ANB-Lys-tRNA}^{\text{amb}}$ was aliquoted into four duplicate tubes, then diluted to 400 μl with buffer A [1mM KOAc (pH 5.0), 5mM MgCl_2]. Two tubes were used to measure the absorbance at 260 nm to obtain the tRNA concentration, while the remaining two tubes were used to determine the amount of [^{14}C]Lys-tRNA^{amb} by liquid scintillation counting. Typically, the $\epsilon\text{ANB-Lys-tRNA}^{\text{amb}}$ preparations had specific activities that ranged from 500-1100 pmol Lys/ A_{260} unit. The decrease in the specific activity after modification was due to

deacylation of the Lys-tRNA^{amb} during the reaction at high pH and the subsequent workups.

The extent of lysine modification was assayed by paper electrophoresis as described earlier (Johnson et al., 1976). Briefly, ϵ ANB-Lys-tRNA^{amb} (~15,000dpm) was hydrolyzed in freshly prepared 50mM triethylamine at 37°C for 90 minutes and dried under nitrogen gas. The sample was resuspended in water and spotted onto electrophoresis paper (Whatmann 3mm) at the origin (20 cm from the anode, 80 cm from the cathode). Free lysine, N ^{α} -acetyl-Lys and N ^{ϵ} -acetyl-Lys standards were also spotted onto the same electrophoresis paper in different lanes, and all samples were separated in buffer B [10% (v/v) glacial acetic acid, 1% (v/v) pyridine] at 25V/cm for 3 hours. After drying overnight, in a fume hood, the sample lane was cut into one hundred 1 cm strips and then counted in a liquid scintillation counter, while the strips containing the standards were stained with ninhydrin to determine the position of the unlabeled α -labeled, and ϵ -labeled lysine. Typically, greater than 82% of the Lys was labeled with ANB at the ϵ -amino group of Lys, while <3% was labeled at the α -amino group, and <12% remained unmodified.

Preparation of wheat germ extract

Nuclease treated wheat germ extract was prepared by Yiwei Miao and Yuanlong Shao as described by Erickson and Blobel (1983), except that the material was resolved by chromatography using a Sephadex G-25 column and stored in 40mM HEPES (pH 7.4), 100mM KOAc (pH 7.5), 5mM Mg(OAc)₂, 2mM glutathione and 100 μ M EGTA. The gel filtration step was necessary to remove the amount of endogenous amino acids

in the wheat germ extract. This was critical with respect to lysine and methionine, because endogenous Lys and Met would compete with ϵ ANB-Lys-tRNA^{Lys} and [³⁵S]Met for incorporation into polypeptides. The wheat germ extract was in buffer that contained 2mM glutathione rather than dithiothreitol (DTT) because the latter was a much stronger reducing agent and chemically reacts with the aryl azide, thereby quenching or preventing the photocrosslinking.

Sf9 microsomes

To prepare virus-infected Sf9 microsomes, Sf9 cells were infected with the E2 strain of AcMNPV (moi=10) and collected 33 hours post infection (Infrastructure for all cell culture, virus work was provided by Summers laboratory staff). 30 g of cells were diluted with 4 ml/per gram cell mass of buffer A [50 mM triethanolamine (pH 7.5), 50 mM KOAc, 6 mM Mg(OAc)₂, 1 mM EDTA, 1 mM DTT and 0.5 mM phenylmethylsulfonyl fluoride] and homogenized with 10-12 strokes using a motor-driven drill homogenizer, avoiding foam formation and heating. The homogenate was centrifuged for 10 min at 1000g. The supernatant was recentrifuged for 10 min at 10,000g. Crude rough microsomes were collected by centrifugation of the 10,000g supernatant for 2.5 h at 140,000g (Beckman Ti50.2 rotor at 40,000 rpm) through a cushion of 1.3 M sucrose in buffer A. The pellets were resuspended by manual homogenization in a Dounce homogenizer in buffer B [250 mM sucrose, 50 mM triethanolamine (pH 7.5) and 1 mM DTT] to a concentration of 50 A₂₈₀ units/ml. The microsomes were active, as judged by their ability to target and translocate preprolactin

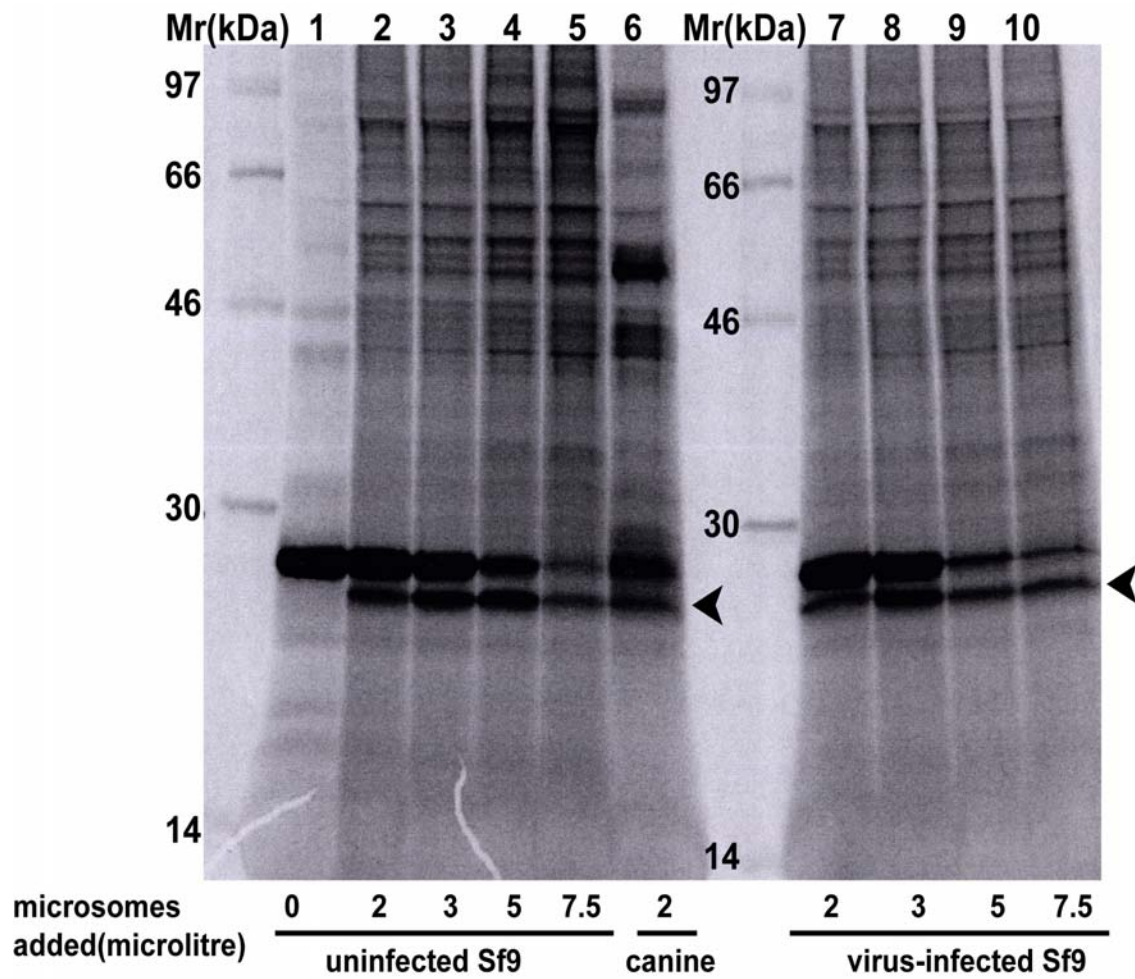


Figure 23. Translocation competence of Sf9 microsomes. Signal sequence processing of preprolactin using different aliquots of virus-infected and uninfected Sf9 microsomes. Processed product is indicated by the arrowhead.

in rabbit reticulocyte lysate at levels comparable to canine pancreatic microsomes (Fig. 23, lanes 7-10).

Uninfected Sf9 microsomes were prepared using the same procedure as described above with the exception that homogenization involved 6-8 dounces using a motor-driven drill homogenizer, avoiding foam formation and heating. The microsomes were active, as judged by their ability to target and translocate preprolactin in rabbit reticulocyte lysate at levels comparable to canine pancreatic microsomes (Fig. 23, lanes 1-6).

Microsomes were also isolated (33 h p.i.) from Sf9 cells infected with the recombinant virus expressing E66SM Δ T7. Recombinant virus development, cell culture and microsome isolation was performed by Summers laboratory staff (Sharon Braunagel and Genevieve Ledwell).

Purification of signal recognition particle and canine pancreatic microsomes

The purification of SRP from canine pancreatic tissue was performed by Yuanlong Shao and Yiwei Miao as previously described (Walter and Blobel, 1983a). The isolation of column-washed rough microsomal membranes was also performed as described elsewhere (Walter and Blobel, 1983b), except that the microsomes were eluted with, and stored in 50mM HEPES (pH 7.5) and 1mM glutathione after treatment with *Staphylococcus* Nuclease (Boehringer-Mannheim).

PCR-generated translation intermediates

Using 5'-primers designed to include the start methionine, and the SP6 polymerase binding site and 3'-primers designed to generate DNA products of appropriate lengths, PCR was performed on the relevant genes.

In vitro run-off transcription

Typically a 100 μ l in vitro run-off transcription consisted of the following: 2 μ g of PCR-amplified DNA fragments (see above), 80mM HEPES (pH 7.5), 16mM MgCl₂, 2mM spermidine, 10mM DTT, 0.3mM GTP, 3mM each of ATP, UTP, and CTP, 500 μ M diguanosine triphosphate [G(5')ppp(5')] (Amersham) which serves as a synthetic mRNA cap, 150 units of RNasin (Promega Biotech) and 100 units of purified SP6 RNA polymerase. The reaction was incubated at 37°C for 90 min and then 3.2 μ l of 100mM GTP was added and the reaction was continued for another 30 min. Following this, a standard ethanol precipitation was performed and the mRNA was resuspended in 120 μ l of ddH₂O. The yield and homogeneity of the transcription products were confirmed on a 1.6% agarose/TAE gel.

In vitro translations using wheat germ extract

mRNAs generated from the in vitro run-off transcriptions were translated in a cell-free protein synthesis system using wheat germ extract. A typical reaction volume was standardized to 50 μ l although increments of this volume (e.g. 100 μ l etc.) were often used. The reactions were performed in 1.5ml eppendorf tubes at 26°C for 40 min. The translations contained 100mM KOAc (pH 7.5), 20mM HEPES (pH 7.5), 3.2mM Mg(OAc)₂, 200 μ M spermidine, 8 μ M S-adenosylmethionine (Sigma), 0.0024% (v/v)

NikkolTM (octaethyleneglycol-mono-N-dodecyl ether, Nikkol Chemicals), 2mM glutathione (pH 7.5), and 20% (v/v) wheat germ extract. An energy-generating system (containing ATP, GTP, creatine phosphate, creatine phosphokinase, and nineteen amino acids excluding methionine), RNAsinTM (ribonuclease inhibitor, Promega), and protease inhibitors (antipain, leupeptin, pepstatin, chymostatin, trasylol; Sigma) were also included in the translations. [³⁵S]-methionine (MP Biomedical) was added to the *in vitro* translation reaction at a final concentration of 0.5 μ Ci/ μ l.

The *in vitro* translations were normally checked by either hot trichloroacetic acid (TCA) precipitation to assess the efficiency of the translation reaction or by sodium dodecylsulfate polyacrylamide gel electrophoresis (SDS-PAGE) to assess the integrity of the protein products and also for molecular weight determination.

In vitro translations using rabbit reticulocyte lysate

mRNAs generated from the *in vitro* run-off transcriptions were translated in a cell-free protein synthesis system using nuclease-treated rabbit reticulocyte lysate (Promega). The reactions were performed in 1.5ml eppendorf tubes at 30°C for 40 min. The translations contained amino acid mixture minus methionine (Promega), RNAsinTM (ribonuclease inhibitor, Promega), and microsomes. [³⁵S]-methionine (MP Biomedical) was added to the *in vitro* translation reaction at a final concentration of 0.5 μ Ci/ μ l.

The *in vitro* translations were normally checked by either hot trichloroacetic acid (TCA) precipitation to assess the efficiency of the translation reaction or by sodium dodecylsulfate polyacrylamide gel electrophoresis (SDS-PAGE) to assess the integrity of the protein products and also for molecular weight determination.

Trichloroacetic acid precipitation

The in vitro translations were often checked by hot trichloroacetic acid (TCA) precipitation followed by filtration through nitrocellulose filters. Typically, 2 μ l of a translation mix was removed and added to a 13 x 100 mm glass test tube that contained 1 ml of 10% (w/v) TCA, and 3% (w/v) casamino acids (CAA). The samples were subsequently incubated at 85°C for 10 min using a water bath (the heating in acid destroyed any RNA molecules, but precipitated polypeptides). The test tubes were placed in ice for 2 min to cool the sample prior to filtration. The samples were vortexed and then filtered under vacuum through a 25mm Metrical membrane filter (45 μ m pore size; Gelman Sciences) that had been prewashed with 3 ml of cold 5% (w/v) TCA. The precipitate on each filter was then washed three times with 3 ml of cold 5% (w/v) TCA. The filters were dried under a heat lamp for 10 min and then counted in a liquid scintillation counter (Beckman Coulter). Translations that lacked any added mRNA served as the reference and their counts were operationally defined as background.

An alternative method that was often used to check in vitro translation was to precipitate the translation reaction with cold TCA and then analyze the samples by SDS-PAGE. Typically, after the translation reaction was completed, an equal volume of cold 25% (w/v) TCA was added to each sample. The samples were incubated on ice for 10 min and then sedimented at 4°C for 5 min in a microcentrifuge tube at maximum speed. The supernatants were removed by aspiration, and the pellets were washed with 1ml of acidic acetone (19 volumes acetone: 1 volume 0.1M HCl). The samples were again sedimented at 4°C for 2 min and the pellets were dried under vacuum in a Speed Vac

concentrator (Savant) for 15 min. The pellets were ultimately resuspended in sample buffer and electrophoresed on SDS-PAGE gels.

Generation of integration intermediates

Integration intermediates were generated by including in the *in vitro* translation reactions (50 μ l), SRP and column-washed rough microsomes (CRMs) at final concentrations of 40nM and 8 equivalents (1 eq = 50 A280 units/ μ l; Walter and Blobel, 1983b) respectively. Fully assembled integration intermediates with nascent chains of a defined length were prepared *in vitro* by translating mRNAs that were truncated in the coding region. Ribosomes halt when they reach the ends of such mRNAs, but they do not dissociate from the mRNA because the absence of a stop codon prevents normal termination from occurring. Thus, the nascent chain remains bound to the ribosome as a peptidyl-tRNA, and the length of the nascent chain is dictated by the length of the truncated mRNA added to the translation. To examine the environment of a TMS at different stages of integration, we prepared integration intermediates with [³⁵S]Met-labeled nascent chains of different lengths, each with a single photoreactive probe located at or near the center of its TMS.

Photoreactive probes were incorporated into nascent chains by translating the mRNA in the presence of N^ε-(5-azido-2-nitrobenzoyl)-Lys-tRNA^{amb} (ϵ ANB-Lys-tRNA^{amb}) that recognizes an amber stop codon. To ensure that each nascent chain received only a single probe, each coding sequence contained only a single in-frame amber stop codon. It is important to note that the modified Lys-tRNA incorporates an uncharged amino acid

into the protein instead of a charged lysine residue, so this experimental approach does not compromise the hydrophobicity of the TMS.

Integration intermediates to be used that are to be used in photocrosslinking studies were generated by in vitro translation reactions similar to those described above, with a few modifications. The final concentration of [³⁵S]methionine in the translation was increased to 2μCi/μl so that the photoadducts could be detected on SDS-PAGE gels. Seventy-two pmoles of εANB-Lys-tRNA^{amb} were included in the incubations in the dark to allow incorporation of the photoreactive probes into nascent polypeptide chains. All translations were performed at 26°C for 40 min in the dark.

Photoreactions

The translation reaction was stopped by placing the samples on ice for 10 min prior to ultraviolet radiation exposure. In some experiments, puromycin was added to a final concentration of 2mM and incubated at 26°C for 30 min either prior to or after photolysis. The samples were photolyzed at 0°C for 15 min using a 500-W mercury arc lamp (Oriel) at a distance of 12cm through a filter combination (Oriel 59855 and 66236) that provides a 300-400nm bandpass.

After photolysis, the microsomal membranes were isolated by sedimentation through a sucrose cushion [0.5M sucrose/100mM KOAc (pH 7.5)/20mM HEPES (pH 7.5)/3.2mM Mg(OAc)₂] at 100,000g for 4 min in a TLA 100 rotor (Beckman). The supernatants were discarded, while the membrane pellets were resuspended in sample buffer (with DTT) and analyzed by SDS-PAGE.

Chemical crosslinking

All chemical crosslinking reactions performed in this work were done following the translation of the substrate using nuclease-treated rabbit reticulocyte lysate (Promega). In vitro translations (30°C, 45 min, 100µl) were performed in the presence of nuclease-treated Rabbit reticulocyte lysate (Promega), amino acid mixture minus methionine (Promega), RNasin (Promega), 30 equivalents of Sf9 rough microsomes (Saksena, 2004), and 50µCi of [³⁵S] Met (1Ci = 37GBq). After translation, samples were sedimented through a 100µl sucrose cushion [0.5M sucrose/20mM Hepes, pH 7.5/100mM KOAc/3.2mM Mg(OAc)₂] in a Beckman TLA ultracentrifuge at 4°C for 4mins at 100,000 rpm in a TLA 100 rotor. The resulting membrane pellet was resuspended in 100µl of crosslinking buffer (25mM Na-phosphate/150mM NaCl, pH 7.0) and the crosslinking reagent BS³ (Pierce) was added to 2.5mM or 50µM in some cases. Samples were incubated at 22°C for 30mins. In the case where SMPB (Pierce) was used as the chemical crosslinker, the membrane pellet was resuspended in 100µl of crosslinking buffer (20mM Hepes, pH 7.5/20mM KOAc/5mM MgCl₂) and the crosslinking reagent was added to 50µM. Samples were incubated at 22°C for 30 mins and the crosslinking reagent quenched by the addition of 40mM DTT and 40mM Tris-HCl (pH 7.5). The quenching reaction was allowed to proceed for 20 mins at 22°C.

Purification of crosslinked products using TALON beads

Following crosslinking, the samples were treated with a denaturing solution (4M urea/1% SDS) for 30 min at 37°C, prior to being incubated with 40µl of Dynabeads

TALON (Dynal Biotech) pre-equilibrated (22°C , 1hr) with 0.75 ml of washing & binding buffer (50mM Na-phosphate, pH 8.0/300mM NaCl/0.01% Tween-20). After allowing 35 mins at 22°C for the binding reaction to occur, the sample-containing tubes were placed on a magnet until the beads migrated to the side of the tube and the supernatant was discarded. The beads were washed four times with 0.7 ml of the washing & binding buffer (50mM Na-phosphate, pH 8.0/300mM NaCl/0.01% Tween-20), following which the bound material was eluted using 40µl SDS-sample buffer. The eluted material was heated at 95°C for 10 mins prior to being analyzed by SDS-PAGE.

Alkaline extraction

The standard operational criterion to determine whether a protein is integrated into microsomal membranes is to assess its solubility in alkaline (pH 11-12) buffers (Fujiki et al., 1982). A protein is considered membrane-integrated if the protein is insoluble in alkaline buffers.

Samples to be analyzed by alkaline extraction were subjected to alkaline conditions after photolysis. Typically, Na₂CO₃ (pH 11.5) was added to each photolyzed sample to a final concentration of 100mM, and then incubated on ice for 20 min. The samples were sedimented through an alkaline cushion [0.5M sucrose/100mM Na₂CO₃ (pH 11.5)] at 100,000g for 4 min in a TLA 100 rotor (Beckman). The supernatant and membrane pellet fractions were separated and analyzed by SDS-PAGE.

High-salt wash

Samples to be analyzed by high salt wash were treated with 0.5M KOAc (potassium acetate) and incubated on ice for 20min. Following the incubation, samples were

sedimented through a high salt cushion (20mM HEPES, 500mM KOAc, 3.2mM Mg(OAc)₂, 0.5M sucrose) at 100,000g for 4 min in a TLA 100 rotor (Beckman). The supernatant and membrane pellet fractions were separated and analyzed by SDS-PAGE.

Immunoprecipitations

Prior to immunoprecipitation, the microsomal membranes were isolated by sedimentation as described above. For immunoprecipitations using affinity-purified antibodies raised against the C-terminal 14 residues of Sec61 α (Research Genetics, Huntsville, AL), the membrane pellet was solubilized in 50 μ l of resuspension buffer [2% (w/v) SDS, 100mM Tris-HCl (pH 7.5)] by heating at 55°C for 30 min. The samples were thoroughly mixed, transferred to new 1.5 ml microfuge tubes, and then diluted to 500 μ l with buffer A [140mM NaCl, 10mM Tris-HCl (pH 7.5), 2% (v/v) Triton X-100]. Individual samples were precleared by adding 40 μ l of protein A-Sepharose (Sigma) and rocking at room temperature for 1 hr before the sepharose beads were removed by sedimentation. Sec61 α specific antibodies were added to each sample and rocked at 4°C overnight. On the following day, 40 μ l of 2x-diluted protein A-Sepharose in buffer A was added to each sample and the incubation was allowed to continue for another 3 hours at 4°C. The immunoprecipitate was recovered by sedimentation, washed twice with buffer A, and then washed a final time with the same buffer containing no detergent. Immunoprecipitated material was separated by SDS-PAGE as before (Do et al., 1996) and visualized using a Bio-Rad FX phosphorimager.

For immunoprecipitations using affinity-purified antibodies raised against the C-terminal 13 residues of TRAM (Research Genetics, Huntsville, AL), the membrane

pellet was solubilized in 50 μ l of resuspension buffer [1% (w/v) SDS, 100mM Tris-HCl (pH 7.5)] by heating at 55°C for 30 min. Each sample was diluted to 500 μ l with buffer B [150mM NaCl, 50mM Tris-HCl (pH 7.6), 2% (v/v) Triton X-100, 0.2% (w/v) SDS] and rocked overnight at 4°C after the addition of TRAM-specific antibodies. On the following day, 40 μ l of 2x-diluted protein A-Sepharose in buffer A was added to each sample and the incubation was allowed to continue for another 3 hours at 4°C. The immunoprecipitate was recovered by sedimentation, washed twice with buffer B, and then washed a final time with the same buffer containing no detergent. The immunoprecipitated material was separated by SDS-PAGE, and visualized using a Bio-Rad FX phosphorimager.

For immunoprecipitations using antibodies specific for SRP54 (provided by Ingmarie Nilsson), FP25K (generated by Robert Harrison), E26 (generated by Hideo Beniya), p39 (provided by Loy Volkman), polyhedrin and E25 (generated by Sharon Braunagel), T7 tag (Novagen), and karyopherin alpha (BD Biosciences), the same conditions were used as described above for the TRAM antibody. The antibody raised against bacterially expressed E26 (antisera #12500) was a generous gift of Jared Burks.

SDS-PAGE electrophoresis

Samples of in vitro translations or photocrosslinking experiments were separated by sodium dodecylsulfate polyacrylamide electrophoresis (SDS-PAGE). The resolving gel was ~14cm in height, 19cm wide, and 0.8mm thick. Samples were loaded into sample wells in a 2 cm stacking gel located on top of the resolving gel. Unless indicated otherwise, the majority of the resolving gels used in this dissertation were linear 10-15%

(w/v) polyacrylamide gradient gels [diluted from a 30% (w/v) acrylamide, 0.8% bisacrylamide stock solution]. The resolving gel also contained 400mM Tris (pH 8.8), 0.08% (w/v) SDS, 0.02% (v/v) N, N, N', N'-tetramethyl ethylenediamine, and 0.017% ammonium persulfate (all materials were purchased from Sigma Chemicals). The stacking gel was 4% (w/v) polyacrylamide that contained all the other components of the resolving gel except that this gel was buffered in 60mM Tris (pH 6.8).

Samples were prepared for electrophoresis either by boiling for 10 min or by incubating at 37°C for 10 min in sample buffer [120mM Tris base, 3.6% (w/v) SDS, 7.5mM EDTA, 125mM DTT, 15% (v/v) glycerol, and a trace amount of bromophenol blue]. The samples were run at 15 milliamperes through the stacking gel and then separated at 30 milliamperes through the resolving gel using a running buffer that contained 400mM glycine/50mM Tris base/0.1% (w/v) SDS (pH 8.8).

After SDS-PAGE, the gels were stained for 15 min at room temperature with gentle shaking in 50% (v/v) methanol/10% (v/v) glacial acetic acid/ and 0.125% (w/v) Coomassie Brilliant Blue (Sigma). The gels were destained for at least 30 min at room temperature with shaking in 35% (v/v) methanol/10% (v/v) glacial acetic acid. The gels were then washed thoroughly with distilled water prior to drying at 80°C to remove the acetic acid, because the Bio-Rad phosphorimaging screens will be damaged by residual acids. The dried gels were then exposed on the phosphorimaging screens and visualized using a Bio-Rad GS-250 phosphorimager.

SDS-PAGE, western transfer and immunoblotting

Following SDS-PAGE (described above), gels were either stained with Commassie blue (0.1% Commassie R-250, 10% methanol) and destained/fixed (45% acetic acid, 10% methanol), or transferred to Immobilon-P membrane (Millipore, Billerica, MA, catalog # IPVH 000 10) using the tank transfer method. Blots were treated with blocking solution (3% non fat dried milk, 50mM Tris-HCl, 150mM NaCl, 0.05% Tween-20, pH 7.4) for 30 minutes at RT, then incubated with primary antibody (diluted in blocking solution) for either 2 hours at RT, or overnight at 4°C. Blots were washed three times (10 minutes per wash, RT) with TBS-T (50mM Tris-HCl, 150mM NaCl, 0.05% Tween-20, pH 7.4), followed by incubation with secondary antibody conjugated to horseradish peroxidase (HRP) (1:10000, blocking solution, 1 hour, RT). The blots were washed three times with TBS-T, and developed using the Western LightningTM chemiluminescence reagent kit (Perkin Elmer, Boston, MA, NEL100) and Kodak X-Omat Blue XB-1 film (Eastman, Kodak Company, New Haven, CT).

cDNA expression-library screen

Sf9 cDNA expression library was a generous gift of Christian Gross and was screened using the E26 antibody under the guidance of Sharon Braunagel.

Primary screen. 100µl of undiluted Sf9 cDNA expression library was added to 0.6mls of plating cells (BB4) followed by incubation at 37°C for 30 min. The adsorbed phage was mixed with 15 ml of prewarmed (42°C) top agarose (0.7% agarose/0.2% maltose/10mM MgSO₄) and plated on NZCYM plates. The plates were left for 6 hrs at 37°C and once pin-sized zones of clearing (plaques) became visible, they were overlaid

with nitrocellulose membranes {137MM (pore size:0.45µm) Pure Nitrocellulose transfer and immobilization membrane, Schleicher & Schnell, Dassel, Germany} presoaked in 10mM IPTG. Once the membranes were placed, appropriate registration marks were made on both the membrane and the plate surface to allow accurate superimposition of any positive plaque on the membrane with the corresponding plaque on the plate.

Following an overnight incubation, the nitrocellulose membranes were lifted from the plates, treated with a blocking solution [150mM NaCl, 10mM Tris (pH 8.0), 3% (w/v) non fat dried milk, 0.1% Tween 20] (22°C, 45min), and incubated with 30µl of antisera # 12499 (4°C, 12 hrs). After incubation with the antibody, the membranes were washed three times (15min/wash) with TTBS [150mM NaCl, 10mM Tris (pH 8.0), 0.1% Tween 20] and then incubated with 2µl of [¹²⁵I]-Protein A {MP Biomedical} (22°C, 6 hrs). Membranes were washed three times with TTBS as described above, air dried and exposed for 3 days to a X-ray plate (XOMAT-AR, Kodak) for visualization. Making use of the registration marks, the positive plaques on the NZCYM plates were identified and cored into a sterile tube containing 0.5ml of phage buffer (0.1M NaCl, 8mM MgSO₄.7H₂O, 50mM Tris pH 7.5, 0.01% gelatin) and 20% chloroform. Secondary and tertiary screens were conducted in the same way as described above except that 200µl of plating cells was mixed with 100µl of the cored phage stock.

In vivo excision and rescue. 200µl of XL-1 Blue cells (OD₆₀₀=1.0) were mixed with 200µl of an appropriate dilution (10⁻¹/10⁻²/10⁻³) of the cored phage stock (derived from the tertiary screen), 10µl of R408 helper phage [1x10¹¹ pfu/ml – 1x10⁶ pfu/ml] (Stratagene), and incubated at 37 °C for 15 min. 5.0 ml of 2XYT media was added to the

sample and incubated overnight in a 37°C shaking incubator. Following overnight incubation, the samples were heated at 70°C for 20 min and the phagemids packed as filamentous phage particles were recovered in the supernatant following centrifugation (4°C, 4min, 4500 rpm). 200µl of the supernatant was added to 200µl of XL-1 Blue cells (OD₆₀₀=1.0), incubated at 37°C for 15 min, and 25µl of the mix was plated on LB/amp⁵⁰ plates. The pBluescript plasmid with the cloned cDNA insert was isolated from the resultant colonies by using the Qiagen DNA Miniprep kit.

DNA sequencing

Polymerase chain reaction (PCR) was performed using a MJ Research DNA Engine Peltier Thermal Cycler, PTC-200 (MJ Research, Inc., Reno, NV). Double stranded DNA sequencing was performed using the ABI PRISM Big Dye Terminator Cycle Sequencing Core kit with Amplitaq DNA Polymerase. Sequencing reactions were performed by Gene Technologies Laboratory (Texas A&M University) using an ABI 373 XL or 373 XL DNA sequencer (Applied Biosystems Inc., Foster City, CA). Enzymes were purchased from Promega (Madison, WI) unless otherwise noted.

Primer extension analysis

Transcript initiation was mapped using primer extension techniques (Sambrook et al., 1989) under the guidance of Sharon Braunagel. The oligonucleotide 5' GGGATCAATTCAACTTGCTCCTGATGC 3' was 5' end labeled with T₄ polynucleotide kinase and probed against 105µg of total cellular RNA. Extension products were generated using Superscript II-Reverse transcriptase in the presence of 2.3µg actinomycin D, 28 units RNasin, and 0.5mM dNTPs for 1 hr at 42°C. Extension

products were precipitated and digested with 0.1N NaOH for 30 min at room temperature, resuspended in 80% formamide loading buffer, and boiled for 3 min before loading onto a denaturing gel (7.0 M Urea, 6% polyacrylamide, 100mM Tris-borate, 20mM EDTA, pH 8.3). Transcript initiation sites were identified by comparison with a concurrent DNA sequence using the same oligonucleotide as used for generating the extension products. A maxiprep of clone 2 was used as a template for the sequencing reaction using the SequenaseTM 2.0 DNA sequencing kit (USB). The three different primer extension products were resolved individually by modulating the time of the electrophoretic runs.

The oligos used for the primer extension analyses are:

2-2 IP: 5' GGATCAATTCAACTTGCTCCTGATGC 3'

2-2 IP-2: 5' GCGGGGGCTGCACCACCAACAGTTG 3'

The oligo 2-2 IP was used to determine the transcription initiation site for the first and second primer extension products. While, the third transcription initiation site was determined using the oligo: 2-2 IP-2. The DNA sequencing gels used to resolve the primer extension products were run for varying lengths of time to individually resolve the three products.

CHAPTER III

COTRANSLATIONAL INTEGRATION AND INITIAL SORTING AT THE ER TRANSLOCON OF PROTEINS DESTINED FOR THE INM*

Experimental design

Any proteins directly involved in the sorting of newly synthesized polypeptides (hereafter termed substrates) into the INM or other membranes will recognize some structural feature(s) of the substrate that directs each protein to a particular location. Because the SM sequence is sufficient to direct a polypeptide to the INM (Hong et al., 1997; Braunagel et al., 2004), this sequence must contain the structural features that constitute an INM-sorting signal. If sorting is protein-mediated, then recognition of this sequence would require a direct interaction between the SM sequence and a protein involved in sorting. Thus, one approach to identifying the proteins that mediate sorting to the INM is to determine which proteins are adjacent to, and presumably interact with, an INM substrate as it progresses through different stages of the sorting process. A direct method for detecting interacting proteins is crosslinking, since a substrate can only react covalently with proteins that are in close proximity. Furthermore, the use of photosensitive crosslinking reagents allows one to create fully assembled intermediates at different stages of substrate synthesis and sorting prior to initiating the crosslinking

* Part of the data reported in this chapter is reprinted with permission from “Cotranslational integration and initial sorting at the endoplasmic reticulum translocon of proteins destined for the inner nuclear membrane” by Saksena et al., 2004. *PNAS*, 101, 12537-12542. Reprinted in accordance with Copyright © 1993-2004 by The National Academy of Sciences of the United States of America, all rights reserved

reaction. Since increasing the length of the truncated mRNA (and hence the nascent chain) yields intermediates that are progressively further along the processing pathway, alterations in the proteinaceous environment surrounding the substrate can therefore be monitored at different stages of integration by varying the length of the nascent chain. By comparing different lengths of INM and non-INM substrates, the stage at which the processing of an INM substrate diverges from that of a protein destined to function in another membrane can be established experimentally.

Crosslinking experiments in a complex biochemical system that includes the substrate, ribosomes, ER microsomes, and many associated factors can yield a myriad of crosslinked proteins. However, by selectively positioning photoreactive probes only in the substrate, one can limit the crosslinking targets solely to those proteins adjacent to the substrate. Since the nascent or full-length substrate typically comprises less than 0.1% of the polypeptide in an *in vitro* translation incubation, selective labeling of the substrate can only be achieved by incorporating the photoreactive probes into the substrate polypeptides as they are being made by the ribosome. To accomplish this, the translation incubation must contain a modified aminoacyl-tRNA (aa-tRNA) that recognizes a particular mRNA codon, but incorporates an amino acid with a photoreactive probe covalently attached to the side chain. The probe will then be incorporated into the substrate nascent protein chain wherever the mRNA contains a codon recognized by the aa-tRNA analogue. Johnson & colleagues were the first to demonstrate the successful incorporation of non-natural amino acids into polypeptides *in vitro* using aa-tRNA analogues (Johnson et al., 1976), and this approach has since been

used successfully by many groups to examine various aspects of protein trafficking using either photoreactive and/or fluorescent probes (Johnson et al., 2001; Johnson et al., 1999; Woolhead et al., 2004).

Fully-assembled integration intermediates with nascent chains of a homogeneous, defined length can be prepared *in vitro* by translating, in the presence of ER microsomes and signal recognition particle (SRP), mRNAs that are truncated within the coding region. Ribosomes halt when they reach the end of the mRNA, but the nascent chains do not dissociate from the tRNA and ribosome because the absence of a stop codon prevents normal termination from occurring. The length of the nascent chain in the ribosome•nascent chain complex (RNC) is therefore determined by the length of the truncated mRNA added to the translation. Translations contain [³⁵S]Met to radiolabel the synthesized substrate and N^ε-(5-azido-2-nitrobenzoyl)-Lys-tRNA^{amb} (εANB-Lys-tRNA^{amb}) to incorporate a photoreactive probe into the substrate {Krieg et al., 1986 ; Flanagan et al., 2003}. Since the εANB-Lys-tRNA^{amb} amber suppressor tRNA recognizes and translates an amber stop codon, the position of the probe in the substrate is dictated by the location of the single amber stop codon in the mRNA. Since our goal was to identify proteins that may interact with the SM sequence, we positioned an amber stop codon within the nonpolar region of the SM-containing proteins for many experiments in this study. (Note that the lysine is no longer charged after modification by the probe.) Moreover, to examine all sides of the putative α-helix formed by the hydrophobic TMS in the SM, a single amber codon was substituted in place of each of four sequential in-frame codons in each mRNA examined.

Targeting of the SM to the ER membrane occurs cotranslationally and is SRP-dependent

Full-length E66 has been observed to insert into membranes post-translationally, albeit at low efficiency (Hong et al., 1997). Hence, it was first necessary to ascertain whether E66 is normally targeted to the ER membrane in an SRP-dependent manner and integrated cotranslationally. Thus, E66 was modified by extending its N-terminus to position a consensus glycosylation acceptor sequence sufficiently far (18 residues) from the nonpolar TMS to be glycosylated when the -N-S-T- is translocated into the ER lumen (Nilsson et al., 1993). The resulting construct, here termed E66G (Fig. 24A), has also been used to determine the normal orientation of E66 in the INM (Braunagel et al., 2004).

The targeting to the ER membrane of most ribosome•nascent chain complexes synthesizing eukaryotic membrane proteins is SRP-dependent (Keenan et al., 2001). When E66G was translated in the presence of canine column-washed rough ER microsomes (CRMs) containing SRP, much of the nascent E66G was glycosylated (Fig. 24B, lane 1). However, when the CRMs were added after nascent E66G had been released from the ribosomes, no E66G was glycosylated (Fig. 24B, lane 2), thereby showing that the signal sequence-containing nascent E66G could not be targeted and translocated post-translationally. The SRP dependence of this targeting was further examined using microsomes that had been stripped of their SRP and residual ribosomes by washing in EDTA and high salt (EKRM). E66G proteins synthesized either in the presence (Fig. 24B, lane 3) or in the absence (Fig. 24B, lane 4) of EKRM were not

glycosylated, but were glycosylated if SRP was included with EKRM in the incubation from the beginning (Fig. 24B, lane 5). Thus, the targeting, translocation, integration, and glycosylation of E66G is SRP-dependent and occurs co-translationally.

The above results suggest that the SM sequence acts as a signal sequence to target RNCs synthesizing E66G to the translocon. If true, one would predict that the SM sequence would bind to SRP, and that this association could be detected by nascent chain photocrosslinking to the 54 kDa subunit of SRP (SRP54) (Krieg et al., 1986). An amber stop codon was substituted into the nonpolar core of E66 at position 12 to create a construct designated E66-A12 (Fig. 24A; other amber codon-containing constructs are identified similarly), and a truncated mRNA transcribed from this DNA was translated in the presence of SRP and either ϵ ANB-Lys-tRNA^{amb} or unmodified Lys-tRNA^{amb}, but in the absence of microsomes to block the targeting pathway at the RNC•SRP intermediate. Upon illumination, a ~61 kDa photoadduct containing the 70-residue nascent chain and a larger protein was formed (Fig. 24C, lane 4), and this target protein was shown to be SRP54 by immunoprecipitation with SRP54-specific antibodies (Fig. 24C, lane 5). As expected, no photoadduct was observed in the absence of light (Fig. 24C, lane 2) or probe (Fig. 24C, lane 1). Furthermore, a nascent chain lacking the SM sequence (termed E66- Δ 33; generated by Tao Hong), but containing a photoreactive probe at position 12, did not photocrosslink to SRP54 (Fig. 24C, lane 3), thereby showing the requirement of the SM sequence for nascent chain binding to SRP.

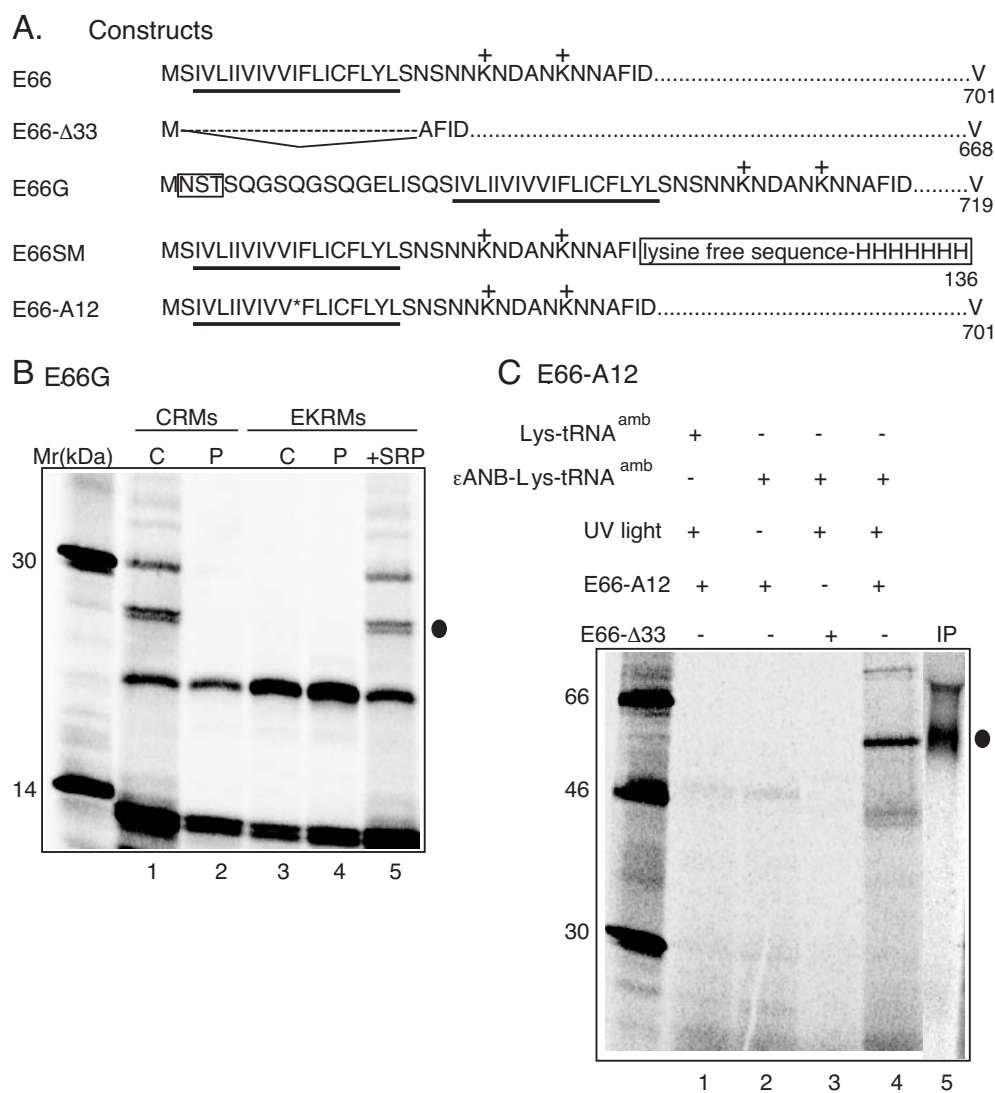


Figure 24. Targeting of E66 to the ER membrane is cotranslational and SRP-

dependent. (A) The N-terminal sequence of E66 and some derivatives used in this study. The TMS is underlined and the glycosylation sequence is boxed. The asterisk denotes the position of the amber codon within the E66-A12 construct. (B) The N-terminal 200 residues of E66G were translated in the presence (cotranslationally or C; lanes 1,3,5) or absence (microsomes were then added post-translationally or P; lanes 2,4) with the indicated microsomes. The sample in lane 5 also received 40 nM canine SRP. The closed circle denotes the glycosylated protein. (C) Translation intermediates containing 70-residue nascent chains of the indicated E66 derivatives were prepared in the presence of unmodified Lys- tRNA^{amb} or εANB-Lys- tRNA^{amb} as indicated. Only the sample in lane 2 was not exposed to UV light. The sample in lane 5 was immunoprecipitated with antibodies to SRP54 prior to analysis by SDS-PAGE, and the closed circle denotes the SRP54-nascent chain photoadduct.

Viral SM sequence proximity to translocon proteins

A number of studies by different groups have demonstrated that a signal or signal-anchor (SA) sequence is adjacent to translocon proteins after SRP-dependent targeting (Johnson & van Waes, 1999; Alder & Johnson, 2004). To determine whether the SM sequence also passes through the translocon, parallel samples of 70-residue E66 nascent chains were translated in the presence of SRP, microsomes, ϵ ANB-Lys-tRNA^{amb}, and truncated mRNAs with an amber stop codon at position 10, 11, 12, or 13 (Fig. 25A). After photolysis, the extents of photocrosslinking of each E66 derivative to both Sec61 α and TRAM were determined by immunoprecipitation using affinity-purified antibodies specific for Sec61 α and TRAM (SDS-PAGE analyses of the total samples did not reveal any other major photoadducts; and no photoadducts were observed in the absence of light or ANB; data not shown). As shown in Fig. 25B, E66 reacts covalently with Sec61 α primarily via probes positioned at residues 10 and 12. Probes at positions 11, 13, and, to a lesser extent, 10 photocrosslink to TRAM. As others have observed and discussed elsewhere (McCormick et al., 2003), the disparity in the magnitude of photocrosslinking from adjacent positions in the TMS of the SM reveals that it is not oriented randomly within the translocon, nor is the SM TMS free to rotate in or next to the translocon. Instead, the SM TMS appears to be bound in a fixed orientation by one or more translocon proteins. If the SM TMSs were randomly oriented and not bound to the translocon, then one would expect to see a symmetric photocrosslinking pattern in which each probe position reacts more or less equally with a given target protein (note that the probes are at the end of a 12 Å-long flexible lysine side chain, so a 1.5 Å difference in

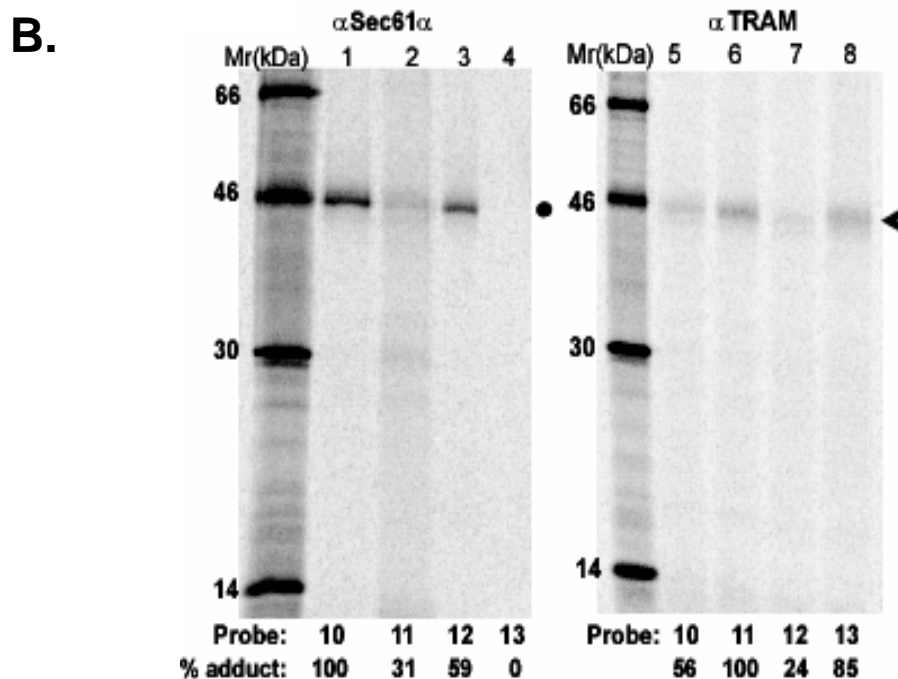
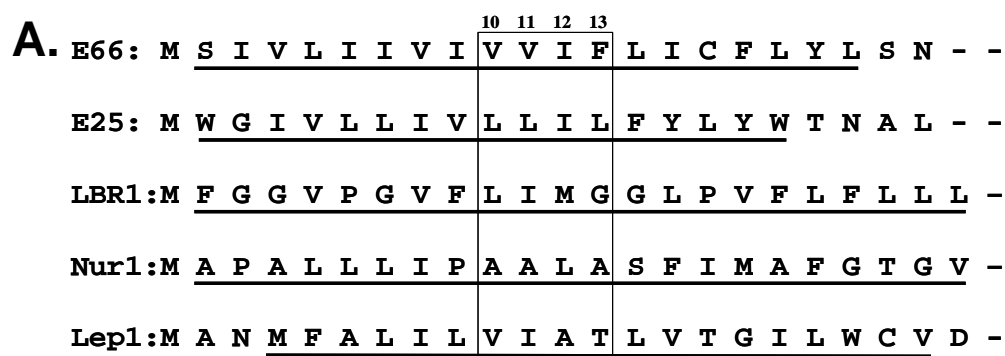


Figure 25. Photocrosslinking of viral INM-directed TMSs to translocon proteins.

(A) The N-terminal sequences of E66 and E25 are shown with the TMS underlined, as are the N-terminal sequences of the constructs containing the first TMS of LBR (LBR1), nurim (Nur1), and Lep (Lep1). In each case, an amber codon was substituted for the codon shown at position 10, 11, 12, or 13 (boxed in figure) to position the photoreactive probes at a single nascent chain location in each sample. The probes extend from different sides of the TMS α -helix surface. (B) Integration intermediates containing 70-residue E66-A10, E66-A11, E66-A12, or E66-A13 nascent chains were photolyzed, immunoprecipitated with affinity-purified antibodies to Sec61 α (lanes 1-4) or TRAM (lanes 5-8), and analyzed by SDS-PAGE. Photoadducts to Sec61 α and TRAM are indicated by the closed circle and arrowhead, respectively. The relative extent of photoadduct formation was quantified by comparing each photoadduct band intensity with that of the most intense photoadduct band in the gel (taken to be 100%).

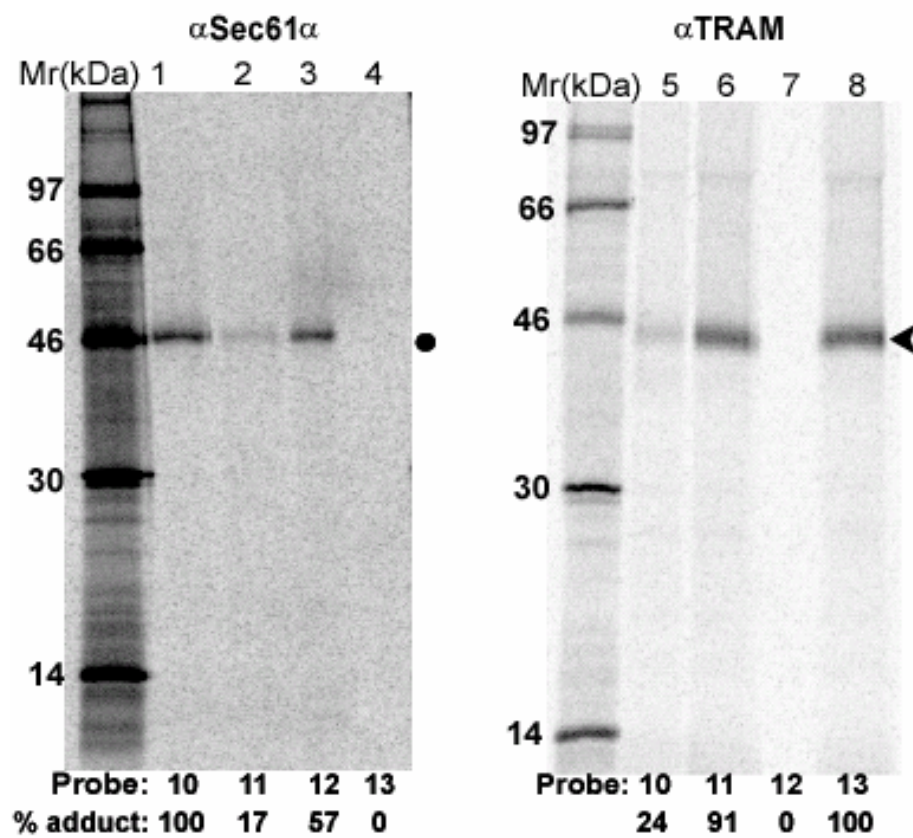


Figure 26. Photocrosslinking of E25 TMS. Integration intermediates containing 70-residue E25-A10, E25-A11, E25-A12, or E25-A13 nascent chains were photolyzed and analyzed as in Fig. 25.

bilayer depth of probes located at adjacent residues in the TMS helix could not explain the differences in photoadduct formation for adjacent probe locations seen in Fig. 25B). Thus, following SRP-dependent targeting, the TMS of the E66 SM sequence appears to occupy and be bound to a specific site within the translocon. To assess the generality of these results, we examined the proximity to the translocon of nascent ODV-E25 (E25), a viral membrane protein that is also sorted to the INM.

As above, an amber stop codon was substituted into position 10, 11, 12, or 13 (Fig. 25A) to yield constructs designated E25-A10, etc. When truncated mRNAs coding for 70 residues of each of these nascent chains were translated in parallel and then photolyzed, the photocrosslinking patterns were very similar to those of nascent E66. Sec61 α was in close proximity to residues 10 and 12 in the E25 TMS, while residues 11 and 13 were adjacent to TRAM (Fig. 26). Thus, the locations of the E66 and E25 TMS sequences within the translocon are indistinguishable early in integration. Furthermore, both viral TMSs were clearly adjacent to TRAM: an average of 11% of the nascent chains photocrosslinked to translocon proteins, and approximately half of the photoadducts contained TRAM.

Mammalian INM TMS proximity to translocon proteins

The unexpected photocrosslinking of viral TMSs to TRAM raised two questions. Is the close association with TRAM a property of viral proteins, or is this close association a property of INM-directed proteins, but not other membrane proteins? To ascertain which of these two possibilities, if either, is correct, the same approach was used to examine two mammalian proteins that localize in the INM: lamin B receptor (LBR) and

nurim. Both LBR and nurim are multi-spanning membrane proteins, but the first TMS and the flanking charged amino acids of both LBR (Soullam et al., 1995) and nurim (Rolls et al., 1999) are important for directing the protein to the INM. Thus, constructs that retained these features were generated and termed LBR1 and Nur1, respectively. After co-translational insertion into the membrane, the LBR1 sequence adopts an orientation opposite to that of the first TMS in native LBR (Worman et al., 2000; Smith et al., 1993); however, this difference in TMS orientation has no detectable effect on protein sorting to the INM because both LBR and LBR1 are each directed to the INM (submitted). Derivatives of LBR1 and Nur1 were then prepared by substituting an amber stop codon for a codon at positions 10, 11, 12, or 13 (Fig. 25A).

When 70-residue nascent chains of the LBR1 constructs were translated, targeted, and photolyzed, SDS-PAGE analyses of the TRAM- and Sec61 α -specific immunoprecipitates revealed that the photocrosslinking was asymmetric and the pattern was very similar to that seen with the viral INM TMSs. Sec61 α was adjacent to positions 10 and 12 in the LBR TMS, while positions 11, 13, and, to a lesser extent, 10 were in close proximity to TRAM (Fig. 27). As was seen with the viral INM-directed proteins, 11-12% of the total LBR1 and Nur1 nascent chains synthesized were photocrosslinked to TRAM plus Sec61 α . The first LBR TMS and the viral TMSs therefore appear to occupy similar sites in the translocon.

When the Nur1 TMS sequence was examined, the photocrosslinking targets were the same, but the photocrosslinking efficiencies at different probe locations differed significantly from those of other INM TMSs. The extent of photocrosslinking to TRAM

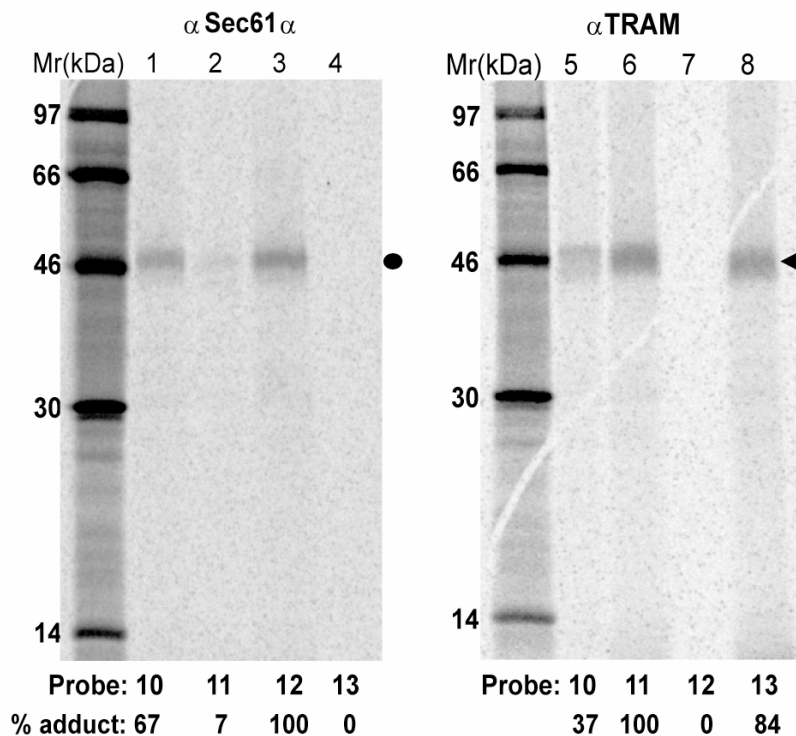


Figure 27. Photocrosslinking of mammalian INM-directed TMSs to translocon proteins. Integration intermediates containing 70-residue LBR1-A10, -A11, -A12, or -A13 nascent chains were photolyzed, immunoprecipitated with affinity-purified antibodies to Sec61 α (lanes 1-4) or TRAM (lanes 5-8), and analyzed by SDS-PAGE. Photoadducts to Sec61 α and TRAM are indicated by the closed circle and arrowhead, respectively. The relative extent of photoadduct formation was quantified by comparing each photoadduct band intensity with that of the most intense photoadduct band in the gel (taken to be 100%).

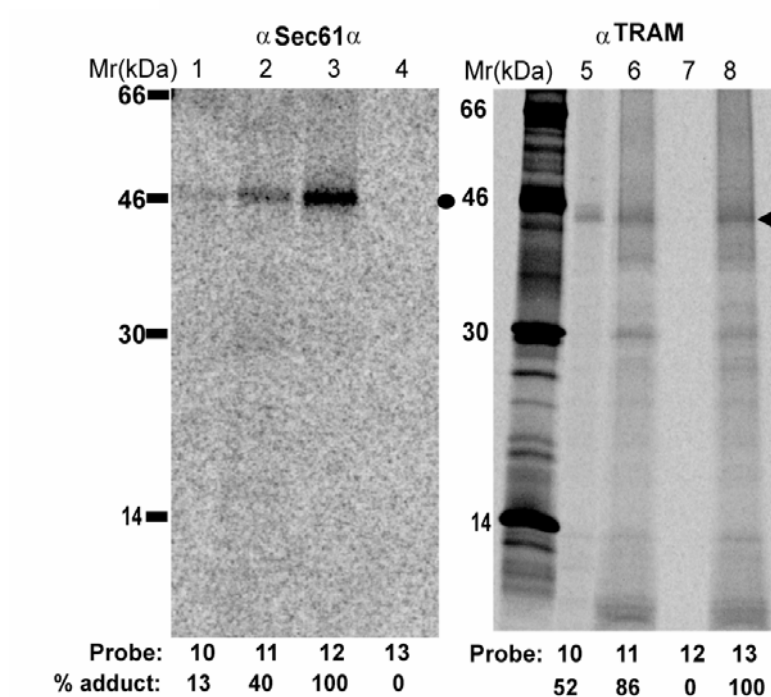


Figure 28. Photocrosslinking of Nur1 TMS to translocon proteins. Integration intermediates containing 70-residue E66-A10, E66-A11, E66-A12, or E66-A13 nascent chains were photolyzed, immunoprecipitated with affinity-purified antibodies to Sec61 α (lanes 1-4) or TRAM (lanes 5-8), and analyzed by SDS-PAGE. Photoadducts to Sec61 α and TRAM are indicated by the closed circle and arrowhead, respectively. The relative extent of photoadduct formation was quantified by comparing each photoadduct band intensity with that of the most intense photoadduct band in the gel (taken to be 100%).

from positions 11 and 13 of Nur1 were similar to those observed with LBR1 (Fig. 27 & 28), while photocrosslinking to Sec61 α was most efficient from position 12 and much less efficient from position 11 (Fig. 28). Only a trace of photocrosslinking to Sec61 α was obtained from position 10, in contrast to the trace photocrosslinking obtained from position 11 in the other three INM TMSs (Figs. 25, 26, 27). The asymmetry of the photocrosslinking to Sec61 α and TRAM shows that the first nurim TMS is bound in a fixed orientation within the translocon. Furthermore, the nurim TMS clearly occupies a site in the translocon adjacent to TRAM. But the differences in photocrosslinking yields from different probe positions indicate that the nurim TMS does not interact with the translocon in exactly the same way as the viral TMSs.

Non-INM TMS proximity to translocon proteins

To determine whether the crosslinking patterns shown in Figs. 25-28 were unique to INM-directed membrane proteins, two non-INM TMSs were examined using the same techniques. The first TMS of leader peptidase (Lep1) has been shown previously to photocrosslink, at least transiently (Mothes et al., 1997; Heinrich et al., 2000; Heinrich et al., 2003) and in an asymmetric fashion (McCormick et al., 2003), with Sec61 α . We therefore determined whether Lep1 also photocrosslinked to TRAM. The Lep1 construct was substituted with a single amber stop codon at each of four adjacent codons in the first TMS (Fig. 25A), and a 70-residue nascent chain of each of these constructs was translated, targeted, photolyzed, and examined as above. In contrast to the results obtained with INM-directed TMSs, Sec61 α photocrosslinked to the Lep1 TMS from positions 11, 13, and, to a lesser extent, 10 (Fig. 29). But no photocrosslinking to TRAM

was detected from any of the four probe positions (for comparison, the extent of TRAM photocrosslinking obtained in a parallel sample containing a 70-residue E66-A11 nascent chain is shown in lane 9 of Fig. 29). Thus, the Lep1 TMS appears to occupy a fixed position within the translocon, but this site differs markedly from that occupied by the INM-directed TMSs.

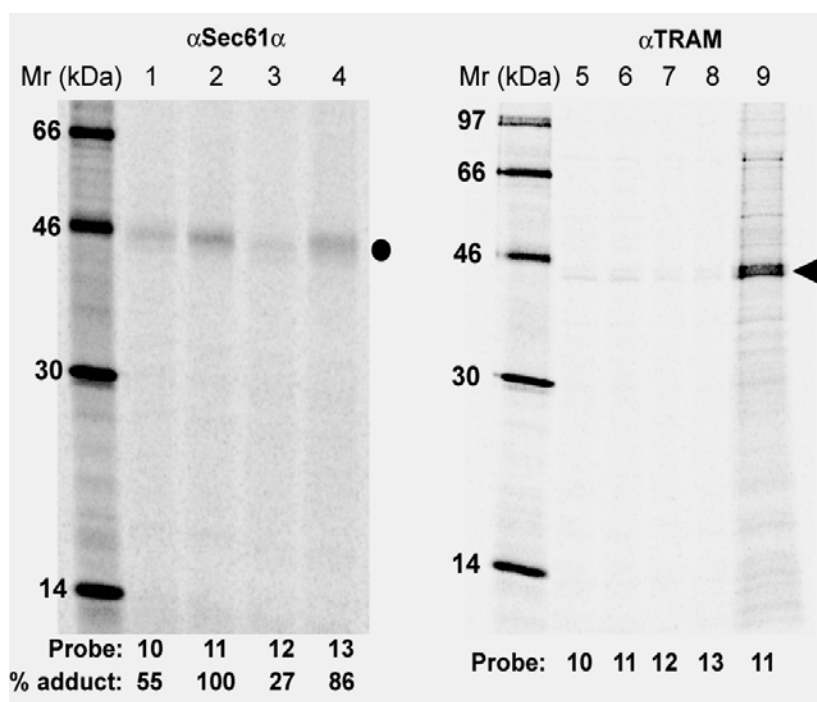


Figure 29. Photocrosslinking of Lep1 to translocon proteins. Integration intermediates containing 70-residue nascent chains of Lep1-A10, Lep1-A11, Lep1-A12, or Lep1-A13 were photolyzed and analyzed as in Fig. 22. Lep1-Sec61 α photoadducts are indicated by the closed circle. As a positive control, a parallel sample containing 70-residue E66-A11 integration intermediate was immunoprecipitated with TRAM antibody (lane 9).

Similarly, four probe locations in the TMS of transferrin receptor (TfR) photocrosslink asymmetrically to Sec61 α , but they do not photocrosslink at all to TRAM (McCormick et al., 2003). Thus, the TfR TMS occupies a specific site in the translocon during co-translational integration, but this site differs substantially from that occupied by the INM-directed TMSs.

Nascent chain length-dependence of photocrosslinking

Previous studies have shown that TMSs of non-INM proteins are retained in the translocon even when the length of the nascent chain is far in excess of that required to release the TMS into the lipid bilayer (McCormick et al., 2003; Do et al., 1996). Moreover, the lengthening of the nascent chain did not substantially alter the asymmetric photocrosslinking patterns obtained with different TMSs (McCormick et al., 2003). To assess the retention of INM TMSs in the translocon, we monitored the photocrosslinking of E66SM-A10 as a function of nascent chain length in parallel incubations (E66SM was created by fusing the N-terminal 33 amino acids of E66 to a lysine-free sequence described previously in Braunagel et al., 2004). After photolysis, the samples were split for immunoprecipitation with antibodies specific for either Sec61 α or TRAM. The extent of E66SM-A10 (Fig. 30) photocrosslinking to Sec61 α decreases rapidly as the nascent chain lengthens. At 70 residues, the TMS has just emerged from the ribosome, and lengthening the chain by 5-17 residues results in a substantial decrease in nascent chain photocrosslinking to Sec61 α . By the time the nascent chain reaches 100 residues, the E66 TMS has moved away from Sec61 α .

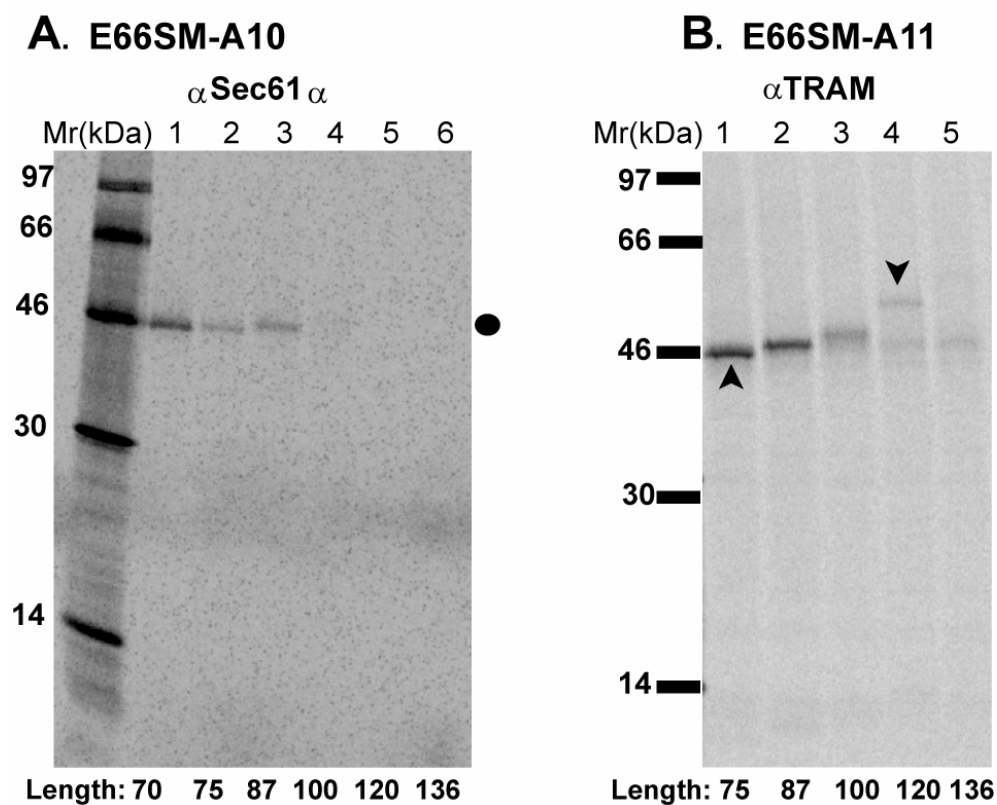


Figure 30. Nascent chain length-dependence of E66 photocrosslinking to translocon proteins. Photoadducts were detected by immunoprecipitation with antisera specific for either Sec61 α (A) or TRAM (B). Nascent chain lengths (amino acids) in the photolyzed E66SM-A10 (A) or -A11 (B) integration intermediates are indicated below the gel. Normally-terminated full-length 136-residue E66SM is shown in lanes A6 and B5. Photoadducts are identified as in Figs. 25-28.

In contrast, the E66 TMS was adjacent to TRAM until later in the process. The extent of E66SM-A11 (Fig. 30) photocrosslinking to TRAM was the same for nascent chain lengths of 75-87, but photoadducts were still visible when the nascent chain reached 120 residues (Fig. 30). Thus, during its passage through the translocon, the E66 SM appears to remain adjacent to TRAM for a longer period of time than to Sec61 α .

SM sequence crosslinking to non-translocon proteins

Another approach that can be used to identify proteins that associate with the SM sequence is chemical crosslinking. Since the E66SM construct contains only two lysine codons near the C-terminal end of the SM sequence (Fig. 25A), the crosslinking of the E66SM substrate to another protein via bis(sulfosuccinimidyl)suberate (BS³), a lysine-specific homobifunctional reagent, would require a Lys residue on the target protein to be in close proximity to a Lys residue in the substrate. Since the sample contains many proteins with surface-exposed lysine amino groups, the detection of a specific covalent complex would be explained most reasonably by the association of the substrate SM sequence with a particular target protein.

Using this approach, we showed that the SM sequence in full-length E66SM was chemically crosslinked to viral proteins FP25K and/or E26 (Braunagel et al., 2004). This crosslinking was observed in nuclei from insect Sf9 cells that had been infected with a recombinant baculovirus expressing E66SM. The crosslinking of E66SM with FP25K and/or E26 could be the result of a stable interaction occurring within the virion or represent a trafficking intermediate. To discern which of the two possibilities was true, E66SM was translated in the presence of ER microsomes isolated from virus-infected

Sf9 cells and then treated with the chemical crosslinker BS³. As was observed with the crosslinking experiments conducted in nuclei derived from virus-infected Sf9 cells, antibodies specific for the T7 epitope, immunoprecipitated a crosslinked complex of ~32 kDa (Fig. 31, lane 4). Antibodies specific for the viral proteins FP25K and E26 were able to immunoprecipitate the crosslinked complex (Fig. 31, lanes 5 & 6). To confirm that the crosslinked complex did not represent a stable interaction occurring within the virion, antibodies that would precipitate the virus in various stages of maturation were used: p39, ODV-E25 and polyhedrin (precipitate nucleocapsids, mature virus and partially occluded virus respectively). None of the antibodies precipitated the crosslinked complex (Fig. 31, lanes 1-3), indicating that the crosslinked complex does not represent protein-protein interactions occurring within the assembled virion but rather represents a trafficking intermediate within the ER membrane.

Having demonstrated that the full-length (ribosome released & membrane integrated) E66SM crosslinks with FP25K and/or E26, we wanted to determine at what point in E66SM integration the SM sequence interacts with FP25K and/or E26. Using microsomes from infected Sf9 cells, we observed essentially no crosslinking of E66SM nascent chains to FP25K (Fig. 32A) or E26 (Fig. 32B). Crosslinked species containing the substrate and one of the two putative sorting factors were only seen with full-length E66SM substrate polypeptides (Fig. 32). Thus, it appears that FP25K and/or E26 associate with the SM sequence after it has been released from the translocon into the lipid bilayer.

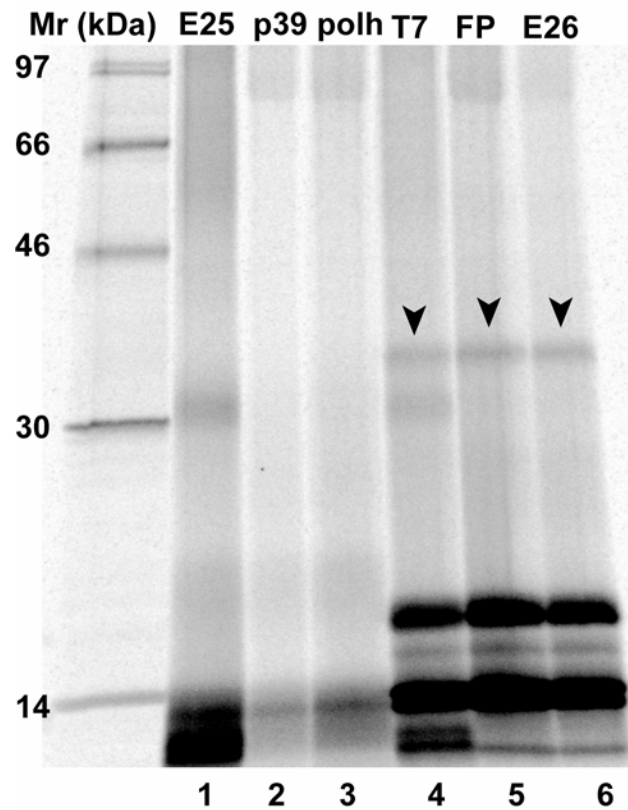


Figure 31. The E66SM crosslinks with FP25K and/or E26. Full-length (normally terminated & ribosome released) E66SM protein was translated in the presence of virus-infected Sf9 microsomes, chemically crosslinked, and immunoprecipitated with antisera specific for either ODV-E25 (lane 1); p39 (lane 2); polyhedrin (lane 3); T7 tag (lane 4); FP25K (lane 5) and E26 (lane 6). The crosslinked product precipitated by the antibody is indicated by the arrowheads.

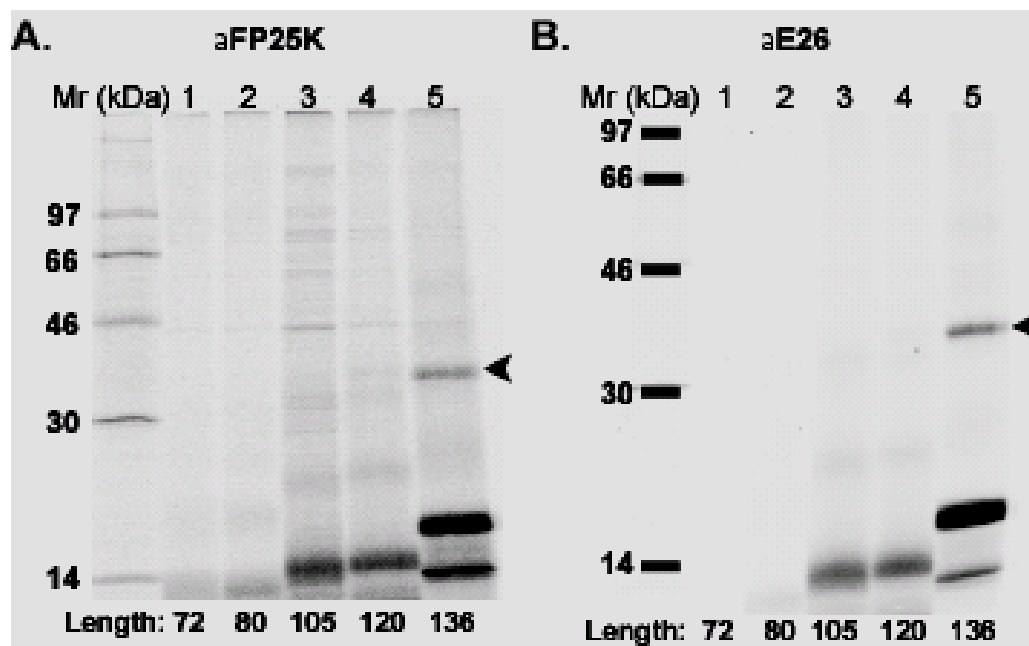


Figure 32. Nascent chain length-dependence of SM chemical crosslinking to FP25K and E26. (A) Nascent or full-length E66SM proteins were translated in the presence of virus-infected Sf9 microsomes, chemically crosslinked, and immunoprecipitated with antisera specific for either FP25K (A) or E26 (B) as before (Braunagel et al., 2004). Nascent chain lengths in integration intermediates are as indicated. Covalent crosslinks between full-length E66SM and FP25K or E26 are identified by the arrowhead adjacent to lane 5 in each gel.

Membrane association of FP25K & E26

Most FP25K is present in the cell as a soluble, cytoplasmic protein (Rosas-Acosta et al., 2001). Clusters of FP25K associating with the ER at the nuclear periphery have been observed using immunogold labeling, but this observation is rare (Harrison et al., 1995). Thus, the identification of a membrane-associated form of FP25K that crosslinks to E66SM raised questions regarding the nature of its membrane association. When virus-infected insect (Sf9) microsomes were washed with high salt (0.5M KOAc), FP25K was found to fractionate in the supernatant fraction (as detected by immunoblotting) (Fig. 33). In contrast, a significant proportion of E26 was able to associate with the membrane pellet after treatment with high salt (Fig. 33). The fractionation pattern that we observed with E26 was similar to the one obtained with the ER integral membrane protein Sec61 α (Fig. 34). Thus, while the membrane association of FP25K appears to be mediated via electrostatic interactions (either with the head groups of phospholipids, other integral membrane proteins etc.), the membrane association of E26 appears to be more stable. Although, E26 lacks any predictable TMS, the presence of an amphipathic helix, C-terminal amidation site(s) have allowed us to explain its membrane association. More recently, E26 has also been shown to undergo palmitoylation during viral infection (unpublished data), which could be another explanation for its membrane association.

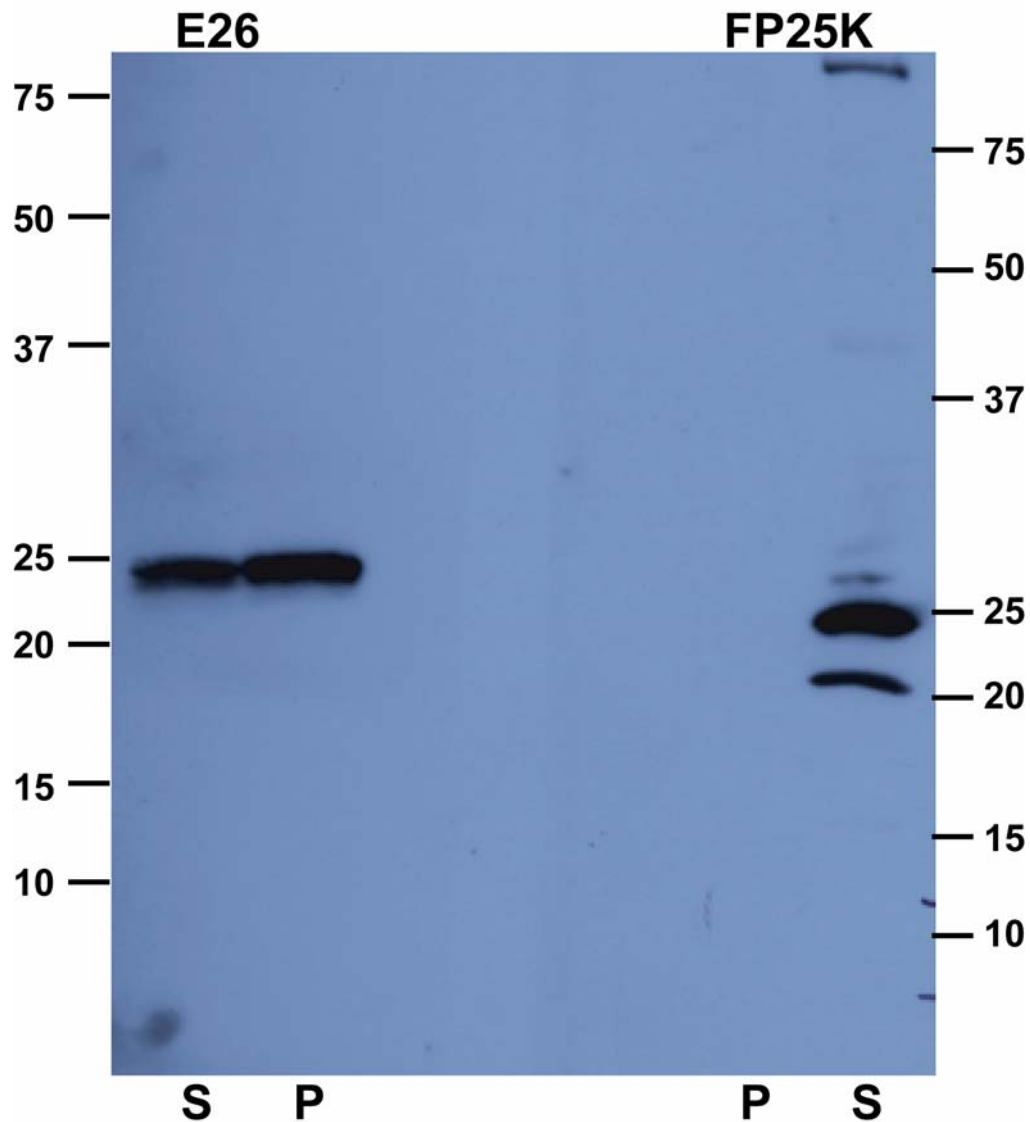


Figure 33. Membrane association of FP25K & E26. Virus-infected Sf9 microsomes were washed with high salt (0.5M KOAc) and sedimented using a high salt cushion. The resulting membrane pellet (P) and supernatant (S) fractions were analyzed by immunoblotting using antibodies specific for FP25K & E26.

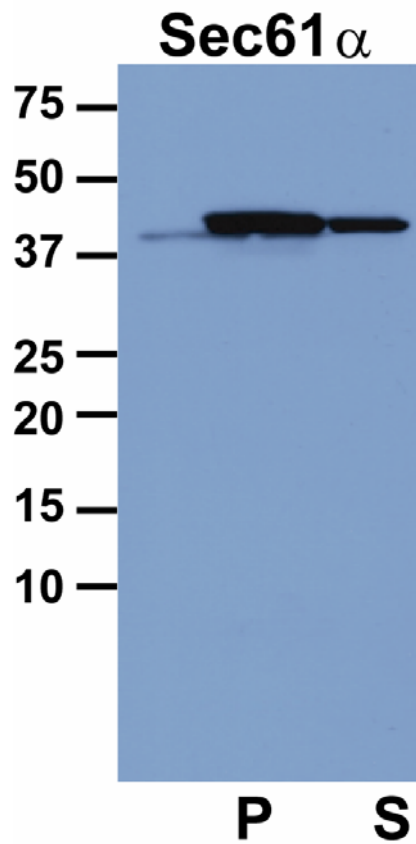


Figure 34. Membrane association of Sec61 α . Microsomes derived from canine pancreas were washed with high salt (0.5M KOAc) and sedimented using a high salt cushion. The resulting membrane pellet (P) and supernatant (S) fractions were analyzed by immunoblotting using antibodies specific for the translocon protein Sec61 α .

However, one of the most important observations to consider is that the ER membrane-associated forms of both FP25K and E26 represent only a small portion of the total FP25K or E26.

Not every substrate crosslinks to FP25K and E26

Lep1 contains lysines in approximately the same positions as E66SM, and hence it is pertinent to ask whether Lep crosslinks to FP25K or E26. No chemical crosslinks to FP25K (Fig. 35A, lane 1) or E26 (Fig. 35A, lane 3) were observed with nascent, puromycin-released Lep intermediates after integration into ER microsomes from infected cells. In contrast, efficient crosslinks to FP25K (Fig. 35A, lane 2) and E26 (Fig. 35A, lane 4) were seen with full length E66SM after integration into infected ER microsomes and incubation with bis(sulfosuccinimidyl)suberate. The difference in the crosslinking efficiencies of Lep1 and SM were not based on differences in levels of translation (Fig. 35B). We therefore conclude that FP25K and E26 do not crosslink (and presumably do not bind to) every protein, but that they are selective in their association with substrates.

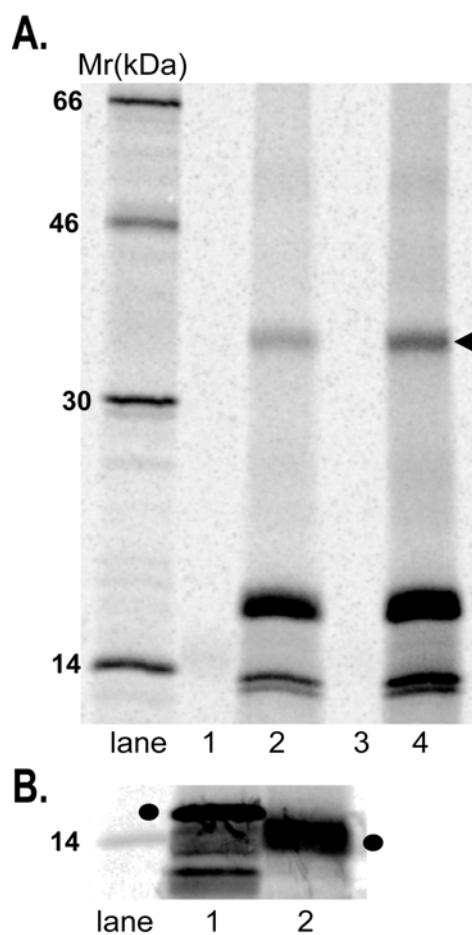


Figure 35. FP25K and E26 are selective in their association. (A) Integration intermediates containing 110-residue nascent chains of Lep1 were translated in the presence of virus-infected S19 ER microsomes, treated with 2 mM puromycin, chemically crosslinked, immunoprecipitated with antibodies to FP25K (lane 1) or E26 (lane 3), and analyzed by SDS-PAGE. In parallel samples, full-length E66SM was translated, crosslinked, and immunoprecipitated with antibodies to FP25K (lane 2) or E26 (lane 4). Covalent crosslinks between full length E66SM and FP25K or E26 are identified by the arrowhead adjacent to lane 4. (B) Aliquots of translation reactions containing either full-length E66SM protein (lane 1) or puromycin-released 110mer-Lep1 protein (lane 2) were removed prior to crosslinker addition and then analyzed by SDS-PAGE. The closed circle adjacent to lanes 1 & 2 identifies the translation products.

Discussion

Several important conclusions can be drawn from the data reported here. First, the asymmetric photocrosslinking to TRAM and to Sec61 α of each TMS examined here reveals that each is bound to a protein(s) within the mammalian translocon (cf. McCormick et al., 2003). Second, the proteinaceous environment within the translocon is very similar for both cellular and viral INM TMSs. Third, the proteinaceous environment within the translocon differs markedly for INM TMSs and for TMSs directed elsewhere. Fourth, an integrated viral SM sequence is crosslinked to two viral proteins after being released from the translocon in ER microsomes purified from infected insect cells. Fifth, this study confirms the widely-held presumption that some INM-directed proteins are targeted to the ER membrane by SRP and integrated cotranslationally at the translocon. Other INM proteins may be inserted post-translationally as C-tail-anchored proteins (Wattenberg et al., 2001). Taken together, these results strongly suggest that some membrane protein sorting to the INM is initiated within the translocon early in the integration process, is protein-mediated, and involves substrate recognition by and interaction with a sequence of proteins that function as sorting factors to facilitate the movement of proteins to the INM.

As discussed elsewhere (McCormick et al., 2003), the binding of a substrate TMS to a translocon protein is revealed by the non-random and asymmetric photocrosslinking of the TMS to TRAM and/or Sec61 α from different photoreactive probe locations that encircle the middle of the cylindrical TMS α -helix. This high-resolution approach for characterizing a TMS's environment within the translocon has so far been applied to 11

TMSs in this (Figs. 25-28) and in a previous study (McCormick et al., 2003). Since each of these 11 TMSs was not free to rotate and randomize its orientation relative to TRAM and Sec61 α in the translocon, each TMS binds to a translocon protein(s). This interaction presumably plays a direct (but as-yet undefined) mechanistic and/or regulatory role in the integration process.

When the translocon environments of the viral E66 and E25 TMSs were examined, the photocrosslinking of these two TMSs to TRAM and Sec61 α were found to be indistinguishable (Figs. 25B & 26). In addition, a similar photocrosslinking pattern was obtained when the proximity of the first TMS of mammalian LBR to translocon proteins was investigated (Fig. 27). The close similarity of the photocrosslinking results for these three INM proteins seems more than coincidental. Furthermore, the first TMS of mammalian nurim also photocrosslinked to TRAM and Sec61 α from the same probe positions as the other three TMSs, though the extent of Sec61 α photocrosslinking from positions 10 and 11 of Nur1 was reversed from that of the other three substrate TMSs (Fig. 28). Most striking, however, was the observation that 4 of 4 INM TMSs were efficiently photocrosslinked to TRAM. Furthermore, these TMSs were in very similar, but not identical, proteinaceous environments or sites within the translocon based on the photocrosslinking-detected proximities of different TMS surfaces to Sec61 α and TRAM.

In contrast, of the 10 total non-INM-directed TMSs whose photocrosslinking to Sec 61 α and TRAM has been examined by different groups, only the two native TMSs of the VSV G protein (McCormick et al., 2003; Do et al., 1996) and the Ii invariant chain (Martoglio et al., 1995) were crosslinked to TRAM via photoreactive probes in the

middle of the TMS. Two non-native Lep derivatives with 1 or 2 charged residues inserted into the TMS were also photocrosslinked to TRAM (Heinrich et al., 2000). But the non-INM VSV G TMS was not located in the same site in the translocon as the INM TMSs. In fact, of the 7 non-INM TMSs that have been examined at high resolution using photoreactive probes on different TMS surfaces, none gave a photocrosslinking pattern similar to the 4 INM TMSs (McCormick et al., 2003) (Figs. 25-28). Although the Ii and two charged Lep TMSs have yet to be examined using the same approach, the clear distinction between the high-resolution photocrosslinking patterns of the 4 INM and 7 non-INM TMSs strongly suggests that the two classes of TMS occupy different sites within the translocon.

It is, of course, possible that INM and non-INM TMS binding sites within the translocon overlap to some extent. Consistent with the close juxtaposition of potentially different interaction sites within the translocon, both nascent secretory and nascent membrane proteins have previously been photocrosslinked to TRAM, usually from sites that flank the TMS or the nonpolar signal sequence core (e.g., Johnson & van Waes, 1999; Falcone et al., 1999). On the other hand, because of variations in probe length, reactivity, location, and target atom, one must be cautious in extrapolating from a crosslink to a specific structural arrangement between two macromolecules. For example, the second TMS in opsin was chemically crosslinked to TRAM (Meacock et al., 2002), but no crosslinking to TRAM was detected when photoreactive probes were positioned in the middle of the second opsin TMS in a chimeric protein (McCormick et al., 2003). Thus, high-resolution experiments using multiple different probes will be

necessary to assess the extent to which the INM and non-INM TMS binding sites in the translocon overlap spatially and dynamically.

Based on photocrosslinking data obtained with charged Lep1 mutants, Heinrich et al. (2000) proposed that TRAM interacts with TMSs that were charged or hydrophilic. Yet of the four INM-directed TMSs found adjacent to TRAM during integration, none contains a charged amino acid (Fig. 25A). Furthermore, based on the White-Wimley values ($\Delta G_{\text{woct}} - \Delta G_{\text{wif}}$) for quantifying amino acid movement from the aqueous to the nonpolar phase, the free energies of transfer of the 4 INM TMSs range from -3.0 kcal/mole for the first nurim TMS to -10.5 kcal/mole for the E66 TMS (a more negative number indicates a more hydrophobic sequence)(Braunagel et al., 2004; White et al., 1999). Thus, even the E66 TMS, which is the most hydrophobic of the 11 TMSs that we have thoroughly examined to date, is positioned adjacent to and photocrosslinks to TRAM during co-translational integration. It therefore appears that TRAM functions in a different or an additional role than that proposed by Heinrich et al. (2000).

We have here compared the photocrosslinking targets of probes that are in different constructs, but are positioned the same number of residues from the N-terminus. Another approach would be to compare the photocrosslinking targets for probes positioned the same number of amino acids from another reference point, such as the N-terminal residue in the putative TMS. But since only small variations in photocrosslinking patterns were observed with E66, E25, LBR1, and Nur1 TMSs (Figs. 25-28), it appears that the differences in TMS length and location (i.e., the number of residues between the N-terminus and the putative start of the TMS) shown in Fig. 25A do not significantly

alter the positioning of the TMS within the translocon. Instead, TMS-translocon interactions are apparently dictated by some other feature of the TMS (see below). This conclusion is supported most strongly, of course, by the fact that the Lep1 TMS does not photocrosslink to TRAM (Fig. 29).

What, then, is the key structural determinant of the SM that is recognized by the translocon? The sample size is still too small to provide a clear answer to this question, but there are some interesting clues in the results presented here. First, as was noted above, we have here examined constructs containing the first TMSs of LBR and nurim because these TMSs are important in terms of sorting to the INM (Soullam et al., 1995; Rolls et al., 1999) and we wished to facilitate comparisons with the INM-directed viral proteins that contain only a single TMS. Yet the orientation of the LBR1 TMS in the bilayer is opposite to the bilayer orientation of the same TMS in native LBR. Strikingly, and unexpectedly, both LBR1 and native LBR are sorted and directed to the INM (submitted). Since the LBR TMS is directed to the INM no matter what its orientation, it appears that the structural features recognized by the sorting machinery as a signal for INM-directed TMSs are not dependent upon the orientation of the TMS in the translocon. Second, both E66 and E25 are directed to the INM, even though E25 lacks the cytosolic positive charge that is characteristic of a SM sequence. Since the E66 and E25 TMSs photocrosslink to TRAM and Sec61 α identically (Figs. 25B & 26), it appears that the positive charge that flanks the TMS is not involved in positioning an INM TMS at a particular site within the translocon. Moreover, both E66 and Lep1 have positive charges flanking the TMS, yet their TMSs occupy different locations in the translocon

(Fig. 25B, 29). It therefore appears that the properties of the TMS itself dictate where it moves in the translocon, while the positive charge may be important for interactions that occur after leaving the translocon, such as recognition and/or association with FP25K and/or E26 (Figs. 32, 35). These results, taken together, strongly suggest that the characteristic structural elements that identify a protein as an INM protein and initiate sorting to the INM are located within the TMS itself. Further experiments with multiple INM-directed TMSs and derivatives will be required to determine what TMS features correlate with INM sorting.

The distinctive photocrosslinking pattern observed with INM TMSs indicates that INM and non-INM TMSs occupy distinctly different sites within the translocon, which in turn suggests that INM-directed TMSs are first identified and sorted by components of the translocon. Since INM TMSs are adjacent to both Sec61 α and TRAM (Figs. 25-28), either or both could be actively involved in recognizing and sorting INM TMSs; future experiments will clarify their involvement. Also, since an INM TMS remains adjacent to TRAM longer than to Sec61 α (Fig. 30), it is possible that TRAM may be involved in the hand-off of INM TMSs to the next participant in the putative INM sorting pathway. Upon leaving the translocon, the viral INM-directed proteins interact with other viral proteins that are required for sorting to the INM. Since viruses typically appropriate host mechanisms to achieve their objectives, the identification membrane-associated viral proteins that are predicted as required for the sorting of viral proteins to the INM strongly suggests that a similar host protein(s) may also be involved in INM sorting.

CHAPTER IV

IDENTIFICATION OF ACCESSORY PROTEINS INVOLVED IN THE SORTING OF E66 TO THE INM

Experimental design

The first 33 amino acids of E66 (referred to as the SM) contain the information for sorting proteins to the INM (Hong et al., 1997; Braunagel et al., 2004). Because the SM sequence is sufficient to direct a polypeptide to the INM, this sequence must contain the structural features that constitute an INM-sorting signal. If sorting is protein mediated, then recognition of this sequence would require a direct interaction between the SM sequence and a protein involved in sorting. A direct method for detecting interacting proteins is crosslinking because a substrate can react covalently only with proteins that are in close proximity.

Crosslinking experiments in a complex biochemical system that includes the substrate of interest, ribosome, ER microsomes, and many associated factors can yield a myriad of crosslinked proteins. However, by selectively positioning photoreactive or chemical probes only in the substrate (of interest), one can limit the crosslinking targets solely to those proteins adjacent to the substrate. In order to accomplish this, we have performed crosslinking experiments using the E66SM construct (Braunagel et al., 2004), which contains the first 33 amino acids of E66 (SM) fused to a K/C free domain of BCL-2. The K/C free sequence of the BCL-2 domain allows for selective incorporation of probes (amine- or sulfhydryl reactive) into the SM region of the fusion protein and thus enables us to directly monitor the proteinaceous environment of the SM sequence. In

addition, the encoded fusion protein carries a C-terminal (His)₇ tag as well as the T7 epitope that can be used either singly or in tandem for detection and/or purification of crosslinked complexes.

The SM sequence is adjacent to two cellular proteins: SMAP-10 & SMAP-25

Since, the SM-C construct contains only two lysine codons near the C-terminal end of the SM sequence (Fig. 36A), the proteinaceous environment of the SM sequence can be directly monitored using a lysine-specific crosslinking reagent, and any crosslinked product(s) can be detected and/or purified via the (His)₇ tag (using TALON beads). Also, since the sample contains many proteins with surface-exposed lysine amino groups, the detection of a specific covalent complex would be explained most reasonably by the association of the substrate SM sequence with a particular target protein. Using this approach, we showed that the SM sequence was chemically crosslinked to viral proteins FP25K and/or E26, either in nuclei from insect Sf9 cells that had been infected with a recombinant baculovirus expressing SM-C or when SM-C was cotranslationally integrated into ER microsomes from infected cells *in vitro* (Braunagel et al., 2004; chapter III in this study).

The potential existence of viral proteins that associate (crosslink) with the SM sequence led us to examine more closely the environment of the SM sequence in ER microsomes purified from uninfected Sf9 cells. When the proximity of SM-C to other proteins was examined by chemical crosslinking, a prominent crosslinked species with a relative mobility (*M_r*) of about 10 kDa was observed (Fig. 36B, lane 2). This cellular protein was tentatively named SM-associated protein or SMAP-10. In addition to

SMAP-10, the SM-C also crosslinked to another cellular protein with a relative mobility (M_r) of about 25kDa (Fig. 36B, lane 2) that was tentatively named SMAP-25. No crosslinks to SMAP-10 or SMAP-25 were seen when the samples were not treated with chemical crosslinker (Fig. 36B, compare lanes 1 & 2).

To assess the generality of this observation, SM-C was translated in an *in vitro* incubation containing ER microsomes purified from canine pancreas. As shown in Fig. 36B (lane 4), SM-C crosslinks to a ~10 kDa protein with an efficiency similar to that seen in the insect microsomes (Fig. 36B, lane 2). It therefore appears that even divergent (insect and mammalian) species contain an endogenous protein that associates with the SM sequence after it has been released from the translocon.

Since the TMS within the SM sequence contains a cysteine residue, we wished to determine whether crosslinks to SMAP-10 could also be observed using sulfhydryl group- reactive crosslinkers. To this end, crosslinking reactions were performed using homo-and hetero-bifunctional sulfhydryl group-reactive crosslinkers (BMH and MBS respectively). As shown in Fig. 37A, crosslinks to SMAP-10 were seen in both the cases (lanes 2 and 3), and the highest efficiency of crosslinking was observed using BMH (compare lanes 1-3). This indicates that SMAP-10 contains cysteine residue(s) that are adjacent to the TMS of the SM sequence.

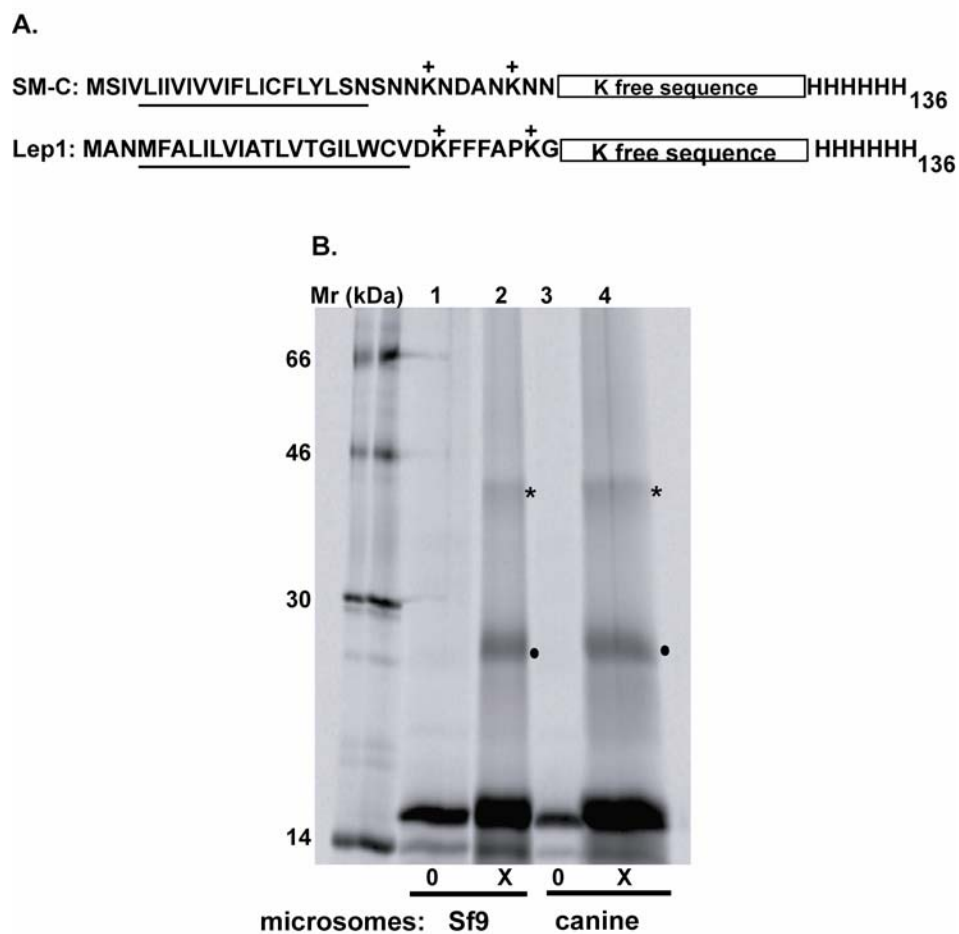


Figure 36. Chemical crosslinking of E66SM to SMAP-10 & SMAP-25. (A) The N-terminal sequence of the SM-C and Lep1 constructs is shown with the TMS underlined. (B) The (His)₆-tagged SM-C construct was translated in the presence of Sf9 microsomes (lanes 1 & 2) or canine pancreatic microsomes (lanes 3 & 4), and either treated with 50 μM BS³ (lanes 2 & 4) or with crosslinking buffer alone (mock) (lanes 1 & 3). Following crosslinking, the samples were incubated with TALON beads to purify the (His)₆-tagged translation product and any crosslinked product(s). The samples that received the crosslinking buffer alone (mock) or the chemical crosslinker are identified by the symbols “0” and “X” respectively. Covalent crosslinks between SM-C and SMAP-10 or SMAP-25 are identified by the closed circle and asterix respectively.

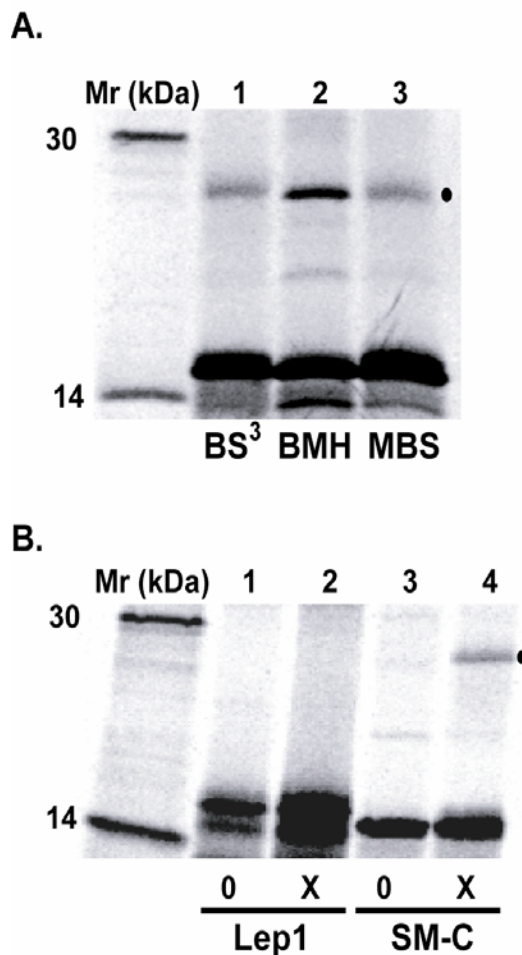


Figure 37. SMAP-10 crosslinking using different chemical crosslinkers and substrates. (A) SM-C construct was translated in the presence of Sf9 microsomes and crosslinking reactions were performed using three different chemical crosslinker: BS³, BMH and MBS. The crosslinked product(s) were purified using TALON beads. Crosslinks to SMAP-10 are identified by the closed circle. (B). (His)₆-tagged SM-C and Lep1 constructs were translated in the presence of Sf9 microsomes and either treated with 50μM BS³ (lanes 2 & 4) or with crosslinking buffer alone (mock) (lanes 1 & 3). The crosslinked product(s) were purified using TALON beads as in (A).

We previously demonstrated that the viral proteins FP25K and E26 do not associate with the first TMS of leader peptidase (Lep1) even though Lep1 contains lysines in approximately the same position as the SM sequence (chapter III in this study). To test whether cellular SMAP-10 exhibits similar substrate specificity, the Lep1 construct (Fig. 36A) was translated *in vitro* and treated with the lysine-specific crosslinker. No crosslinks to SMAP-10 were observed with Lep1 (Fig. 37B, lane 2) in contrast to the efficient crosslinking observed with SM-C (lane 4).

Having demonstrated that cellular SMAP-10 exhibits substrate specificity similar to the viral proteins FP25K and E26, we wanted to test whether SMAP-10 associates (crosslinks) with the SM sequence only after release from the translocon {as observed with the viral proteins (chapter III in this study)}, or if it can associate prior to translocon release. To this end, we examined the proximity of SM-C nascent chains (nascent implying a ribosome-bound integration intermediate) to other proteins by chemical crosslinking at different stages of integration. Although crosslinks to SMAP-10 were seen with the different SM-C nascent chains (Fig. 38, lanes 1-5), the efficiency of SM-C crosslinking to SMAP-10 increased dramatically upon release from the translocon (denoted as 136-R; Fig. 38, lane 6). These experiments reveal that the SM sequence is in close proximity to SMAP-10 before and after leaving the translocon.

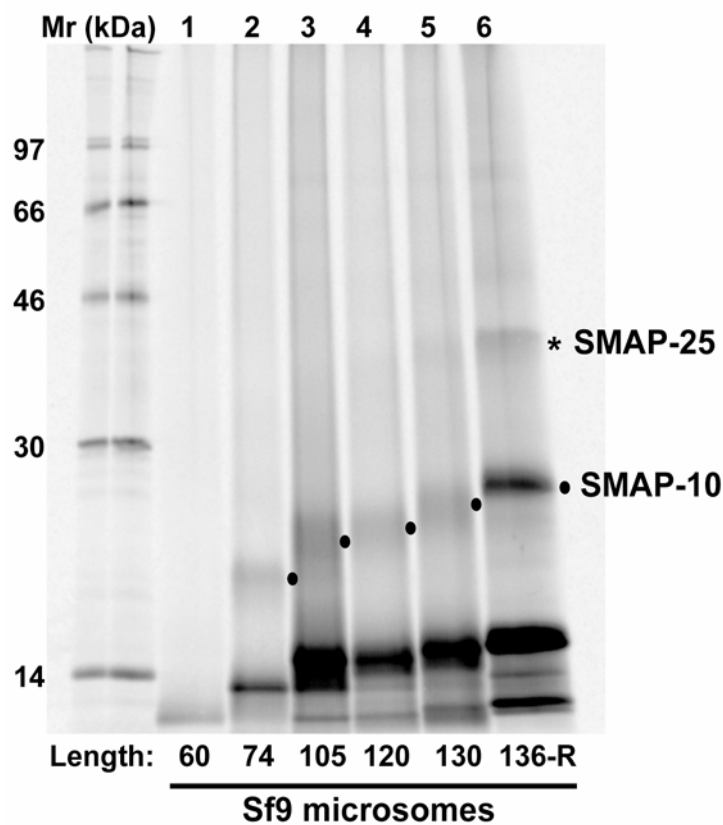


Figure 38. SM sequence is in close proximity to SMAP-10 before and after the leaving the translocon. (His)₆-tagged nascent or full-length (ribosome-released) SM-C proteins were translated in the presence of Sf9 microsomes, chemically crosslinked (using 50 μ M BS³), and subjected to TALON purification. Nascent chain lengths (amino acids) in the chemically-crosslinked SM-C integration intermediates are indicated below the gel. Normally terminated (ribosome-released) full-length SM-C (indicated as 136-R) is shown in lane 6. Covalent crosslinks between the SM-C integration intermediates and SMAP10 or SMAP25 are identified as above.

BV/ODV –E26 shares epitopes with SMAP-10

Since viruses are highly skilled at manipulating cellular pathways, and the Mr of SMAP-25 is similar to the molecular mass of the two viral proteins (FP25K & E26) that have been shown to crosslink with SM-C, antibodies specific for viral FP25K & E26 were tested for cross-reactivity with a cellular protein of similar Mr using Sf9 extracts. Antisera specific for FP25K demonstrated no cross-reactivity, however antibodies raised against bacterially expressed E26 cross-reacted predominantly with a cellular protein of ~25kDa, and to a lesser extent with a cellular protein of ~10kDa. Since, this cross-reactivity was seen in both Sf9 extracts and Sf9 microsomes (Fig. 39) we decided to test whether the E26 antiserum could recognize either SMAP-10 or SMAP-25.

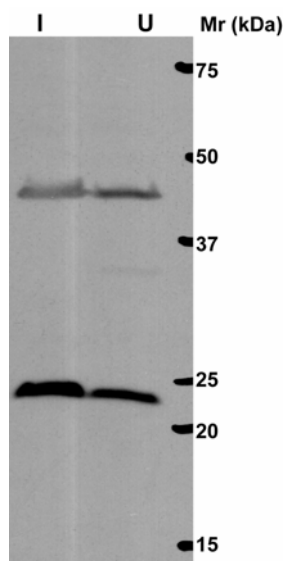


Figure 39. E26 antiserum crossreacts with a ~25kDa cellular protein. Thirty equivalents each of virus-infected microsomes (I) and uninfected Sf9 microsomes (U) were resolved by S-PAGE and immunoblotted using the E26 antiserum (generous gift of Jared Burks).

To this end, the SM-C construct was translated *in vitro* in the presence of Sf9 microsomes, and following crosslinking, the samples were either incubated with TALON beads or the E26 antiserum. As shown in Fig. 40, the E26 antiserum was able to precipitate a radiolabeled product (lane 2) having the same Mr as the crosslinked complex purified via the (His)₆ tag on the SM-C (Fig. 40 lane 1 & Fig.36B lane 2), indicating that the molecular mass of the protein recognized by the E26 antiserum is similar to SMAP-10. The immunoprecipitation reaction was specific, since the preimmune serum failed to precipitate the crosslinked complex (Fig. 40, lane 3).

Having shown that SMAP-10 can associate with the SM sequence both before and after it leaves the translocon (Fig. 38), we decided to test whether the cellular protein recognized by E26 antiserum also demonstrated the same ability. As shown in Fig. 41A, the protein recognized by E26 antiserum was able to associate with the SM sequence both before (Fig. 41A, lanes 1-5) and after it was released from the translocon (denoted as 136-R; Fig. 41A, lane 6). Thus, as previously observed with SMAP-10 (Fig. 38), the cellular protein recognized by E26 antiserum appears to be translocon-associated (Fig. 41A) and not unique to insect microsomes, but also present in microsomes derived from mammalian (canine pancreatic) cells (Fig. 41B).

Put together, these results suggest that the E26 antiserum recognizes epitopes within Sf9 SMAP-10. As such, the antiserum should serve as a useful tool in the identification of SMAP-10, and hence was used to screen an Sf9 cDNA expression library.

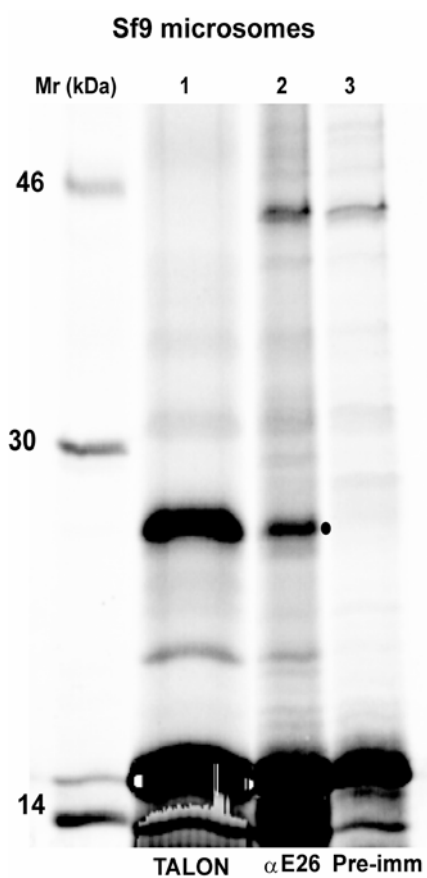
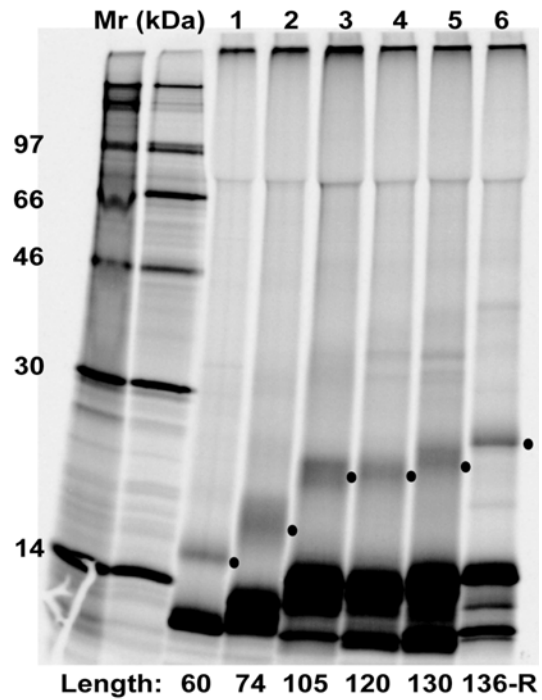


Figure 40. E26 shares epitopes with cellular SMAP-10. The SM-C construct was translated in the presence of Sf9 microsomes. Following translation, the membrane pellet was recovered by sedimentation, treated with the chemical crosslinker, and the crosslinked products were either purified using TALON beads (lane 1), or immunoprecipitated using the E26 antisera (lane 2), or immunoprecipitated using pre-immune antiserum (lane 3).

A. Sf9 microsomes



B. Canine pancreatic microsomes

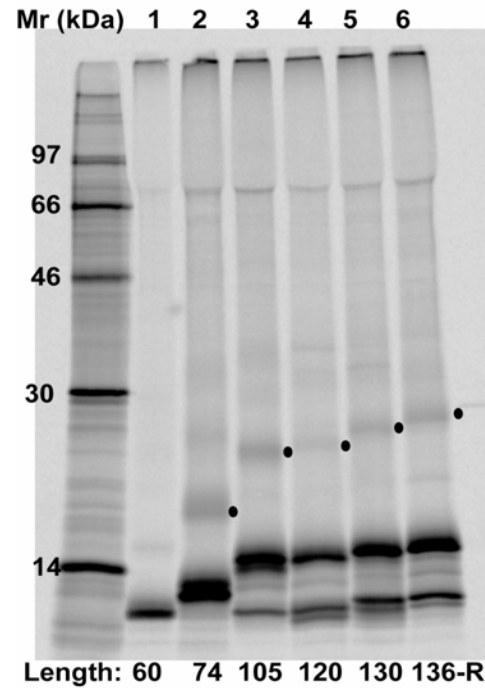


Figure 41. Immunoprecipitations using E26 antiserum. Crosslinked adducts containing SM-C derived from Sf9 (A) or canine pancreatic (B) microsomes were detected by immunoprecipitation using the E26 antiserum. Nascent chain lengths in the samples were the following: 60 in lane 1; 74 in lane 2; 105 in lane 3 ; 120 in lane 4; 130 in lane 5. Samples containing normally terminated SM-C polypeptide chains (denoted as 136-R) are shown in lane 6. Crosslinked adducts are indicated by the closed circles.

**Antibody screening of an Sf9 cDNA expression library using E26 antibody
identifies clone 2**

A lambda-ZAP cDNA expression library comprised of cDNA fragments derived from Sf9-mRNA (provided by Christian Gross) was used to infect *E.coli* (BB4) cells at an appropriate dilution. The resultant plaques containing phage particles expressing a beta-galactosidase fusion of the cDNA insert were transferred onto nitrocellulose membranes and probed with the E26 antisera (provided by Jared Burks). Following incubation with the antibody, the blots were treated with [¹²⁵I]-Protein A to allow for visualization of the positive plaques using autoradiography. The results of a typical primary screen and secondary screen are depicted in Fig. 42. Typically, an isolated positive plaque obtained from the primary screen generated several positive plaques on the secondary screen. A total of 40 primary positive plaques were subjected to secondary and tertiary rounds of antibody screening prior to phagemid rescue, excision and sequencing of the cDNA insert(s).

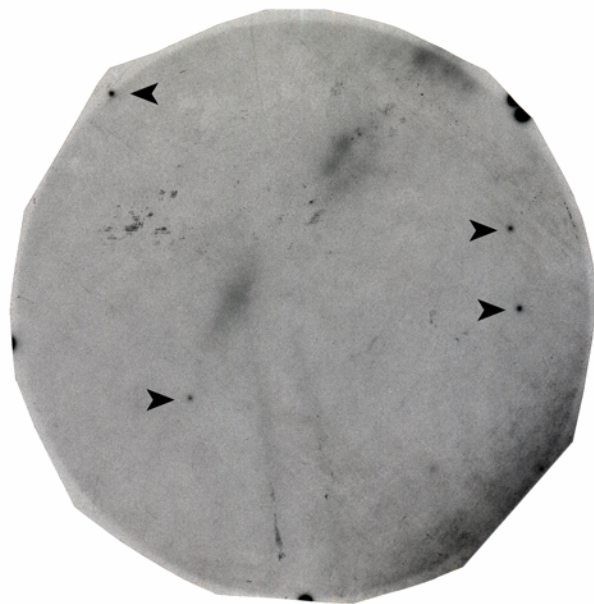
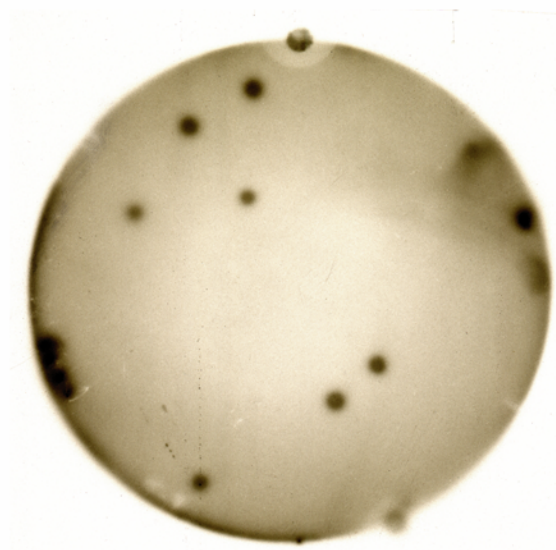
A. Primary screen**B. Secondary screen**

Figure 42. Sf9 cDNA expression library screen. The results of a typical primary and secondary screen are depicted in (A) and (B) respectively. The positive plaques are identified by the arrowheads in (A).

Sequence analyses revealed that a significant majority (33/40) of the plaques contained only the C-terminal 20-30 amino acids (including the in frame stop codon) of the insert, which proved to be insufficient (too short) to provide any meaningful information regarding the identity of SMAP-10. However six plaques were found to contain the same cDNA insert (454 amino acids) referred to as clone 2 (Fig. 43). The high representation of clone 2 sequence in the positives identified by the E26 antiserum and the identification of a large region of the ORF (454 amino acids) led us to focus on it, to determine the identity of SMAP-10. Another positive identified in the screen, clone 15 (504 amino acids) was also analyzed but it did not associate with the viral SM-C.

While, the E26 antiserum crossreacted with SMAP-10 (Fig. 40), the protein encoded by clone 2 consists of at least 454 amino acids. Although, the molecular mass of the clone 2- encoded protein was far in excess of 10kDa we tested whether any portion (N- or C- terminal domain/internal fragment) of clone 2 could associate (crosslink) with SM-C. ER microsomes containing membrane-integrated and (His)₆-tagged SM-C were added to translation reactions programmed with transcripts encoding T7-tagged versions of a series of clone 2 derivatives (Fig. 44A & 44B). Since two derivatives (Met₃₁₀₋₄₅₄ & Met₃₅₆₋₄₅₄; Fig. 44B: construct # 5 & 6) lacked any lysine residue, the crosslinking reactions were performed using the sulfhydryl-reactive crosslinker, SMPB rather than the lysine-specific crosslinker BS³. The presence of unique tags on the *in vitro* generated clone 2 derivative(s) (T7 tag) and the membrane-integrated SM-C {(His)₆ tag} allows the specific detection of a crosslinked complex.

```

GGCAGCGGGT CTGGCGGTGC GGGCGCGGAG GAGTCTCCT CCGAGGAGGG CGAGGTCCGG CGTCTGCAGG CGCTGCTGGA
G S G S G G A G A E E S S S E E G E V G R L Q A L L E
27
GGCGCGGGC CTGCCGCCG ATCTACTCGG GCGCTGGGC CCGCGCATGC AGCATCTGCT GCATAGGACT GCTACTGCCA
A R G L P P H L L G A L G P R M Q H L L H R T V T A
53
ACTCCGCTGC ATCTAAAGCG GCACAGCTAC TGGCCGGTCT GCAAGCGACC GGTGACGAAG GCCAGCAGCT GCAGGCTGTG
N S A A S K A A Q L L A G L Q A T G D E G Q Q L Q A V
80
ATCGAGATGT GTCAGCTGCT GGTGATGGC AATGAGGACA CGCTGGCCGG CTCCCCGTC AGACAAGTCG TGCCCGCGT
I E M C Q L L V M G N E D T L A G F P V R Q V V P A L
107
CGTCAATCTA CTCGCTGCTG AACACAACTT TGACATGATG AACCATGCGT GTCGTGCCCT GACGTACATG CTGGAGGCGC
V N L L A A E H N F D M M N H A C R A L T Y M L E A
130
TGCCCGCAG TAGCGCGCG GTGGCGCTGG CCGTGCCCGC CTTCCTGGAC AAGTTGCAGG CCATCACCTG CATGGACGTG
L P R S S G A V A L A V P A F L D K L Q A I T C M D V
160
GCCGAGCAA GCCTCACGGC GCTCGACATG CTCTCCCGAC GACTCTCAA AGCTATATTA CAAGCGCGTG GCGTGTACG
A E Q S L T A L D M L S R R H S K A I L Q A R G V S A
187
TTGCTGACT TACTTGGATT TCTTCTCCAT CAACGCACAG CGCGCCGCC TCTCCATTAC AGCCAACTGC TGTCAGAACC
C L T Y L D F F S I N A Q R A A L S I T A N C C Q N
213
TCACTCCGA TGAGTCCAT CTAGTAGGG ACTCTCTACA ACTATTGGCT AATAGACTTA CTCACAAGA CAAGAAATCA
L T P D E F H L V R D S L Q L L A N R L T Q Q D K K S
240
GTAGAATGCG TATGCCTGC GTTCTCGCGA CTCGTGGACA GTTCCAAACA TGATCCGGCT CGCCTACAGG AGATCGCTAC
V E C V C L A F S R L V D S F Q H D P A R L Q E I A T
267
TCCAGAACTG CTCACTAATT TACAACAAT GTTGGTGGTG CAGCCCCCGC TGATATCCGG CGCGACGTTT ATCACAGTGC
P E L L T N L Q Q L L V V Q P P L I S G A T F I T V
303
TGCGGTGCT GTGGGTCTG TGCGCCGCT GTCCCGCAGT GGCCCTGGCC CTGCACCAGC GCTCCATCGC TGACACGCTG
L R L L W V M C A A C P Q L A L A L H Q R S I A D T I
310
CTCTGTCTGC TCACCGGGT CACGCTGCAT CAGGAGCAAG TTGAATTGAT CCCGCGTCTC CCGCAAGAGT TGTACGAGAT
L C L L T G S T L H Q E Q V E L I P R L P Q E L Y E I
348
CACCTGCCTG ATAGGCGAGC TGATGCCGCG CCTGCCACA GACGGCATCT TCGCAGTAGA CTCACATCTA GACAGACCTT
T C L I G E L M P R L P T D G I F A V D S H L D R P
356
GGTCCGCTT TACCGAGCG ACTGCCACT GGCAGTGGAG GGATGATAGA GGAGTATGGC GGTCTACTC GTGGGCGGAG
W S A S T E R T A H W Q W R D D R G V W R S Y S W A E
401
AGCCGCGCGC TGGAGGCGG CGCGGCGCG GCGGAGAGGG AGGTGTGCCT GACGACGCTG GGCCGCTCCT ACACCGTGGA
S R A L E A G A A A G E R E V C L T T L G R S Y T V D
439
CCTCACCGCC ATGCAGAGTT TCGAGTCACA GAGGGAGTCT TCATCATGA
L T A M Q S F E S Q R E S S S *
454

```

Figure 43. Clone 2 identified in the screen using E26 antiserum. The annotated sequence of clone 2 identified in the library screen is shown. The PE oligo used for primer extension analysis is underlined. The transcription initiator sequences identified by primer extension are indicated by the red asterisk, and the corresponding initiator methionine residues are highlighted in yellow.

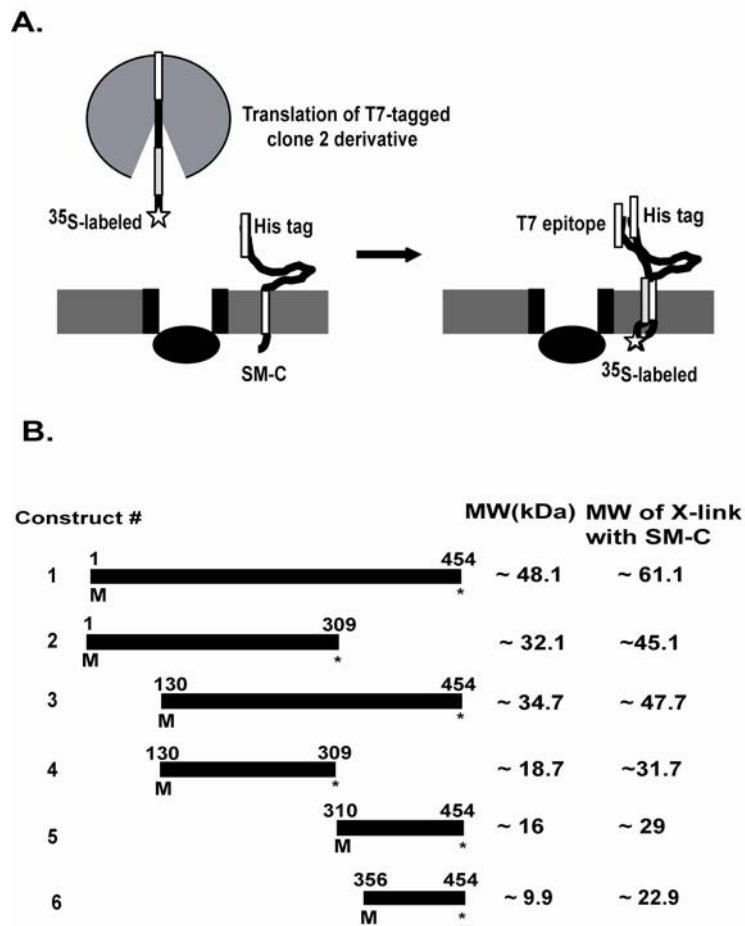


Figure 44. Clone 2 derivatives and set up of chemical crosslinking reactions. (A). The set-up of the chemical crosslinking reaction is depicted. The different clone 2 derivatives are translated in the presence of SM-C microsomes. Any complex containing the clone 2 derivative chemically-crosslinked to SM-C (in the membrane) can be either purified using TALON beads, since the SM-C in the membrane is (His)₆ tagged or immunoprecipitated using antibodies specific for the T7 epitope, since the *in vitro* translated product is radiolabeled (indicated by the asterix) and T7 tagged. (B). The different derivatives of clone 2 generated *in vitro* are shown. The asterix indicates the in frame stop codon either naturally occurring in the clone 2 ORF (codon 454) or introduced by PCR (codon 309) to generate internal truncates of clone 2. The expected molecular weight (MW) of the different clone 2 derivatives and chemically crosslinked products (if any) with SM-C are indicated.

No crosslinked complexes containing SM-C (whose expected molecular masses are indicated in Fig. 44B) were purified (using TALON beads) when crosslinking experiments were performed using different derivatives of clone 2 initiating at Met₃₅₆ (Fig. 45, lane 2), Met₁₃₀ (data not shown) or the initiator methionine (Met₁) (data not shown). In contrast, the clone 2 derivative initiating at Met₃₁₀ was able to crosslink with SM-C in the microsomes: this association was dependent on the presence of crosslinker (Fig. 45, lanes 3 & 4), and the crosslinked product (of the expected molecular weight: Fig. 44B) could be purified using TALON beads. The crosslinked product could also be immunoprecipitated using antibodies specific for the T7 epitope (lane 5). The results of the crosslinking experiment demonstrated that a derivative of clone 2 (Met₃₁₀₋₄₅₄) contains the structural features necessary for association with SM-C.

Similar crosslinking experiments were conducted using a series of *in vitro* generated derivatives of clone 15 (data not shown). However, no crosslinking to SM-C was observed with any of the clone 15 derivatives.

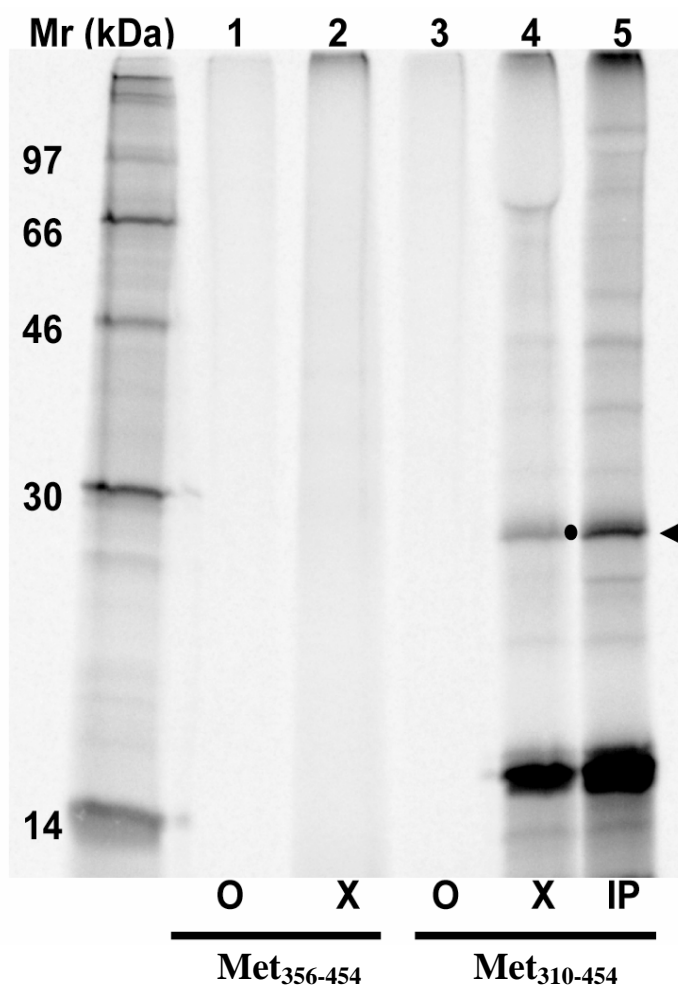


Figure 45. Crosslinking of clone 2 derivatives. *In vitro* generated transcripts initiating either at Met₃₁₀ or Met₃₅₆ and T7 tagged at the C-terminus were generated using SP6 RNA polymerase. The transcripts were translated *in vitro* in the presence of SM-C microsomes, treated either with crosslinking buffer alone (lanes 1 & 3) or with 50 μ M SMPB (lanes 2, 4 & 5), and either purified using TALON beads (lanes 1-4) or immunoprecipitated using antibodies specific for the T7 epitope (lane 5). The crosslinked product purified by the TALON beads and immunoprecipitated by antibodies specific for the T7 epitope is indicated by the closed circle adjacent to lane 4 and the arrowhead adjacent to lane 5 respectively.

We had previously determined that the ~10kDa cellular protein recognized by E26 antiserum remains membrane-associated when alkaline conditions (sodium carbonate at pH 11.5) are used to strip the microsomal membranes of peripherally associated proteins (data not shown). When a similar test was performed using the different derivatives of clone 2, the Met₃₁₀₋₄₅₄ derivative remained membrane associated (Fig. 46, lane 4). In contrast, membrane association of the Met₃₅₆₋₄₅₄ derivative (lanes 1 and 2) and the other clone 2 derivatives (lanes 5-12) was sensitive to alkaline treatment. Thus, the Sf9 cDNA (clone 2) identified using the E26 antisera encodes within its sequence a protein, Met₃₁₀₋₄₅₄ that has the following features: (1) has a molecular mass { 16 kDa } similar to that predicted for SMAP-10; (2) contains epitope(s) that are shared with viral E26; (3) crosslinks with the SM-C; and (4) remains membrane-associated under alkaline conditions.

Met₃₁₀₋₄₅₄ is a translocon-associated protein

Crosslinking data shows that SMAP-10 is adjacent to the SM sequence before it is released from the translocon (Fig. 38), indicating that it is a translocon-associated protein. Since, antibodies specific for Met₃₁₀₋₄₅₄ are currently not available, we used an alternate approach to directly test its ability to associate with translocon components. Met₃₁₀₋₄₅₄ was translated *in vitro*, and incubated posttranslationally with canine pancreatic microsomes and two different concentrations of SMPB. When the crosslinking reactions were analyzed by SDS-PAGE, a prominent crosslinked product of ~56kDa was observed (Fig. 47A lanes 1 & 4), indicating crosslinks to one of the

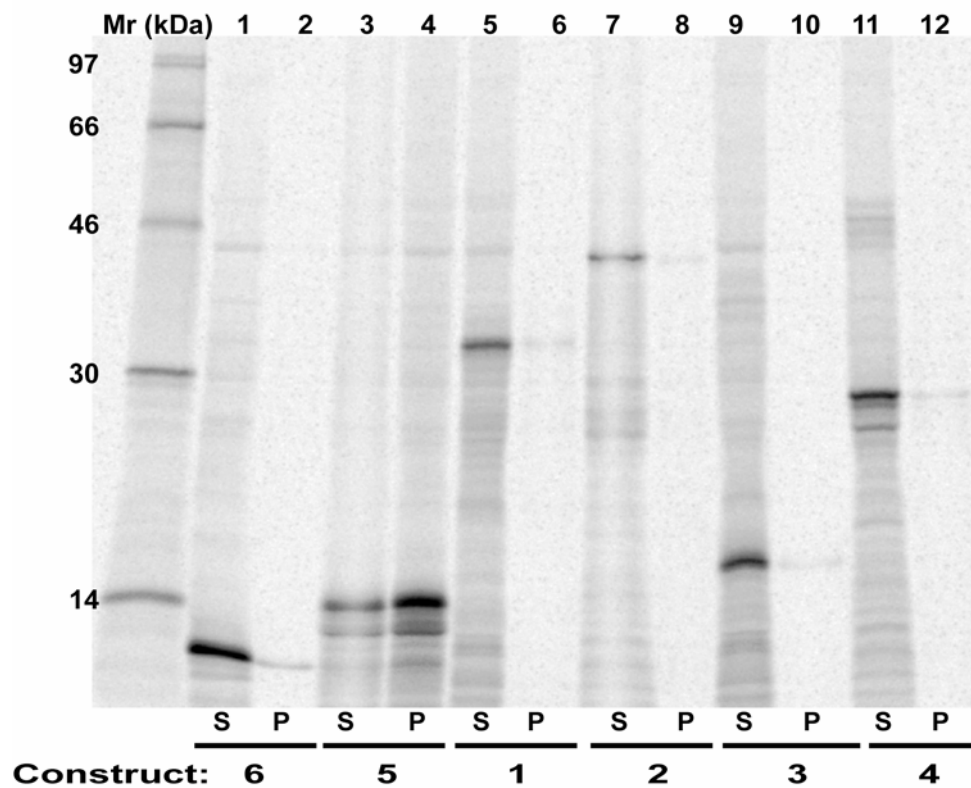


Figure 46. Membrane association of clone 2 derivatives. The membrane association of the different clone 2 derivatives was examined by performing *in vitro* translations followed by treatment with Na_2CO_3 (pH 11.5) and sedimentation through an alkaline cushion. S, proteins in the supernatant fraction after carbonate extraction; P, nonextracted proteins in the carbonate pellet.

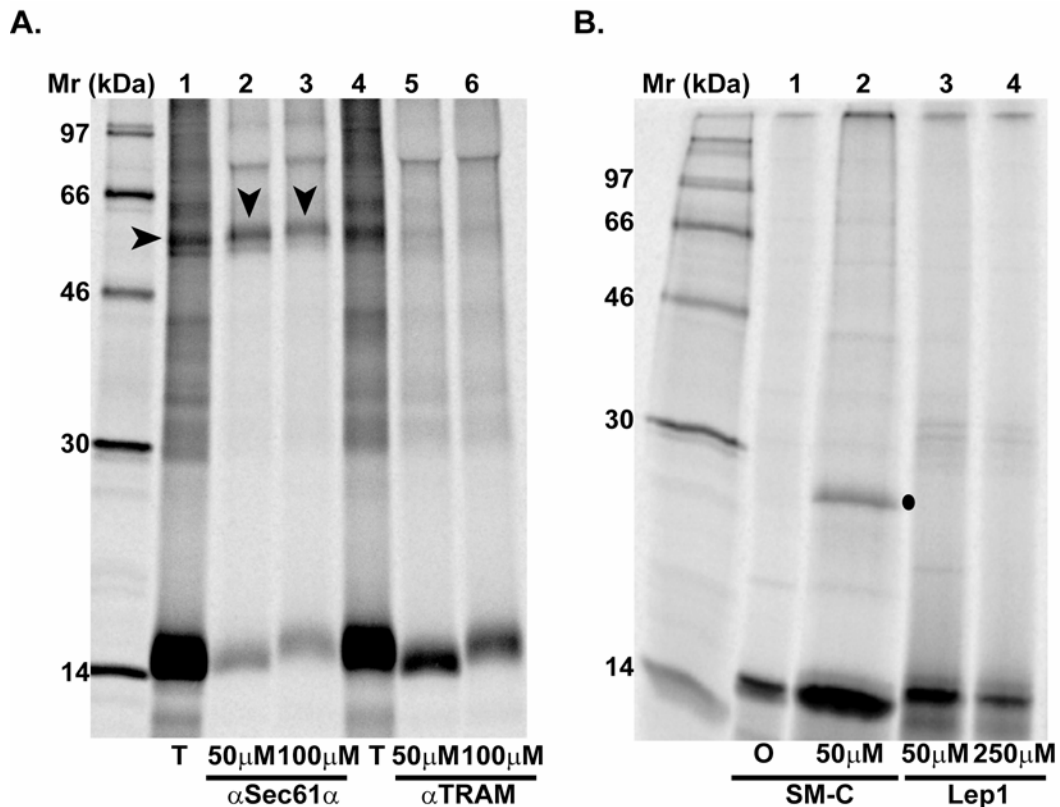


Figure 47. $Met_{310-454}$ is a translocon-associated protein, which is selective in substrate selection. (A). $Met_{310-454}$ was translated *in vitro*, incubated posttranslationally with canine pancreatic microsomes and treated with either 50 μ M SMPB (lanes 2, & 5) or with 100 μ M SMPB (lanes 3 & 6). Following the crosslinking reaction, the samples were immunoprecipitated by using either antibodies specific for Sec61 α (lanes 2 & 3), or antibodies specific for TRAM (lanes 5 & 6). Aliquots of the crosslinking reactions analysed in lanes 2 & 5, were removed prior to immunoprecipitation and analysed in lanes 1 & 4. The crosslinked product and immunoprecipitated material are identified by the arrowheads. (B). $Met_{310-454}$ was translated in the presence of Sf9 microsomes containing cotranslationally integrated SM-C and Lep1. Following crosslinking with the BS³, the samples were incubated with TALON beads, and analyzed by SDS-PAGE. The crosslinker concentrations used are indicated and the sample labeled 'O' represents the sample which received only the crosslinking buffer (mock).

translocon protein(s) Sec61 α or TRAM (both of which are ~40kDa). Crosslinks to Sec61 α were seen at both the crosslinker concentrations tested as judged by the ability of antibodies specific for Sec61 α to immunoprecipitate the crosslinked complex (lanes 2 & 3). In contrast, extremely inefficient or no crosslinking was seen with the translocon protein TRAM (Fig. 47A, lanes 5 & 6). The ability of Met₃₁₀₋₄₅₄ to be chemically-crosslinked to the translocon component Sec61 α , suggests that analogous to SMAP-10, it is a translocon-associated protein and thus is able to gain access to the SM sequence while it is still being synthesized by the ribosome (Fig. 38).

Having demonstrated that Met₃₁₀₋₄₅₄ is associated with the translocon, we wished to determine whether it exhibited the same substrate specificity as SMAP-10. To this end, we examined the ability of *in vitro* translated Met₃₁₀₋₄₅₄ to associate (crosslink) with (His)₆-tagged SM-C and Lep1 cotranslationally integrated into Sf9 microsomes. As shown in Fig. 47B, the crosslinked complex containing Met₃₁₀₋₄₅₄ chemically crosslinked to SM-C was purified using TALON beads (lane 2). In contrast, no crosslinked complex containing Met₃₁₀₋₄₅₄ crosslinked to Lep1 was purified, indicating that analogous to SMAP-10, Met₃₁₀₋₄₅₄ is selective in substrate association.

Met₃₁₀₋₄₅₄ is derived via internal initiation of transcription

There are multiple ways to produce a smaller protein from a larger cDNA. It is possible that although the E26 antisera recognized clone 2; a smaller copy number, alternatively spliced cDNA is the source of the cellular SMAP-10 like protein (Met₃₁₀₋₄₅₄). It is equally possible that this smaller protein is a product of proteolytic or post translational processing, or transcriptional initiation at an internal methionine residue

(selection of alternative initiation sites). Examination of the clone 2 (cDNA) sequence revealed the presence of two internal arthropod promoter motifs (CAGT and GATA) associated with transcription initiation elements, including a TATA box and an appropriately spaced Met start codon (Met₃₁₀). Thus, it was straightforward to test if transcripts corresponding to internal transcription initiation sites of clone 2 were produced.

To test for internal transcripts (if any) derived from internal initiation, we isolated total cellular RNA from Sf9 cells and performed primer extension analyses using a primer [PE oligo] that anneals downstream of Met₃₁₀ (Fig. 43). The results of primer extension analyses show that three internal transcripts are produced from this larger cDNA (Fig. 48A). One transcript initiation site corresponds with a known insect promoter (GATA box) with an appropriately spaced (24nts) upstream TA rich sequence. The first methionine residue associated with this promoter sequence is Met₃₁₀, and this transcript would encode the Met₃₁₀₋₄₅₄ isoform of clone 2 (Fig. 43). The second transcript which initiates at a cryptic sequence (CGACT) (Fig. 46B), would encode the Met₃₅₆₋₄₅₄ isoform of clone 2 (Fig. 43). Thus, consistent with our hypothesis Met₃₁₀₋₄₅₄ represents an isoform of clone 2 derived via internal initiation of transcription.

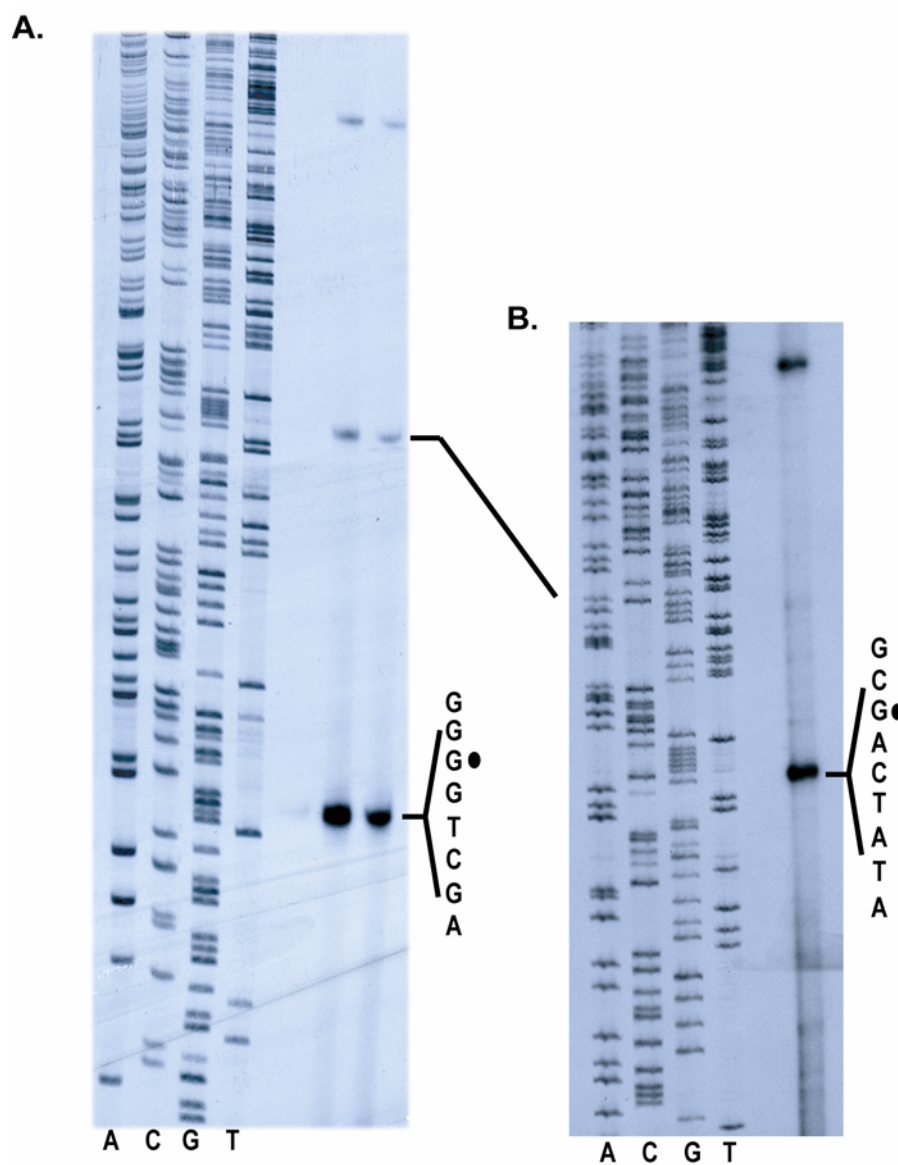


Figure 48. Primer extension analysis. Transcription initiation sites were mapped using 100 μ g of Sf9 RNA. The sequence of the oligo used for primer extension (PE oligo), and the sequence of clone 2 where it anneals are indicated in Fig. 43. (A) and (B) represent the resolution of the two internal initiation products.

Met₃₁₀₋₄₅₄ is an isoform of Sf9 importin α

The combined data suggest that the smaller isoform of the clone 2-encoded protein (Met₃₁₀₋₄₅₄) shares a number of features with SMAP-10: (1) the molecular mass of the encoded protein (16.2kDa) is close to the predicted molecular mass of SMAP-10; (2) both proteins share epitopes with the viral protein E26 (Fig. 40); (3) both proteins associate with the SM sequence before and after it is released from the translocon (Figs. 38 & 41); (4) both proteins appear to be associated with the translocon (Figs. 38, 41 & 47A); (5) both proteins exhibit substrate specificity (Figs. 37B & 47B) and (6) both proteins are insoluble in sodium carbonate at pH 11.5 (Fig. 46). Yet, while the growing evidence suggests that Met₃₁₀₋₄₅₄ and SMAP-10 are the same protein, these observations provide no information regarding the identity of Met₃₁₀₋₄₅₄ or SMAP-10. To gain insights into the identity of clone 2 and its smaller isoform (Met₃₁₀₋₄₅₄), computer-based sequence homology searches were performed.

The BLAST search paradigm (Altschul et al., 1990) revealed that clone 2 displayed significant sequence homology with the nuclear transport adaptor protein: importin α (Fig. 49). If this predicted homology were true, one might expect antibodies specific for importin α to recognize the SM•SMAP-10 (SM•Met₃₁₀₋₄₅₄) crosslinked complex (provided the epitope used to generate the antibodies shared sequence/fold homology with the Met₃₁₀₋₄₅₄ sequence). To test this possibility, antibodies raised in mice against the C-terminal 244 residues (underlined in Fig. 49) of *Drosophila* Karyopherin α 3 or human Rch1 were tested for their ability to precipitate the SM•SMAP-10 crosslinked

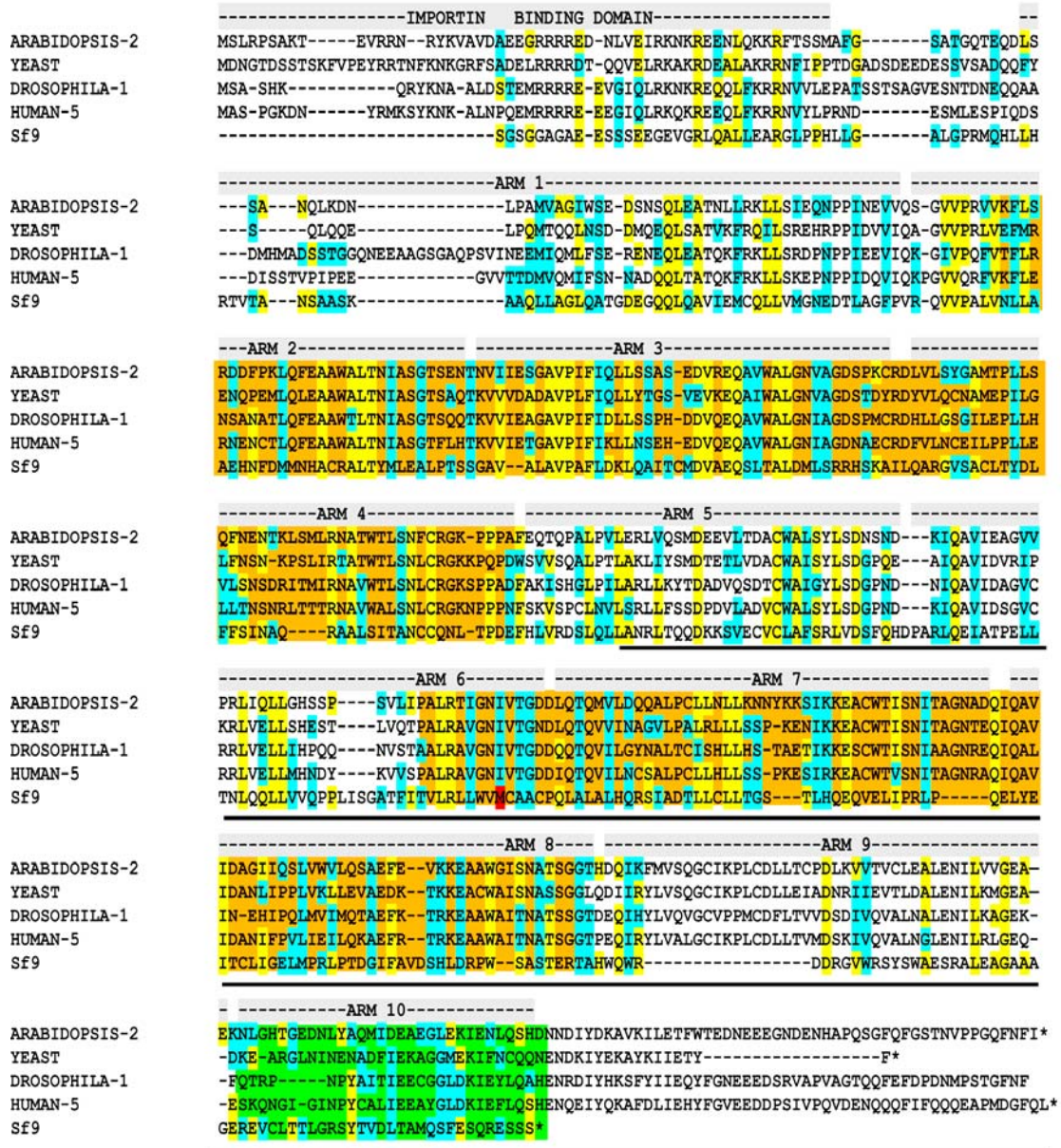


Figure 49. SMAP-10 is an Sf9 importin alpha isoform. The sequences of different importin alpha isoforms from *Arabidopsis* (O04294), *Saccharomyces cerevisiae* (Q02821), *Drosophila melanogaster* (O76521), and *Homo sapiens* (O15131) were aligned with the clone 2-encoded protein (indicated as Sf9 importin alpha). Identical amino acids (based on conservation within the Sf9 importin alpha sequence) are shaded in yellow; similar amino acids are indicated in blue. The major (ARMS 2-4) and minor (ARMS 7-9) NLS-binding sites are highlighted in orange. The exportin (CAS)-binding site (ARM 10) is highlighted in green. The initiator methionine residue (Met₃₁₀) of SMAP-10 is highlighted in red.

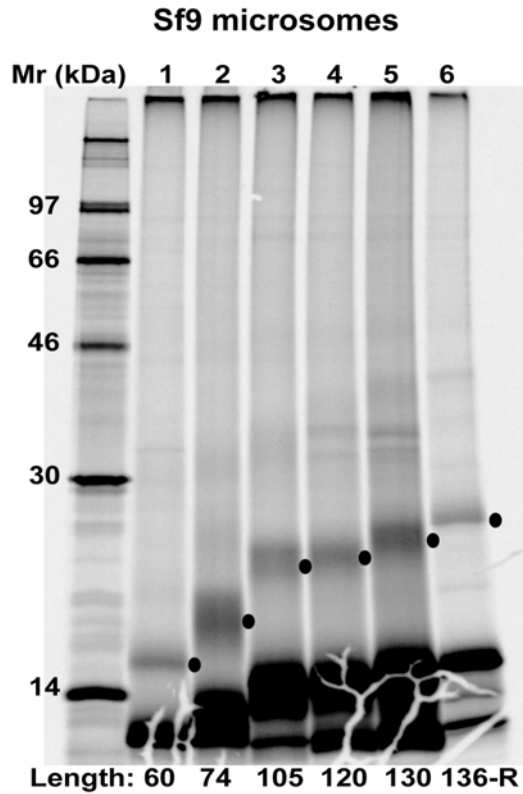


Figure 50. Immunoprecipitation using antibodies specific for Karyopherin alpha.

Crosslinked adducts between SM-C and SMAP-10 derived from Sf9 microsomes were detected by immunoprecipitation using antibodies raised against drosophila karyopherin $\alpha 3$. The epitope used for generating this antibody is underlined (solid black line) in Fig. 44. Nascent chain lengths in the samples were the following: 60 in lane 1 ; 74 in lane 2 ; 105 in lane 3 ; 120 in lane 4 ; 130 in lane 5. Samples containing normally terminated (ribosome-released) SM-C (136-R) polypeptide chains are shown in lane 6. Crosslinked adducts are indicated by the closed circles.

complex. As observed with the E26 antiserum, the importin α antiserum was able to precipitate the complex containing SMAP-10 crosslinked to a variety of SM-C integration intermediates (ribosome bound) (Fig. 50 lanes 1-5) as well as the full-length protein that has been released from the translocon and integrated into the membrane bilayer (denoted as 136-R, lane 6).

In addition to sequence homology searches we (in collaboration with Christos Savva, Texas A&M University) used the program CPHmodels 2.0 {X3M a computer program to extract 3D models} (Lund et al., 2002) to perform homology-based modeling of clone 2 (Sf9 importin α). In this program, a large sequence database is iteratively searched to construct a sequence profile until a template can be found in a database of proteins with known structure. Query and template sequences are subsequently aligned using a score based on profile-profile comparisons. The results of the modeling program revealed that a significant portion (residues 62-302; side chains depicted in yellow in Fig. 51) of the Sf9 importin α (shaded red in Fig. 51) has a three dimensional fold similar (super imposable) to mouse importin α (PDB code: 1IAL) (shaded purple in Fig. 51). The region of mouse importin α that shares a similar fold with Sf9 importin α includes the region between ARM 2 and ARM 6 (including the major NLS-binding site). However, there was not enough sequence homology between the insect and mouse importin α isoforms in the region between ARM 7 and ARM10 for the program to model the Sf9 importin α in three-dimensional space (the region of mouse importin α that could not be used as a template for modeling Sf9 importin α is shaded blue in Fig. 51).

Thus, the results of the modeling program indicate that clone 2 represents an isoform of Sf9 importin α whose C-terminal (ARM 7-ARM10) fold is different from importin α isoforms of other (mouse) species. Interestingly, SMAP-10 (Met₃₁₀₋₄₅₄) initiates very close to the start of ARM 7, and hence represents a novel, membrane-bound Sf9 importin.

Homology-based modeling

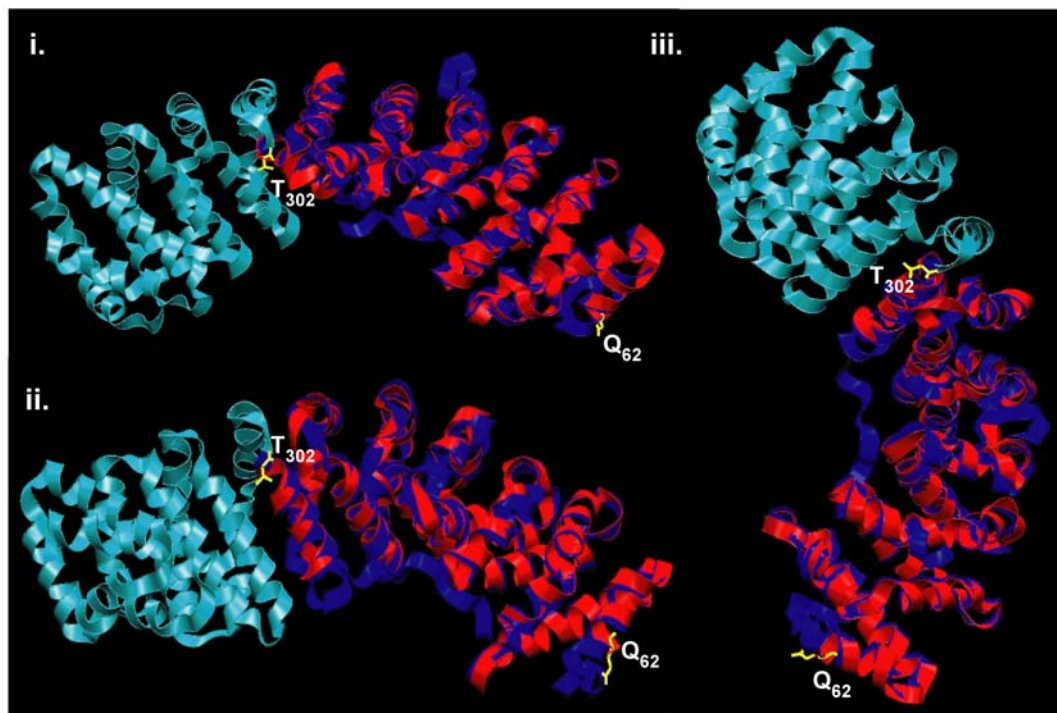


Figure 51. Homology based modeling. The program CPHmodels 2.0 was used to perform homology-based modeling of clone 2 (Sf9 importin α). The predicted three-dimensional fold (homology-based) of Sf9 importin α is shaded in red. Region of Mouse importin α (HIAL) that has good homology with Sf9 importin α is highlighted in purple, and the region with low homology is shaded in blue. The side chains of the first (Q62) and the last (T302) residue within the Sf9 importin α sequence to be modeled based on homology are indicated in yellow.

Discussion

In this work, we have analyzed the proteinaceous environment of the E66 SM sequence in ER microsomes purified from insect Sf9 cells. Five major conclusions can be drawn from our results. First, we have identified a membrane-bound Sf9 importin α isoform (SMAP-10) that associates with the SM sequence before and after it leaves the translocon. Second, transcription is initiated at at least three internal sites within the Sf9 importin α gene resulting in three different isoforms. One of the isoforms obtained via internal initiation is SMAP-10. Third, SMAP-10 shares epitopes with viral E26, which was previously shown to associate with the E66 SM (Braunagel et al., 2004; this study). Fourth, we demonstrate that SMAP-10 is a translocon-associated protein, which is selective in substrate association, indicating that it may potentially be involved in membrane protein sorting to the INM. Fifth, crosslinks to SMAP-10 are seen in ER microsomes purified from insect and mammalian cells, suggesting that this protein is found in divergent species. Finally, the results of this study and our previous work (Braunagel et al., 2004) suggest that the sorting of INM proteins at the ER membrane is a protein-mediated, multistep process in which the INM sorting signal sequentially associates with various sorting factors.

There is growing evidence that protein transport to the INM is not mediated by simple diffusion in the interconnected ER and nuclear membranes as proposed by the diffusion-retention model (Worman et al., 2000). The INM transport process instead appears to be energy-dependent (Ohba et al., 2004), and mediated by other proteins, which are potentially involved in the active restructuring of the NPC to facilitate protein

movement across the lateral channels (Ohba et al., 2004). Also, if INM transport were governed by simple diffusion alone, one would predict INM localization of a substrate to be independent of any other protein(s) or putative interacting partner(s). However, a recent report by Murthi et al. shows that YIL090W/Ice2p, an integral membrane protein located in the ER, is necessary for efficient tethering of Trm1p-II-GFP (tRNA specific m²G methyltransferase) to the INM. In addition, the INM transport process exhibits remarkable specificity contrary to the randomness predicted by simple diffusion in the interconnected membranes (Smith & Blobel, 1993; Soullam & Worman, 1993; Soullam & Worman, 1995; Ellenberg et al., 1997; Furukawa et al., 1995; Lin et al., 2000; Rolls et al., 1999; Imreh et al., 2003). This specificity reflects the existence of sorting events mediated by putative INM-sorting factors, which confer directionality to protein transport towards the INM and prevent random protein distribution.

This study identifies a membrane-bound, isoform of Sf9 importin α that includes the NLS-binding site (ARMS 7-9), and the CAS binding site (ARM 10), and appears to play a role in the sorting of proteins to the INM. Although it has been proposed that importin α acts as an adaptor molecule between importin β and cNLS-bearing proteins, we show that SMAP-10 associates with the INM sorting signal within E66 without the need for importin β . This is not totally surprising, since soluble importin α has recently been shown to transport CaMKIV to the nucleus through the central channel of the NPC without the need for importin β (Kotera et al., 2005). Although one needs to be careful while drawing parallels between importin α -mediated transport through the central channel of the NPC and importin α -mediated transport in the membranes of the nuclear

envelope, the fact that soluble importin α can facilitate nuclear import in an importin β -independent process, allows us to speculate that the same case may be applicable in membrane protein transport. The crosslinking data presented in this paper does not provide any information regarding function of the SM•SMAP-10 interaction, however, based on what is known about the function(s) of soluble importin α , it is tempting to speculate that SMAP10 functions as a nuclear transporter (carrier) that facilitates protein sorting to the INM. As described by Kotera et al (Kotera et al., 2005), at least three requirements must be satisfied for a molecule to be classified as a nuclear transporter: the ability to form a complex with a cargo protein, the ability to penetrate the NPC on its own, the ability to release the cargo and return to the cytoplasm for another round of trafficking.

By examining the proximity of SM-C nascent chains to other proteins using chemical crosslinking at different stages of integration, we examined the first requirement for SMAP-10 to be classified as a nuclear transporter (carrier). Although, crosslinks to SMAP-10 were seen with the SM-C integration intermediates (Fig. 38, lanes 1-5), the highest efficiency of SM-C crosslinking to SMAP-10 was observed with the full length protein that had been released from the translocon (lane 6). The increased crosslinking may result from easier access of the reagent to the lysines in the absence of the translocon, a more favorable alignment of the lysines or cysteines in the SM•SMAP-10 complex after the proteins leave the translocon, and/or an increase in SM•SMAP-10 association in the absence of the translocon proteins that bind to SM (chapter III in this study). Whatever the case, these experiments confirm the formation of a complex

between the SM sequence (putative cargo/substrate) and SMAP-10 (carrier) (Figs. 36, 38). Although, the structures of the *Saccharomyces Cerevisiae* and *Mus musculus* importin α 's bound to cNLS peptides have revealed two NLS-binding sites consisting of ARM repeats 2-4 (major NLS-binding site) and 7-9 (minor NLS-binding site) (Fontes et al., 2000; Conti et al., 1998; Conti et al., 2000; Fontes et al., 2003), SMAP-10 includes only the minor NLS-binding site (ARM repeats 7-9). While, it is difficult to extrapolate the crosslinking data to function of the interaction, our results suggest that the IBB and the major NLS-binding site are dispensable for interaction with the SM sequence and seem to be consistent with the observations of other groups that the carboxyl terminus of importin α (in isolation) can mediate nuclear import of Human Immunodeficiency Virus Type 1 Vpr (Kamata et al., 2005).

The second requirement is the ability of importin α to penetrate the NPC without importin β . It has been reported that the carboxyl terminus of importin α , which partially or completely includes the region between residues 360-495, binds several nucleoporins such as Nup1p (Belanger et al., 1994), Nup2p (Belanger et al., 1994; Solsbacher et al., 2000), Npap60/Nup50 (Lindsay et al., 2002), and Nup153 (Moroianu et al., 1997), which are FG repeat nucleoporins. While, the homology between SMAP-10 and other importin α isoforms is much lower in the region between residues 360-495 compared to the N-terminus (Fig. 51), we speculate that SMAP-10 could potentially facilitate the passage of the cargo(E66SM)-importin α complex via the lateral channels of the NPC via interactions with nucleoporins.

Currently, the recycling mechanism of the membrane-bound importin α remains unclear, however since SMAP-10 includes the CAS (exportin) binding site it is possible that CAS/RanGTP may potentially be involved in cargo dissociation and recycling. From these results, it seems reasonable to conclude that SMAP-10 satisfies the requirements for being classified as a nuclear transporter. However, a number of issues remain unresolved. For instance, how does importin α associate with membranes? Secondly, since our results suggest that the membrane-bound importin α may be involved in the cotranslational sorting of E66SM to the INM, what, then, is the key structural or sequence determinant of the SM that is recognized by importin α ?

The localization of importin α to either the membrane or cytosolic fractions has been found to be linked to post-translational modification of the protein. The soluble form of importin α present in the cytosolic fraction is more highly phosphorylated than the membrane-bound form (Hachet et al., 2004). An alternate mechanism would involve the presence of either a TMS, an amphipathic helix, or a hydrophobic domain that allows stable and/or reversible membrane association of importin α . Indeed, when the Sf9 importin α sequence identified in this study was analysed using a number of TMS prediction programmes, two separate stretches of amino acid residues were found to be sufficiently hydrophobic to constitute a TMS. One such stretch (residues 304-325 of the putative Sf9 importin α) exists right at the N-terminus of SMAP-10 which may be one possible explanation for its ability to associate with ER microsomes. An alternate explanation could be via the predicted amphipathic helix within SMAP-10 (shaded gray in Fig.43).

The nuclear import signals for soluble proteins generally are basic and often part of DNA- or RNA- binding sites (Kalderon et al., 1984; Makkerh et al., 1996). Indeed, the INM sorting motif (SM) consists of 18 hydrophobic amino acids that form a TMS with positively charged amino acids that are located four to eight residues from the TMS on the nucleoplasmic or cytoplasmic face of the membrane (Braunagel et al., 2004). In addition, deletion of the lysine residues or any changes in the spacing of the lysine residues from the TMS within the SM results in dramatic changes in the efficiency of protein accumulation at the INM, suggesting that the lysine residues in the SM are at or near a functionally important site that influences protein trafficking to the INM. Based on these observations, we speculate that analogous to cargo recognition by soluble importin α , substrate binding of SMAP-10 (membrane-bound form of importin α) is mediated by basic residues.

Does the association of SM sequence with SMAP-10 imply sorting? The sample size is still too small to provide a clear answer to this question, but there are some interesting clues in the results presented here. First, as we have shown elsewhere, the SM sequence is sufficient to direct reporter proteins (such as GFP, beta-galactosidase etc.) to the INM en-route to the viral envelope (Hong et al., 1997), indicating that the SM sequence contains the structural features that constitute an INM sorting signal and recognition of this sequence would require a direct interaction between the SM sequence and a protein involved in sorting. In addition, well-characterized cellular INM proteins have a SM-like sequence (Braunagel et al., 2004) implying that the sorting process of the viral SM closely resembles the sorting of other INM proteins. Thus, the association of SMAP-10

with the INM sorting signal most likely reflects a sorting event shared by other INM proteins. Second, although Lep1 contains lysines in the approximately the same positions as E66SM, the fact that Lep1 shows no crosslinking to SMAP-10 indicates substrate specificity and thus sorting (Fig. 37B & 47B).

Just as transcription, splicing, translation, and protein degradation are carried out by core machinery subjected to the action of regulatory factors, the sorting of proteins at the ER membrane is likely to be regulated similarly. Given that the 'space' around the nascent chain during translocation/integration at the ER membrane is limited, it is likely that the translocon is dynamic providing the nascent chain access to appropriate enzymes and/or sorting factors. How might such events be regulated? In order to specialize the translocon for particular substrates, it is possible that topogenic sequences within the nascent chain are recognized by the translocation machinery to initiate dynamic changes in the translocon. Several experimental results support the existence of such long-range signal transduction pathways, where topogenic sequences within the ribosomal tunnel are able to initiate changes in the translocon structure and dynamics (Liao et al., 1997; Hamman et al., 1998; Woolhead et al., 2004). We have already demonstrated that the translocon seems to discriminate between INM and other membrane proteins while they are nascent chains (chapter III in this study), and thus the identification of a membrane-bound form of importin α that is translocon associated (Fig. 47A), and proximal to the INM sorting signal within E66 (Fig. 36B & 38), suggests that the recruitment of importin α at the translocon may represent translocon dynamics in response to the nascent chain (substrate).

CHAPTER V

SUMMARY

A number of studies have shown that translocon proteins play an active role in the lipid partitioning of TMSs (Do et al., 1996; Heinrich et al., 2000; McCormick et al., 2003). Since the TMS of E66 contains the signal for INM localization (Hong et al., 1997), the first part of the study focused on examining the role of the translocon in the sorting of proteins destined for the INM (chapter III). A photocrosslinking approach based on the cotranslational incorporation of a photoreactive probe into the nascent substrate of interest (Johnson et al., 1976) was used to examine the role of the translocon in membrane protein sorting. Several important conclusions can be drawn from the results presented. First, the asymmetric photocrosslinking to TRAM and to Sec61 α of each TMS examined in this study reveals that each is bound to a protein(s) within the mammalian translocon (cf. McCormick et al., 2003). Second, the proteinaceous environment within the translocon is very similar for both cellular and viral INM TMSs. Third, the proteinaceous environment within the translocon differs markedly for INM TMSs and for TMSs directed elsewhere. Fourth, an integrated viral SM sequence is crosslinked to two viral proteins after being released from the translocon in ER microsomes purified from infected insect cells. Fifth, this study confirms the widely-held presumption that some INM-directed proteins are targeted to the ER membrane by SRP and integrated cotranslationally at the translocon. Other INM proteins may be inserted post-translationally as C-tail-anchored proteins (Wattenberg et al., 2001). Taken together, these results strongly suggest that some membrane protein sorting to the INM

is initiated within the translocon early in the integration process, is protein-mediated, and involves substrate recognition by and interaction with a sequence of proteins that function as sorting factors to facilitate the movement of proteins to the INM.

The striking similarity in the photocrosslinking pattern observed for viral (E66 & E25) and cellular INM TMSs (LBR1 & Nur1), suggests that INM-directed TMSs occupy the same binding site within the translocon. The difference in the photocrosslinking pattern observed for non-INM TMSs (Lep1 & Tfr) suggests that the proteinaceous environment of non-INM TMSs within the translocon is clearly different from that of INM-directed TMSs. Thus, our results suggest a model in which once a TMS arrives in the translocon pore, the translocon is able to 'sense' (by an as yet undefined mechanism) whether it has been engaged with a ribosome synthesizing an INM substrate or a non-INM substrate (Fig. 52). Following this 'sensing' event, the translocon appears to participate in membrane protein sorting by moving TMSs of an INM protein to a binding site (formed by transmembrane helices of translocon proteins) different from the site occupied by TMSs of proteins destined for other cellular membranes. The model thus suggests that all TMSs do not occupy the same binding site within the translocon during membrane integration, and proposes an active role for the translocon in cotranslational protein sorting.

What may regulate the movement of INM-directed TMSs to a binding site within the translocon that is not occupied by other TMSs? It is possible that the INM-binding site within the translocon is associated with sorting factors that function downstream (and possibly posttranslationally) in the sorting of proteins to the INM. This idea is

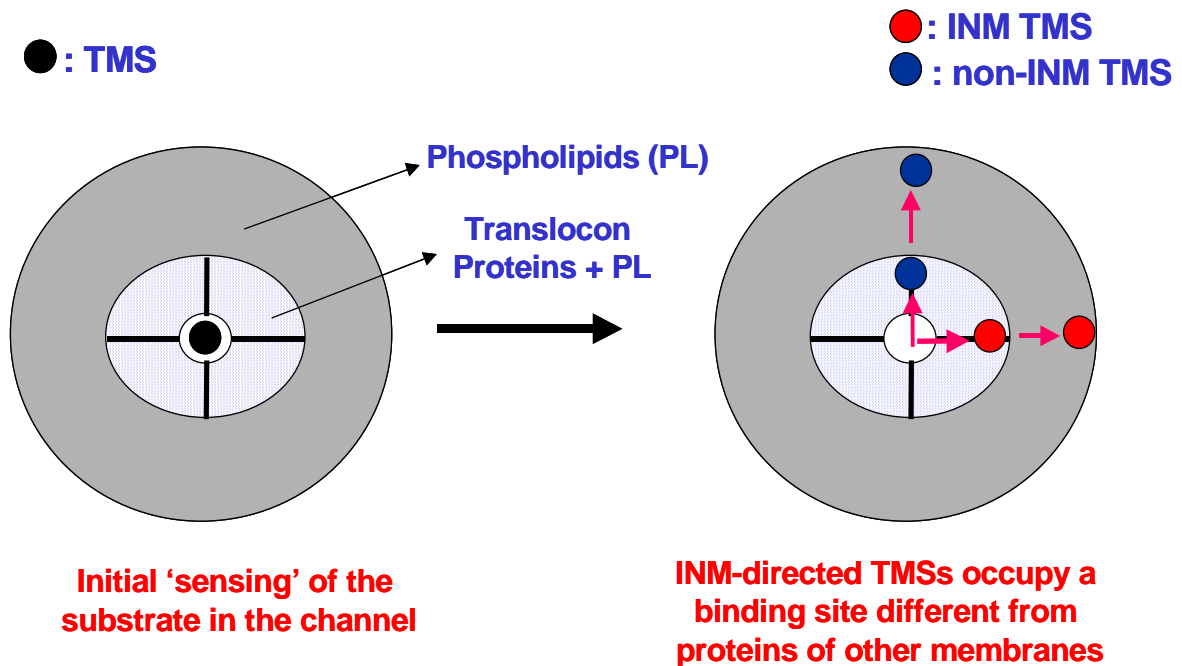


Figure 52. Cotranslational sorting of INM-directed TMSs at the ER translocon.

Although there is a controversy in the field regarding the oligomeric state of the active translocon, for simplicity it is depicted as a tetramer in this schematic. The translocon pore is shown surrounded by translocon proteins with interspersed phospholipids (PLs). The translocon proteins are surrounded by the phospholipids in the membrane of the ER (depicted in gray). Once engaged with a ribosome, the translocon is able to 'sense' whether the TMS in the pore represents an INM protein or a protein of another cellular membrane. Following this initial 'sensing' event, the translocon responds by moving INM-directed TMSs (depicted in red) to a binding site which is different from the binding site occupied by other membrane proteins (non-INM proteins; depicted in blue).

clearly supported by the identification of viral proteins FP25K and E26 that associate with the E66SM posttranslationally, but do not associate with the non-INM protein, Lep1 (Fig. 53).

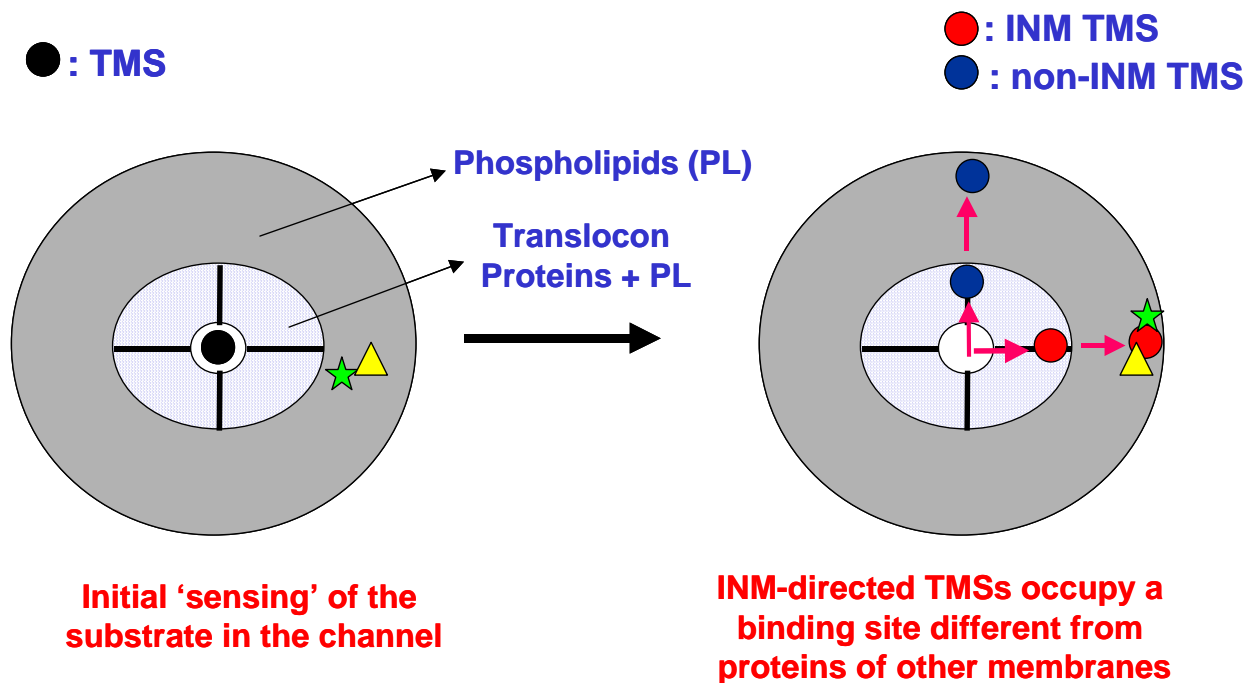


Figure 53. Posttranslational sorting of INM-directed TMSs. Although there is a controversy in the field regarding the oligomeric state of the active translocon, for simplicity it is depicted as a tetramer in this schematic. The translocon pore is shown surrounded by translocon proteins with interspersed phospholipids (PLs). The translocon proteins are surrounded by the phospholipids in the membrane of the ER (depicted in gray). The viral proteins FP25K (indicated by the green asterisk) and E26 (indicated by the yellow triangle) are shown to be proximal to the INM-binding site. This proximity allows for substrate-specific, posttranslational sorting of proteins to the INM.

The identification of viral proteins that associate with the E66SM prompted the second part of this study to focus on the proteinaceous environment of the E66 SM sequence in ER microsomes purified from insect Sf9 cells to identify accessory proteins involved in the sorting of E66 to the INM. Five major conclusions can be drawn from the results presented. First, a membrane-bound Sf9 importin α isoform (SMAP-10) that associates with the SM sequence before and after it leaves the translocon has been identified. Second, transcription is initiated at at least three internal sites within the Sf9 importin α gene resulting in three different isoforms. One of the isoform obtained via internal initiation is SMAP-10. Third, SMAP-10 shares epitopes with viral E26, which was perviously shown to associate with the E66 SM (Braunagel et al., 2004). Fourth, SMAP-10 is a translocon-associated protein, which is selective in substrate association, indicating that it may potentially be involved in membrane protein sorting to the INM. Fifth, crosslinks to SMAP-10 are seen in ER microsomes purified from insect and mammalian cells, suggesting that this protein is found in divergent species. Finally, the results of this study and previous work (Braunagel et al., 2004) suggest that the sorting of INM proteins at the ER membrane is a protein-mediated, multistep process in which the INM sorting signal sequentially associates with various sorting factors.

The identification of a translocon-associated sorting factor (SMAP-10) that associates with the E66SM co- and post-translationally allows us to further refine the model presented in Fig. 52. The crosslinking data (Fig. 47A) suggests that SMAP-10 associates with the translocon protein Sec61 α , yet it provides no clues regarding its binding site. However, based on the substrate specificity exhibited by SMAP-10 (Fig.

47B) it seems reasonable to conclude that SMAP-10 associates with the translocon at a site proximal to the binding site for INM-directed TMSs. This arrangement would explain the ability of SMAP-10 to associate with the E66SM before it is released from the translocon.

How is the translocon association of SMAP-10 regulated? Is it recruited at the translocon in response to translocon-mediated 'sensing' of an INM substrate (Fig. 54) or is it associated with an empty translocon at a site that attracts/pulls and thus determines the binding site for INM-directed TMSs (Fig. 55)? Indeed, while both of these possibilities are likely, it is difficult to discern in our crosslinking experiments, which one is a more accurate depiction of the *in vivo* situation.

The ability of SMAP-10 to associate with the E66SM posttranslationally raises a number of interesting issues. What induces the dissociation of the complex at the INM? After dissociation, how does free SMAP-10 recycle to its binding site at the ER translocon? How is the membrane association of SMAP-10 regulated? A TMS and an amphipathic helix are predicted within the SMAP-10 sequence (Fig. 43). However, since we conclude that SMAP-10 is an isoform of Sf9 importin α , it remains to be tested whether the membrane association of SMAP-10 can be regulated via posttranslational modification of the protein (eg. phosphorylation).

Although this study demonstrates that SMAP-10 associates with the INM-directed viral protein (E66), it remains to be determined whether SMAP-10 participates in the sorting of cellular proteins (LBR, nurim etc.) to the INM. Further, since cellular proteins of the INM including LBR and nurim are multispinning proteins, it will be

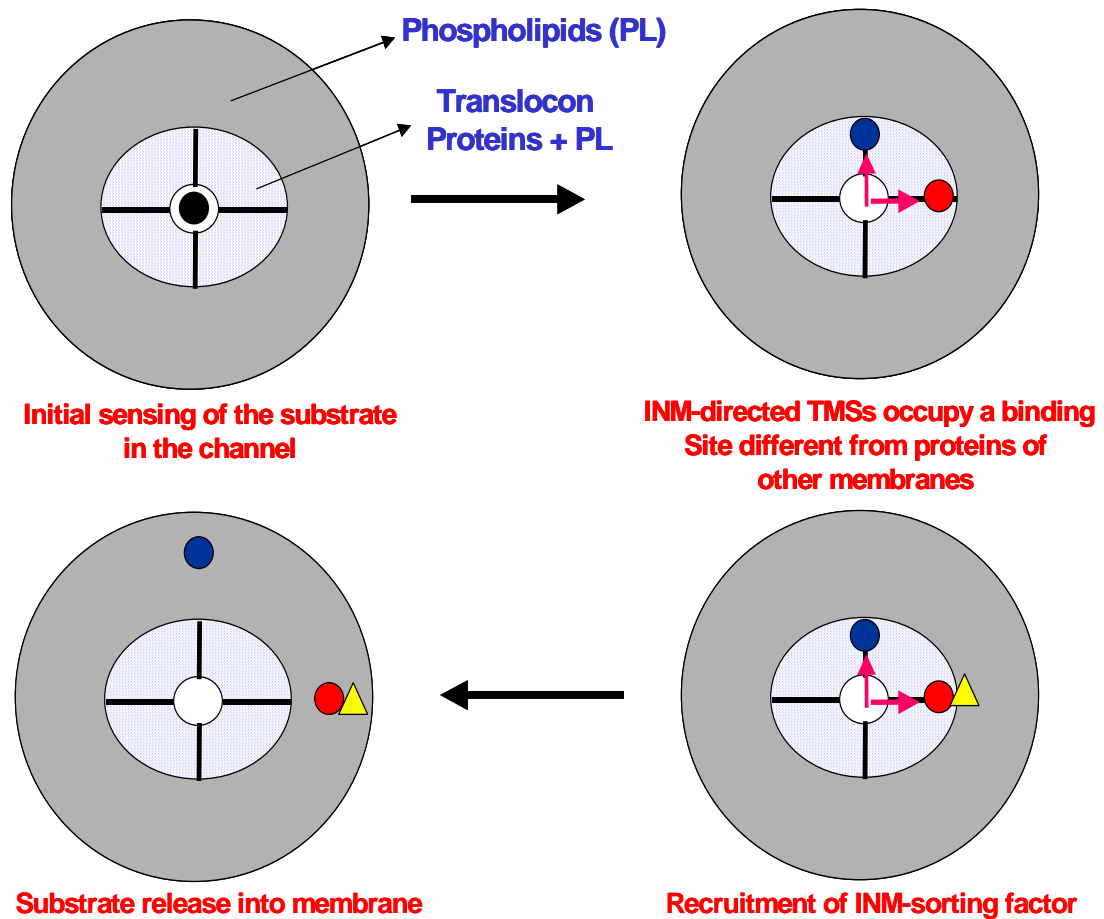


Figure 54. SMAP-10 recruitment at the translocon. The translocon pore is shown surrounded by translocon proteins (tetramer) with interspersed phospholipids (PLs). The translocon proteins are surrounded by the phospholipids in the membrane of the ER (depicted in gray). Translocon-mediated 'sensing' of an INM-directed TMS initiates recruitment of SMAP-10 (indicated by the yellow triangle) at the translocon. SMAP-10 associates with the translocon at a site proximal to the binding site for INM-directed TMSs (depicted in red). This arrangement allows for substrate-specific, cotranslational association of INM-directed TMSs with SMAP-10.

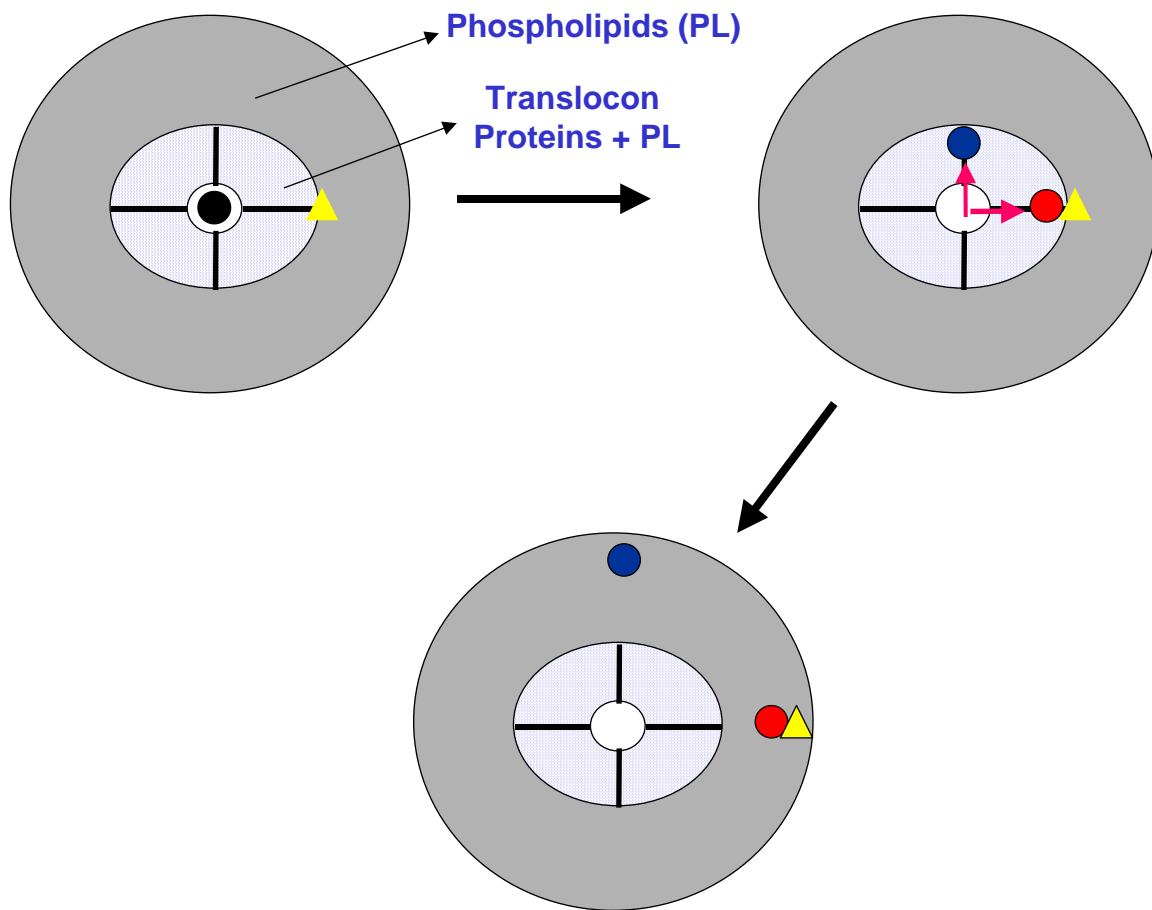


Figure 55. Translocon-bound SMAP-10 determines the binding site for INM-directed TMSs . The translocon pore is shown surrounded by translocon proteins (tetramer) with interspersed phospholipids(PLs). The translocon proteins are surrounded by the phospholipids in the membrane of the ER (depicted in gray). A ribosome-free translocon contains bound SMAP-10 (depicted by the yellow triangle). INM-directed TMSs (depicted in red) that arrives in the translocon pore are shunted/pulled towards the SMAP-10-binding site within the translocon. In contrast, non-INM TMSs (depicted in blue) move to a site that is not adjacent to the SMAP-10-binding site.

interesting to determine whether SMAP-10 associates with all the TMSs of these proteins or with the TMSs that are critical for INM localization?

Clearly, the identification of SMAP-10 has set the stage for some exciting research in the field of protein sorting to the INM. It will be interesting to see the results of studies focused on the identity of SMAP-25 and studies focused on the identification of other proteins that facilitate protein trafficking to the INM.

REFERENCES

- Adams, J.R., and McClintock, J.T. (1991). Nuclear polyhedrosis virus. Atlas of invertebrate viruses, Boca Raton FL: CRC Press, 87-225.
- Aebi, U., Cohn, J., Buhle, L., and Gerace, L. (1986). The nuclear lamina is a meshwork of intermediate-type filaments. *Nature* 323, 560-564.
- Alder, N.N., & Johnson, A.E. (2004). Cotranslational membrane protein biogenesis at the endoplasmic reticulum. *J. Biol. Chem.* 279, 22787-22790.
- Altschul, S.F., Gish, W., Miller, W., Myers, C.W., and Lipman, D.J. (1990). Basic local alignment search tool. *J. Mol. Biol.* 215, 403-410.
- Andrulis, E.D., Neiman, A.M., Zappulla, D.C., and Sternglanz, R. (1998). Perinuclear localization of chromatin facilitates transcriptional silencing. *Nature* 394, 592-595.
- Barlowe, C. (2003). Signals for COPII-dependent export from the ER: whats the ticket out? *Trends Cell Biol.* 13, 295-300.
- Beckmann, R., Spahn, C.M., Eswar, N., Helmers, J., Penczek, P.A., Sali, A., Frank, J., and Blobel, G. (2001). Architecture of the protein-conducting channel associated with the translating 80S ribosome. *Cell* 107, 361-372.

Belanger, K.D., Kenna, M.A., Wei, S., and Davis, L.I. (1994). Genetic and physical interactions between Srp1p and nuclear pore complex proteins Nup1p and Nup2p. *J. Cell Biol.* *126*, 619-630.

Bione, S., Maestrini, E., Rivella, S., Mancini, M., Regis, S., Romeo, G., and Toniolo, D. (1994). Identification of a novel X-linked gene responsible for Emery-Dreifuss muscular dystrophy. *Nat. Genet.* *8*, 323-327.

Bonne, G., Di Barletta, M.R., Varnous, S., Becane, H.M., Hammouda, E.H., Merlini, L., Muntoni, F., Greenberg, C.R., Gary, F., Urtizbera, J.A., et al. (1999). Mutations encoding the gene lamin A/C cause autosomal dominant Emery-Dreifuss muscular dystrophy. *Nat. Genet.* *21*, 285-288.

Braunagel, S.C., Elton, D.M., Ha, M., and Summers, M.D. (1996). Identification and analysis of an *Autographa californica* nuclear polyhedrosis virus structural protein of the occlusion-derived virus envelope: ODV-E56. *Virology* *217*, 97-110.

Braunagel, S.C., Williamson, S.T., Saksena, S., Zhong, Z., Russell, W.K., Russell, D.H., and Summers, M.D. (2004). Trafficking of ODV-E66 is mediated via a sorting motif and other viral proteins: facilitated trafficking to the inner nuclear membrane. *Proc. Natl. Acad. Sci. USA* *101*, 8372-8377.

Brodsky, J.L., and Schekman, R. (1993). A Sec63p-BiP complex from yeast is required for protein translocation in a reconstituted proteoliposome. *J. Cell Biol.* *123*, 1355-1363.

Brown, D.A., and London, E. (1998). Functions of lipid rafts in biological membranes. *Annu. Rev. Cell Dev. Biol.* *14*, 111-136.

Conti, E., Uy, M., Leighton, L., Blobel, G., and Kuriyan, J. (1998). Crystallographic analysis of the recognition of a nuclear localization signal by the nuclear import factor karyopherin alpha. *Cell* *94*, 193-204.

Conti, E. And Kuriyan, J. (2000). Crystallographic analysis of the specific yet versatile recognition of distinct nuclear localization signals by karyopherin alpha. *Structure Fold. Des.* *8*, 329-338.

Corsi, A.K., and Schekman, R. (1997). The luminal domain of Sec63p stimulates the ATPase activity of BiP and mediates BiP recruitment to the translocon in *Saccharomyces cerevisiae*. *J. Cell Biol.* *137*, 1483-1493.

Crowley, K.S., Liao, S., Worrell, V.E., Reinhart, G.D., and Johnson, A.E. (1994). Secretory proteins move through the endoplasmic reticulum via an aqueous, gated pore. *Cell* *78*, 461-471.

Deshaies, R.J., and Schekman, R. (1987). A yeast mutant defective at an early stage in import of secretory protein precursors into the endoplasmic reticulum. *J. Cell Biol.* *105*, 633-645.

Do, H., Falcone, D., Lin, J., Andrews, D.W., and Johnson, A.E. (1996). The cotranslational integration of membrane proteins into the phospholipid bilayer is a multistep process. *Cell* *85*, 369-378.

Dreger, M., Bengtsson, L., Schoneberg, T., Otto, H., and Hucho, F. (2001). Nuclear envelope proteomics: novel integral membrane proteins of the inner nuclear membrane. *Proc. Natl. Acad. Sci. USA* *98*, 11943-11948.

Dreier, L., and Rapoport, T.A. (2000). In vitro formation of the endoplasmic reticulum occurs independently of microtubules by a controlled fusion reaction. *J. Cell Biol.* *148*, 883-898.

Economou, A., and Wickner, W. (1994). SecA promotes preprotein translocation by undergoing ATP-driven cycles of membrane insertion and deinsertion. *Cell* *78*, 835-843.

Ellenberg, J., Siggia, E.D., Moreira, J.E., Smith, C.L., Presley, J.F., Worman, H.J., and Lippincott-Schwartz, J. (1997). Nuclear membrane dynamics and reassembly in living

cells: targeting of an inner nuclear membrane protein in interphase and mitosis. *J. Cell Biol.* *138*, 1193-1206.

Erickson, A.H., and Blobel, G. (1983). Cell-free translation of messenger RNA in a wheat germ system. *Methods Enzymol.* *96*, 38-50.

Falcone, D., Do, H., Johnson, A.E., and Andrews, D.W. (1999). Negatively charged residues in the IgM stop-transfer effector sequence regulate transmembrane polypeptide integration. *J. Biol. Chem.* *274*, 33661-33670.

Fisher, D.Z., Chaudhary, N., and Blobel, G. (1986). cDNA sequencing of nuclear lamins A and C reveals primary and secondary structural homology to intermediate filament proteins. *Proc. Natl. Acad. Sci. USA* *83*, 6450-6454.

Flanagan, J.J., Chen, J.C., Miao, Y., Shao, Y., Lin, J., Bock, P.E., and Johnson, A.E. (2003). Signal recognition particle binds to ribosome-bound signal sequences with fluorescence-detected subnanomolar affinity that does not diminish as the nascent chain lengthens. *J. Biol. Chem.* *278*, 18628-18637.

Fons, R.D., Bogert, B.A., and Hegde, R.S. (2003). Substrate-specific function of the translocon-associated protein complex during translocation across the ER membrane. *J. Cell Biol.* *160*, 529-539.

Fontes, M.R., Teh, T., and Kobe, B. (2000). Structural basis of recognition of monopartite and bipartite nuclear localization sequences by mammalian importin-alpha. *J. Mol. Biol.* 297, 1183-1194.

Fontes, M.R., Teh, T., Jans, D., Brinkworth, R.I., and Kobe, B. (2003). Structural basis for the specificity of bipartite nuclear localization sequence binding by importin-alpha. *J. Biol. Chem.* 278, 27981-27987.

Fraser, M.J. (1986). Ultrastructural observations of virion maturation in *Autographa californica* nuclear polyhedrosis virus infected *Spodoptera frugiperda* cell cultures. *J. Ultrastruct. Mol. Struct. Res.* 95, 189-195.

Fried, H., and Kutay, U. (2003). Nucleocytoplasmic transport: taking an inventory. *Cell Mol. Life Sci.* 60, 1659-1688.

Fujiki, Y., Hubbard, A.L., Fowler, S., and Lazarow, P.B. (1982). Isolation of intracellular membranes by means of sodium carbonate treatment: application to endoplasmic reticulum. *J. Cell Biol.* 93, 97-102.

Furukawa, K., Pante, N., Aebi, U., and Gerace, L. (1995). Cloning of a cDNA for lamina-associated polypeptide 2 (LAP2) and identification of regions that specify targeting to the nuclear envelope. *EMBO J.* 14, 1626-1636.

Furukawa, K., Fritze, C.E., and Gerace, L. (1998). The major nuclear envelope targeting domain of LAP2 coincides with its lamin binding region but is distinct from its chromatin interaction domain. *J. Biol. Chem.* *273*, 4213-4219.

Gant, T.M., and Wilson, K.L. (1997). Nuclear assembly. *Annu. Rev. Cell Dev. Biol.* *13*, 669-695.

Goldfarb, D.S., Corbett, A.H., Mason, D.A., Harreman, M.T., and Adam, S.A. (2004). Importin alpha: a multipurpose nuclear-transport receptor. *Trends Cell Biol.* *14*, 505-514.

Gomord, V., Wee, E., and Faye, L. (1999). Protein retention and localization in the endoplasmic reticulum and the golgi apparatus. *Biochimie* *81*, 607-618.

Gorlich, D., Hartmann, E., Prehn, S., and Rapoport, T.A. (1992a). A protein of the endoplasmic reticulum involved early in polypeptide translocation. *Nature* *357*, 47-52.

Gorlich, D., Prehn, S., Hartmann, E., Kalies K-U, and Rapoport, T.A. (1992b). A mammalian homolog of SEC61p and SECYp is associated with ribosomes and nascent polypeptides during translocation. *Cell* *71*, 489-503.

Gorlich, D., and Rapoport, T.A. (1993). Protein translocation into proteoliposomes reconstituted from purified components of the endoplasmic reticulum membrane. *Cell* 75, 615-630.

Gorlich, D., and Kutay, U. (1999). Transport between the cell nucleus and the cytoplasm. *Annu. Rev. Cell Dev. Biol.* 15, 607-660.

Gruenbaum, Y., Goldman, R.D., Meyuhas, R., Mills, E., Margalit, A., Fridkin, A., Dayani, Y., Prokocimer, M., and Enosh, A. (2003). The nuclear lamina and its functions in the nucleus. *Int. Rev. Cytol.* 226, 1-62.

Gruss, O.J., Carazo-Salas, R.E., Schatz, C.A., Guarguaglini, G., Kast, J., Wilm, M., Le Bot, N., Vernos, I., Karsenti, E., and Mattaj, I.W. (2001). Ran induces spindle assembly by reversing the inhibitory effect of importin alpha on TPX2 activity. *Cell* 104, 83-93.

Hachet, V., Kocher, T., Wilm, M., and Mattaj, I.W. (2004). Importin α associates with membranes and participates in nuclear envelope assembly *in vitro*. *EMBO J.* 23, 1526-1535.

Hamman, B.D., Chen, J.C., Johnson, E., and Johnson, A.E. (1997). The aqueous pore through the translocon has a diameter of 40-60 Å during cotranslational protein translocation at the ER membrane. *Cell* 89, 535-544.

Hamman, B.D., Hendershot, L.M., and Johnson, A.E. (1998). BiP maintains the permeability barrier of the ER membrane by sealing the luminal end of the translocon pore before and early in translocation. *Cell* 92, 747-758.

Hanein, D., Matlack, K.E., Plath, K., Kalies, K.U., Miller, K.R., Rapoport, T.A., and Akey, C.W. (1996). Oligomeric rings of the Sec61p complex induced by ligands required for protein translocation. *Cell* 87, 721-732.

Harreman, M.T., Kline, T.M., Milford, H.G., Harben, M.B., Hodel, A.E., and Corbett, A.H. (2004). Regulation of nuclear import by phosphorylation adjacent to nuclear localization signals. *J. Biol. Chem.* 279, 20613-20621.

Harris, C.R., and Silhavy, T.J. (1999). Mapping an interface of SecY (PrlA) and SecE (PrlG) by using synthetic phenotypes and *in vivo* crosslinking. *J. Bacteriol.* 181, 3438-3444.

Harrison, R.L., and Summers, M.D. (1995). Mutations in the *Autographa californica* multinucleocapsid nuclear polyhedrosis virus 25kDa protein gene result in reduced virion occlusion, altered intranuclear envelopment and enhanced virus production. *J. Gen. Virol.* 76, 1451-1459.

Hegde, R.S., and Lingappa, V.R. (1997). Membrane protein biogenesis: regulated complexity at the endoplasmic reticulum. *Cell* 91, 575-582.

Hegde, R.S., Mastrianni, J.A., Scott, M.R., Defea, K.A., Tremblay, P., Torchia, M., Dearmond, S.J., Pruisner, S.B., and Lingappa, V.R. (1998a). A transmembrane form of the prion protein in neurodegenerative disease. *Science* 279, 827-834.

Hegde, R.S., Voigt, S., and Lingappa, V.R. (1998b). Regulation of protein topology by trans-acting factors at the endoplasmic reticulum. *Mol. Cell* 2, 85-91.

Hegde, R.S., Voigt, S., Rapoport, T.A., and Lingappa, V.R. (1998c). TRAM regulates the exposure of nascent secretory proteins to the cytosol during translocation into the endoplasmic reticulum. *Cell* 92, 621-631.

Hegde, R.S., and Lingappa, V.R. (1999). Regulation of protein biogenesis at the endoplasmic reticulum membrane. *Trends Cell Biol.* 9, 132-137.

Heinrich, S.U., Mothes, W., Bruner, J., and Rapoport, T.A. (2000). The Sec61p complex mediates the integration of a membrane protein by allowing lipid partitioning of the transmembrane domain. *Cell* 102, 233-244.

Heinrich, S.U., and Rapoport, T.A. (2003). Cooperation of transmembrane segments during the integration of a double-spanning protein into the ER membrane. *EMBO J.* *22*, 3654-3663.

Hellemans, J., Preobrazhenska, O., Willaert, A., Debeer, P., Verdonk, P.C. et al. (2004). Loss-of-function mutations in LEMD3 result in osteopoikilosis, Buschke-Ollendorff syndrome and melorheostosis. *Nat. Genet.* *36*, 1213-1218.

Hendrick, J.P., and Hartl, F.U. (1993). Molecular chaperone functions of heat-shock proteins. *Annu. Rev. Biochem.* *62*, 349-384.

Herold, A., Truant, R., Wiegand, H., and Cullen, B.R. (1998). Determination of the functional domain organization of the importin alpha nuclear import factor. *J. Cell Biol.* *143*, 309-318.

High, S., Gorlich, D., Wiedmann, M., Rapoport, T.A., and Dobberstein, T.A. (1991). The identification of proteins in the proximity of signal-anchor sequences during their targeting to and insertion into the membrane of the ER. *J. Cell Biol.* *113*, 35-44.

High, S., Martoglio, B., Gorlich, D., Andersen, S.S., Ashford, A.J., Giner, A.E., Hartmann, E., Prehn, S., Rapoport, T.A., and Dobberstein, B. (1993). Site-specific

photocross-linking reveals that Sec61p and TRAM contact different regions of a membrane-inserted signal sequence. *J. Biol. Chem.* 268, 26745-26751.

Hinshaw, J.E., Carragher, B.O., and Milligan, R.A. (1992). Architecture and design of the nuclear pore complex. *Cell* 69, 1133-1141.

Hoffmann, K., Dreger, C.K., Olins, A.L., Olins, D.E., Shultz, L.D. et al. (2002). Mutations in the gene encoding the lamin B receptor produce an altered nuclear morphology in granulocytes (Pelger-Huët anomaly). *Nat. Genet.* 31, 410-414.

Holmer, L., Pezhman, A., and Worman, H.J. (1998). The human lamin B receptor/sterol reductase multigene family. *Genomics* 54, 469-476.

Hong, T., Braunagel, S.C., and Summers, M.D. (1994). Transcription, translation, and cellular localization of PDV-E66: a structural protein of the PDV envelope of *Autographa californica* nuclear polyhedrosis virus. *Virology* 204, 210-222.

Hong, T., Summers, M.D., and Braunagel, S.C. (1997). N-terminal sequences from *Autographa californica* nuclear polyhedrosis virus envelope proteins ODV-E66 and ODV-E25 are sufficient to direct reporter proteins to the nuclear envelope, intranuclear microvesicles, and the envelope of occlusion derived virus. *Proc. Natl. Acad. Sci. USA* 94, 4050-4055.

Imreh, G., Maskel, D., de Monvel, J.B., Branden, L., and Hallberg, E. (2003). ER retention may play a role in sorting of the nuclear pore membrane protein POM121. *Exp Cell Res.* 284, 173-184.

Johnson, A.E., Woodward, W.R., Herbert, E., and Menninger, J.R. (1976). N-acetyl lysine transfer ribonucleic acid: a biologically active analogue of aminoacyl transfer ribonucleic acids. *Biochemistry* 15, 569-575.

Johnson, A.E., and van Waes, M.A. (1999). The translocon: a dynamic gateway at the ER membrane. *Annu. Rev. Cell Dev. Biol.* 15, 799-842.

Johnson, A.E., Chen, J.C., Flanagan, J.J., Miao, Y., Shao, Y., Lin, J., and Bock, P.E. (2001). Structure, function, and regulation of free and membrane-bound ribosomes: the view from their substrates and products. *Cold Spring Harbor Symp. Quant. Biol.* 66, 531-541.

Joly, J.C., and Wickner, W. (1993). The SecA and SecY subunits of translocase are the nearest neighbors of a translocating preprotein, shielding it from phospholipids. *EMBO J.* 12, 255-263.

Kaffman, A., and O'Shea, E.K. (1999). Regulation of nuclear localization: a key to a door. *Annu. Rev. Cell Dev. Biol.* 15, 291-339.

Kalderon, D., Richardson, W.D., Markham, A.F., and Smith, A.E. (1984). Sequence requirements for nuclear localization of simian virus 40 large T antigen. *Nature* *311*, 33-38.

Kamata, M., Nitahara-Kasahara, Y., Miyamoto, Y., Yoneda, Y., and Aida, Y. (2005). Importin α promotes passage through the nuclear pore complex of Human Immunodeficiency Virus Type 1 Vpr. *J. Virol.* *79*, 3557-3564.

Kawamoto, F., Suto, C., Kumada, N., and Kobayashi, M. (1977). Cytoplasmic budding of a nuclear polyhedrosis virus and comparative ultrastructural studies of envelopes. *Microbiol. Immunol.* *21*, 255-265.

Keenan, R.J., Freymann, D.M., Stroud, R.M., and Walter, P. (2001). The signal recognition particle. *Annu. Rev. Biochem.* *70*, 755-775.

Kobe, B. (1999). Autoinhibition by an internal nuclear localization signal revealed by the crystal structure of mammalian importin alpha. *Nat. Struct. Biol.* *6*, 388-397.

Kotera, I., Sekimoto, T., Miyamoto, Y., Saiwaki, T., Nagoshi, E., Sakagami, H., Kondo, H., and Yoneda, Y. (2005). Importin α transports CaMKIV to the nucleus without utilizing importin β . *EMBO J.* *24*, 942-951.

Krieg, U.C., Johnson, A.E., and Walter, P. (1989). Protein translocation across the endoplasmic reticulum membrane: identification by photocrosslinking of a 39kD integral membrane glycoprotein as part of a putative translocation tunnel. *J. Cell Biol.* *109*, 2033-2043.

Kurzchalia, T.V., Wiedmann, M., Breter, H., Zimmermann, W., Bauschke, E., and Rapoport, T.A. (1988). tRNA-mediated labeling of proteins with biotin. A nonradioactive method for the detection of cell-free translation products. *Eur. J. Biochem.* *172*, 663-668.

Laguri, C., Gilquin, B., Wolff, N., Romi-Lebrun, R., Courchay, K., Callebaut, I., Worman, H.J., and Zinn-Justin, S. (2001). Structural characterization of the LEM motif common to three human inner nuclear membrane proteins. *Structure* *9*, 503-511.

Lee, K.K., Gruenbaum, Y., Spann, P., Lin, J., and Wilson, K.L. (2000). *C. elegans* nuclear envelope proteins emerlin, MAN1, lamin and nucleoporins reveal unique timing of nuclear envelope breakdown during mitosis. *Mol. Biol. Cell* *11*, 3089-3099.

Lee, K.K., Starr, D., Cohen, M., Liu, J., Han, M., Wilson, K.L., and Gruenbaum, Y. (2002). Lamin-dependent localization of UNC-84, a protein required for nuclear migration in *Caenorhabditis elegans*. *Mol Biol. Cell* *13*, 892-901.

Lenart, P., and Ellenberg, J. (2003). Nuclear envelope dynamics in oocytes: from germinal vesicle breakdown to mitosis. *Curr. Opin. Cell Biol.* *15*, 88-95.

Liao, S., Lin, J., Do, H., and Johnson, A.E. (1997). Both luminal and cytosolic gating of the aqueous ER translocon pore is regulated from inside the ribosome during membrane protein biogenesis. *Cell* *90*, 31-41.

Lin, F., Blake, D.L., Callebaut, I., Skerjanc, I.S., Holmer, L., McBurney, M.W., Paulin-Levasser, M., and Worman, H.J. (2000). MAN1, an inner nuclear membrane protein that shares the LEM domain with lamina-associated polypeptide 2 and emerin. *J. Biol. Chem.* *275*, 4840-4847.

Lindsay, M.E., Plafker, K., Smith, A.E., Clurman, B.E., and Macara, I.G. (2002). Npap60/Nup50 is a tri-stable switch that stimulates importin- α : β -mediated nuclear import. *Cell* *110*, 349-360.

Lund, O., Nielsen, M., Lundegaard, C., and Worning, P. (2002). CPH models 2.0: X3M a computer program to extract 3D models. Abstract at the CASP5 conference A102.

Makkerh, J.P.S., Dingwall, C., and Laskey, R.A. (1996). Comparative mutagenesis of nuclear localization signals reveals the importance of neutral and acidic amino acids. *Curr. Biol.* *6*, 1025-1027.

Malone, C.J., Fixsen, W.D., Horvitz, H.R., and Han, M. (1999). UNC-84 localizes to the nuclear envelope and is required for nuclear migration and anchoring during *C. elegans* development. *Development* 126, 3171-3181.

Martin, L., Crimando, C., and Gerace, L. (1995). cDNA cloning and characterization of lamina-associated polypeptide 1C (LAP1C), an integral protein of the inner nuclear membrane. *J. Biol. Chem.* 270, 8822-8828.

Martin, P.E., Du, Y., Novick, P., and Ferro-Novick, S. (2005). Ice2p is important for the distribution and structure of the cortical ER network in *Saccharomyces cerevisiae*. *J. Cell Sci.* 118, 65-77.

Martoglio, B., Hofmann, M.W., Brunner, J., and Dobberstein, B. (1995). The protein-conducting channel in the membrane of the endoplasmic reticulum is open laterally toward the lipid bilayer. *Cell* 81, 207-214.

Matlack, K.E., Misselwitz, B., Plath, K., and Rapoport, T.A. (1999). BiP acts as a molecular ratchet during posttranslational transport of prepro- α factor across the ER membrane. *Cell* 97, 553-564.

McCormick, P.J., Miao, Y., Shao, Y., Lin, J., and Johnson, A.E. (2003). Cotranslational protein integration into the ER membrane is mediated by the binding of nascent chains to translocon proteins. *Mol. Cell* *12*, 329-341.

McKeon, F.D., Kirschner, M.W., and Caput, D. (1986). Homologies in both primary and secondary structure between nuclear envelope and intermediate filament proteins. *Nature* *319*, 463-468.

Meacock, S.L., Lecomte, F.J., Crawshaw, S.G., and High, S. (2002). Different transmembrane domains associate with distinct endoplasmic reticulum components during membrane integration of a polytopic protein. *Mol. Biol. Cell* *13*, 4114-4129.

Mellman, I., & Warren, G. (2000). The road taken: past and future foundations of membrane traffic. *Cell* *100*, 99-112.

Menetret, J.F., Neuhof, A., Morgan, D.G., Plath, K., Radermacher, M., Rapoport, T.A., and Akey, C.W. (2000). The structure of ribosome-channel complexes engaged in protein translocation. *Mol. Cell* *6*, 1219-1232.

Meyer, H.A., Grau, H., Kraft, R., Kostka, S., Prehn, S. et al. (2000). Mammalian Sec61 is associated with Sec62 and Sec63. *J. Biol. Chem.* *275*, 14550-14557.

Morgan, D.G., Menetret, J.F., Neuhof, A., Rapoport, T.A., and Akey, C.W. (2002).

Structure of the mammalian ribosome-channel complex at 17Å resolution. *J. Mol. Biol.* 324, 871-886.

Mori, H., and Ito, K. (2001). The Sec protein-translocation pathway. *Trends Microbiol.*

9, 494-500.

Moroianu, J., Blobel, G., and Radu, A. (1997). RanGTP-mediated nuclear export of karyopherin alpha involves its interaction with the nucleoporin Nup153. *Proc. Natl. Acad. Sci. USA* 94, 9699-96704.

Mosammaparast, N., and Pemberton, L.F. (2004). Karyopherins: from nuclear-transport mediators to nuclear-function regulators. *Trends Cell Biol.* 14, 547-556.

Mothes, W., Prehn, S., and Rapoport, T.A. (1994). Systematic probing of the environment of a translocating secretory protein during translocation through the ER membrane. *EMBO J.* 13, 3937-3982.

Mothes, W., Heinrich, S.U., Graf, R., Nilsson, I., von Heijne, G., Brunner, J., and Rapoport, T.A. (1997). Molecular mechanism of membrane protein integration into the endoplasmic reticulum. *Cell* 89, 523-533.

Muchir, A., and Worman, H.J. (2004). The nuclear envelope and human disease. *Physiology (Bethesda)* *19*, 309-314.

Murthi, A., and Hopper, A.K. (2005). Genome-wide screen for inner nuclear membrane protein targeting in *Saccharomyces cerevisiae*: Roles for N-acetylation and an integral membrane protein. *Genetics* *170*, 1553-1560.

Musch, A., Wiedmann, M., and Rapoport, T.A. (1992). Yeast Sec proteins interact with polypeptides traversing the endoplasmic reticulum membrane. *Cell* *69*, 343-352.

Ng, D.T., Brown, J.D., and Walter, P. (1996). Signal sequences specify the targeting route to the endoplasmic reticulum membrane. *J. Cell Biol.* *134*, 269-278.

Nicchitta, C.V., and Blobel, G. (1990). Assembly of translocation-competent proteoliposomes from detergent-solubilized rough microsomes. *Cell* *60*, 259-269.

Nilsson, I., and von Heijne, G. (1993). Determination of the distance between the oligosaccharyltransferase active site and the endoplasmic reticulum membrane. *J. Biol. Chem.* *268*, 5798-5801.

Ohba, T., Schirmer, E.C., Nishimoto, T., and Gerace, L. (2004). Energy and temperature-dependent transport of integral proteins to the inner nuclear membrane via the nuclear pore. *J. Cell Biol.* *167*, 1051-1062.

Oliver, J., Jungnickel, B., Gorlich, D., Rapoport, T.A., and High, S. (1995). The Sec61 complex is essential for the insertion of proteins into the membrane of the endoplasmic reticulum. *FEBS Lett.* *362*, 126-130.

Osborne, A.R., Rapoport, T.A., and van den Berg, B. (2005). Protein translocation by the Sec61/SecY channel. *Annu. Rev. Cell Dev. Biol.* *21*, 529-550.

Ostlund, C., Ellenberg, J., Hallberg, E., Lippincott-Schwartz, J., and Worman, H.J. (1999). Intracellular trafficking of emerin, the Emery-Dreifuss muscular dystrophy protein. *J. Cell Sci.* *112*, 1709-1719.

Panzner, S., Dreier, L., Hartmann, E., Kostka, S., and Rapoport, T.A. (1995). Posttranslational protein transport in yeast reconstituted with a purified complex of Sec proteins and Kar2p. *Cell* *81*, 561-570.

Pemberton, L.F., and Paschal, B.M. (2005). Mechanisms of receptor-mediated nuclear import and nuclear export. *Traffic* *6*, 187-198.

Pyrpasopoulou, A., Meier, J., Maison, C., Simos, G., and Georgatos, S.D. (1996). The lamin B receptor (LBR) provides essential chromatin docking sites at the nuclear envelope. *EMBO J.* *15*, 7108-7119.

Rapoport, T.A., Jungnickel, B., and Kutay, U. (1996). Protein transport across the endoplasmic reticulum and bacterial inner membranes. *Annu. Rev. Biochem.* *65*, 271-303.

Rapoport, T.A., Goder, V., Heinrich, S.U., and Matlack, K.E. (2004). Membrane-protein integration and the role of the translocation channel. *Trends Cell Biol.* *14*, 568-575.

Rogue, P.J., and Malviya, A.N. (1999). Calcium signals in the cell nucleus. *EMBO J.* *18*, 5147-5152.

Rolls, M.M., Stein, P.A., Taylor, S.S., Ha, E., McKeon, F., and Rapoport, T.A. (1999). A visual screen of a GFP-fusion library identifies a new type of nuclear envelope membrane protein. *J. Cell Biol.* *146*, 29-44.

Rosas-Acosta, G., Braunagel, S.C., and Summers, M.D. (2001). Effects of deletion and overexpression of the *Autographa californica* nuclear polyhedrosis virus FP25K gene on synthesis of two occlusion-derived virus envelope proteins and their transport into virus-induced intranuclear membranes. *J. Virol.* *75*, 10829-10842.

Rose, M.D. (1996). Nuclear function in the yeast *Saccharomyces cerevisiae*. *Annu. Rev. Cell Dev. Biol.* *12*, 663-695.

Rothman, J.E., and Wieland, F.T. (1996). Protein sorting by transport vesicles. *Science* *272*, 227-234.

Saksena, S., Shao, Y., Braunagel, S.C., Summers, M.D., and Johnson, A.E. (2004). Cotranslational integration and initial sorting at the endoplasmic reticulum translocon of proteins destined for the inner nuclear membrane. *Proc. Natl. Acad. Sci. USA* *101*, 12537-12542.

Sambrook, J., Fritsch, E.F., and Maniatis, T. (1989). *Molecular cloning: a laboratory manual*. Cold Spring Harbor Laboratory Press, Cold Spring Harbor, NY.

Sanders, S.L., Whitfield, K.M., Vogel, J.P., Rose, M.D., and Schekman, R.W. (1992). Sec61p and BiP directly facilitate polypeptide translocation into the ER. *Cell* *69*, 353-365.

Schiebel, E., Driessen, A.J.M., Hartl, F-U, Wickner, W. (1991). $\Delta\mu\text{H}^+$ and ATP function at different steps of the catalytic cycle of preprotein translocase. *Cell* *64*, 927-939.

Schindler, M., Holland, J.F., and Hogan, M. (1985). Lateral diffusion in nuclear membranes. *J. Cell Biol.* *100*, 1408-1414.

Schirmer, E.C., Florens, L., Guan, T., Yates, J.R., and Gerace, L. (2003). Nuclear membrane proteins with potential disease links found by subtractive proteomics. *Science* *301*, 1380-1382.

Schuler, E., Lin, F., and Worman, H.J. (1994). Characterization of the human gene encoding LBR, an integral protein of the nuclear envelope inner membrane. *J. Biol. Chem.* *269*, 11312-11317.

Sidrauski, C., and Walter, P. (1997). The transmembrane kinase Ire1p is a site-specific endonuclease that initiates mRNA splicing in the unfolded protein response. *Cell* *90*, 1031-1039.

Smith, S., & Blobel, G. (1993). The first membrane spanning region of the lamin B receptor is sufficient for sorting to the inner nuclear membrane. *J. Cell Biol.* *120*, 631-637.

Snapp, E.L., Reinhart, G.A., Bogert, B.A., Lippincott-Schwartz, J., and Hegde, R.S. (2004). The organization of engaged and quiescent translocons in the endoplasmic reticulum of mammalian cells. *J. Cell Biol.* *164*, 997-1007.

Solsbacher, J., Maurer, P., Vogel, F., and Schlenstedt, G. (2000). Nup2p, a yeast nucleoporin, functions in bidirectional transport of importin alpha. *Mol. Cell Biol.* *20*, 8468-8479.

Soullam, B., & Worman, H.J. (1993). The amino-terminal domain of the lamin B receptor is a nuclear envelope targeting signal. *J. Cell Biol.* *120*, 1093-1100.

Soullam, B., & Worman, H.J. (1995). Signals and structural features involved in integral membrane protein targeting to the inner nuclear membrane. *J. Cell Biol.* *130*, 15-27.

Stirling, C.J., Rothblatt, J., Hosobuchi, M., Deshaies, R., and Schekman, R. (1992). Protein translocation mutants defective in the insertion of integral membrane proteins into the endoplasmic reticulum. *Mol. Biol. Cell* *3*, 129-142.

Stoltz, D.B., Pavan, C., and Da Cunha, A.B. (1973). Nuclear polyhedrosis virus. A possible example of de novo intranuclear membrane morphogenesis. *J. Gen. Virol.* *19*, 145-150.

Summers, M.D., and Arnott, H.J. (1969). Ultrastructural studies on inclusion formation and virus occlusion in nuclear polyhedrosis and granulosis virus-infected cells of *Trichoplusia ni* (Hubner). *J. Ultrastruct. Res.* *28*, 462-480.

Tani, K., Tokuda, H., Mizushima, S. (1990). Translocation of proOmpA possessing an intramolecular disulfide bridge into membrane vesicles of *Escherichia coli*. Effect of membrane energization. *J. Biol. Chem.* *265*, 17341-17347.

Thrift, R.N., Andrews, D.W., Walter, P., and Johnson, A.E. (1991). A nascent membrane protein is located adjacent to ER membrane proteins throughout its integration and translation. *J. Cell Biol.* *112*, 809-821.

Tong, A.H., Lesage, G., Bader, G.D., Ding, H., Xu, H. *et al.* (2004). Global mapping of the yeast genetic interaction network. *Science* *303*, 808-813.

Tyedmers, J., Lerner, M., Bies, C., Dudek, J., Skowronek, M.H. *et al.* (2000). Homologs of the yeast Sec complex subunits Sec62p and Sec63p are abundant proteins in dog pancreas microsomes. *Proc. Natl. Acad. Sci. USA* *97*, 7214-7219.

van den Berg, B., Clemons, W.M. Jr., Collinson, I., Modis, Y., Hartmann, E., Harrison, S.C., and Rapoport, T.A. (2004). X-ray structure of a protein-conducting channel. *Nature* *427*, 36-44.

Voigt, S., Jungnickel, B., Hartmann, E., and Rapoport, T.A. (1996). Signal sequence-dependent function of the TRAM protein during early phases of protein transport across the endoplasmic reticulum membrane. *J. Cell Biol.* *134*, 25-35.

Volkman, L.E., and Goldsmith, P.A. (1985). Mechanisms of neutralization of budded *Autographa californica* nuclear polyhedrosis virus by a monoclonal antibody: inhibition of entry by absorptive endocytosis. *Virology* 143, 185.

Walter, P., and Blobel, G. (1983a). Signal recognition particle: a ribonucleoprotein required for cotranslational translocation of proteins, isolation and properties. *Methods Enzymol.* 96, 682-691.

Walter, P., and Blobel, G. (1983b). Preparation of microsomal membranes for cotranslational protein translocation. *Methods Enzymol.* 96, 84-93.

Walter, P., and Johnson, A.E. (1994). Signal sequence recognition and protein targeting to the endoplasmic reticulum membrane. *Annu. Rev. Cell Dev. Biol.* 2, 499-516.

Waterham, H.R., Koster, J., Mooyer, P., Noort, G.G., Kelley, R.I. et al. (2003). Autosomal recessive HEM/Greenberg skeletal dysplasia is caused by 3 beta-hydroxysterol delta 14-reductase deficiency due to mutations in the lamin B receptor gene. *Am. J. Hum. Genet.* 72, 1013-1017.

Wattenberg, B., & Lithgow, T. (2001). Targeting of C-terminal (tail)-anchored proteins: understanding how cytoplasmic activities are anchored to intracellular membranes. *Traffic* 2, 66-71.

Weis, K. (2003). Regulating access to the genome: nucleocytoplasmic transport throughout the cell cycle. *Cell* *112*, 441-451.

White, S.H., and Wimley, W.C. (1999). Membrane protein folding and stability. Physical principles. *Annu. Rev. Biophys. Biomol. Struct.* *28*, 319-365.

Wiedmann, M., Gorlich, D., Hartmann, E., Kurzchalia, T.V., and Rapoport, T.A. (1989). Photocrosslinking demonstrates proximity of a 34kDa membrane protein to different portions of preprolactin during translocation through the endoplasmic reticulum. *FEBS Lett.* *257*, 263-268.

Wiese, C., Goldberg, M.W., Allen, T.D., and Wilson, K.L. (1997). Nuclear envelope assembly in *Xenopus* extracts visualized by scanning EM reveals a transport-dependent 'envelope smoothing' event. *J. Cell Sci.* *110*, 1489-1502.

Wilkinson, B.M., Critchley, A.J., and Stirling, C.J. (1996). Determination of the transmembrane topology of yeast Sec61p, an essential component of the endoplasmic reticulum translocation complex. *J. Biol. Chem.* *271*, 25590-25597.

Woolhead, C., McCormick, P.J., and Johnson, A.E. (2004). Nascent membrane and secretory proteins differ in their FRET-detected folding far inside the ribosome and in their exposure to ribosomal proteins. *Cell* *116*, 725-736.

Worman, H.J., Yuan, J., Blobel, G., and Georgatos, S.D. (1988). A lamin B receptor in the nuclear envelope. *Proc. Natl. Acad. Sci. USA* *85*, 8531-8534.

Worman, H.J., & Courvalin, J.C. (2000). The inner nuclear membrane. *J. Membr. Biol.* *177*, 1-11.

Worman, H.J., & Courvalin, J.C. (2005). Nuclear envelope, nuclear lamina, and inherited disease. *Int. Rev. Cytol.* *246*, 231-279.

Wu, W., Lin, F., and Worman, H.J. (2002). Intracellular trafficking of MAN1, an integral protein of the nuclear envelope inner membrane. *J. Cell Sci.* *115*, 1361-1371.

Yan, A., and Lennarz, W.J. (2005). Two oligosaccharyl transferase complexes exist in yeast and associate with two different translocons. *Glycobiology* (in press).

Ye, Q., and Worman, H.J. (1994). Primary structure analysis and lamin B and DNA binding of human LBR, an integral protein of the nuclear envelope inner membrane. *J. Biol. Chem.* *269*, 11306-11311.

Ye, Q., and Worman, H.J. (1996). Interaction between an integral protein of the nuclear envelope inner membrane and human chromodomain proteins homologous to *Drosophila* HP1. *J. Biol. Chem.* *271*, 14653-14656.

Zhang, Q., Skepper, J.N., Yang, F., Davies, J.D., Hegyi, L., *et al.* (2001). Nesprins: a novel family of spectrin-repeat-containing proteins that localize to the nuclear membrane in multiple tissues. *J. Cell Sci.* *114*, 4485-4498.

VITA

SURAJ SAKSENA

surajsaksena@neo.tamu.edu

Education:

Graduate Research Assistant, Department of Biochemistry & Biophysics,
Laboratories of Dr. M.D. Summers & Dr. A.E. Johnson, Texas A&M University (2000-
present)

M.S. Biochemistry, Laboratory of Dr. V.K. Chaudhry,

University of Delhi South Campus, New Delhi, India (2000)

B.S. Biochemistry, Sri Venkateswara College, University of Delhi (1998)

Permanent address:

E-1/19 First Floor

Vasant Vihar

New Delhi-110057

India

Full-length Original Research Publications:

Saksena, S., Shao, Y., Braunagel, S.C., Summers, M.D., and Johnson, A.E. (2004) "Co translational integration and initial sorting at the endoplasmic reticulum translocon of proteins destined for the inner nuclear membrane". *Proceedings of the National Academy of Sciences (USA)* 101(34): 12537-12542.

Braunagel, S.C., Williamson, S.T., **Saksena, S.**, Zhong, Z., Russell, W.K., Russell, D.H., and Summers, M.D. (2004) "Trafficking of ODV-E66 is mediated via a sorting motif and other viral proteins: Facilitated trafficking to the inner nuclear membrane". *Proceedings of the National Academy of Sciences (USA)* 101(22): 8372-8377.

Sauri, A., **Saksena, S.**, Salgado, J., Johnson, A.E., and Mingarro, I. (2005) "Double-spanning Plant Viral Movement Protein Integration into the Endoplasmic Reticulum Membrane is Signal Recognition Particle-dependent, Translocon-mediated, and Concerted". *Journal of Biological Chemistry* 280(27): 25907-25912.